2022

Application of physiologically based pharmacokinetic (PBPK) modeling to study the impact of Roux-en-Y gastric bypass (RYGB) surgery on the bioavailability of oral antibiotics

Suvarchala Kiranmai Avvari
Long Island University

Application of Physiologically based Pharmacokinetic (PBPK) Modeling to Study the Impact of Roux-en-Y gastric Bypass (RYGB) Surgery on the Bioavailability of Oral Antibiotics

A thesis submitted in Partial Fulfillment of the Requirement for the Degree of

DOCTOR OF PHILOSOPHY (Ph.D.)

WITH SPECIALIZATION IN PHARMACEUTICS

To the Faculty of

Arnold & Marie Schwartz College of Pharmacy and Health Sciences
Division of Pharmaceutical Sciences
Long Island University
Brooklyn, New York

August 5th, 2022

Presented By

Suvarchala Kiranmai Avvari

Sponsoring Committee

_____

Dr. David R. Taft, Ph.D. – Committee Chair

_____

Dr. Grazia Stagni, Ph.D. - Committee member

_____

Dr. Jaclyn Cusumano, Pharm.D., BCIDP - Committee member

_____

Dr. Pooja Manchandani, Ph.D. - Committee member

_____

Dr. Anthony J. Cutie, Ph.D.
Interim Division Chair

Dedicated to

my parents,

my husband and my daughter

ACKNOWLEDGEMENT:

Firstly, I would like to express my sincere gratitude to my advisor Dr. David Taft for the continuous support of my Ph.D. study and related research, for his patience, motivation, and immense knowledge. His guidance helped me in all the time of research and writing of this thesis. I am extremely grateful that you took me as a student and continued to have faith in me over the years. I could not have imagined having a better advisor and mentor for my Ph.D. study.

I would like to express my sincere thanks to the members of my thesis committee: Dr. Grazia Stagni, Dr. Jaclyn Cusumano, Dr. Pooja Manchandani, for their insightful comments and encouragement, but also for the hard question which incented me to widen my research from various perspectives.

I would also like to extend my gratitude to Dr. Rutesh Dave, The Office of Experiential Education, and Long Island University for supporting me academically through assistantships. I thank my fellow lab mates Jennyfer Mudunuru, Sheila Masinde, Vamshi Jogiraju, Harshith, Kushal Shah for the stimulating discussions, and have helped me pull through all the research aspects.

This journey would not have been possible without the unconditional love, support, and encouragement from my family. I would like to thank my parents, my husband and my sister for being extremely understanding, being a phone call away and being there for me day and night. Very special thanks to my husband, Rama Chilukuri and to my lovely daughter, Divija Chilukuri without them I cannot imagine this dream come true.

ABBREVIATIONS

AGP	Alpha-1-acid glycoprotein
AUC	Area under Concentration
ADAM	Advanced Dissolution Absorption & Metabolism
BMI	Body Mass Index
BPD	Biliopancreatic Diversion
CA	Cefuroxime axetil
CAP	Community Acquired Penumoniae
CDC	Center for Disease Control
CLint	Intrinsic Clearance
CL_{IV}	Clearance following Intravenous administration
CL_R	Renal Clearance
C_{max}	Peak Plasma Concentration
CYP P-450	Cytochrome P-450
F_{oral}	Oral Bioavailability
fa	Fraction of drug absorbed into the intestinal gut wall
fg	Fraction that escapes gut wall metabolism
fh	Fraction that escapes hepatic metabolism
GIT	Gastrointestinal Tract
IAI	Intra-abdominal Infection
IDSA	Infectious Disease Society of America
LAGB	Laparoscopic Adjustable Gastric Banding
MIC	Minimum Inhibitory Concentration
OATP	Organic Anionic Transporter Protein
PBPK	Physiologically Based Pharmacokinetic Modeling
PK/PD	Pharmacokinetics/Pharmacodynamics
P-gp	Poly-glycoprotein
PEPT 1	Human Peptide Transporter 1
RYGB	Roux-en-Y Gastric Bypass
SG	Sleeve Gastrectomy
SSTIs	Skin and Soft Tissue Infections
UTI	Urinary Tract Infections
UGT	UDP-Glucuronosyltransferases
Vss	Steady-state Volume of Distribution
WHO	World Health Organization

Table of Contents

List of Tables

List of Figures

ABSTRACT

ABSTRACT

Understanding the mechanisms that govern drug absorption and elimination is a critical component in pharmaceutical research and development, as the oral route remains the most common method of drug administration. The utilization of *in silico* physiologically based pharmacokinetic modeling and simulation (PBPK M&S) has enabled the extrapolation of modeling and simulation in special populations where concerns regarding alteration in overall drug exposure may arise, such as following gastrointestinal surgery. Roux-en-Y Gastric bypass (RYGB), or partial resection of the gastrointestinal tract, leads to multiple physiological alterations that affect drug absorption. The inability to generalize and predict changes in oral drug bioavailability (F_{oral}) following gastric bypass surgery presents a considerable therapeutical challenge to clinicians.

PBPK M&S is a widely used approach for predicting the bioavailability changes in different clinical scenarios. Infection post-surgery is the most common risk factor and should be monitored and treated with utmost care. There is limited literature assessing the bioavailability changes of oral antibiotics post-gastric bypass surgery. This thesis aimed to determine the impact of gastric bypass surgery on oral drug absorption and metabolism for antibiotics such as azithromycin, cefuroxime axetil, and metronidazole. This was accomplished by applying the PBPK M&S approach to identify and define essential intrinsic elements and parameters, model implementation, and validation within a general model development framework.

The developed post gastric bypass surgery PBPK model provides a framework for investigating physiological mechanisms associated with changes in systemic drug

exposure after oral administration, which may result from the interplay of disintegration, dissolution, absorption, and presystemic metabolism by the intestine and liver. The developed PBPK models of azithromycin, cefuroxime axetil, and metronidazole were used to evaluate the changes in antibiotic exposure in gastric bypass surgery patients after a solid and liquid formulation. The results from solid formulation bioavailability post gastric bypass surgery model simulations suggest that the current dosing regimen for azithromycin and cefuroxime axetil may not be sufficient for treating infections, and dose modifications might be necessary. At the same time, no significant changes were observed for metronidazole bioavailability post-surgery. The results from liquid formulations of these antibiotics suggest that the azithromycin suspension presents enhanced absorption and bioavailability than the tablet formulation. In contrast, the suspension of cefuroxime axetil followed the same trend as solid formulation.

Overall, this thesis demonstrates the application of PBPK M&S in the extrapolation of oral drug exposure to special populations (*e.g.*, RYGB). The PBPK approach shows oral bioavailability to provide clinicians with an evidence-based dose selection to prevent the risk of treatment failure due decreased drug exposure of oral antibiotics post gastric bypass surgery.

BACKGROUND

Background

The World Health Organization (WHO) declared obesity, now a worldwide epidemic, as one of the major concerns for global health. The WHO considered obesity to be the fifth leading risk for global death and a significant burden on health care systems. Body mass index (BMI= body weight (kg)/height $(m)^2$) is the most commonly used measure for classifying adults as overweight or obese, both at the population and the individual level. Table 1 presents the WHO classification of obesity based on BMI with normal weight as a BMI of 18 to 24.9 kg/m^2, overweight as a BMI of 25 to 29.9 kg/m^2, obesity as a BMI of 30 kg/m^2 or more, and morbid obesity as a BMI of >40 kg/m^2 or >35 kg/m^2 in the presence of comorbidities [1]. Morbid obesity (body mass index [BMI] $\geq$ 35 kg/m^2) is an enormous global health challenge, with an exponentially increased global prevalence over the past several decades [2]. In the United States, the number of people who are overweight or obese has increased to outnumber normal-weight individuals by 2:1. In the United States, during the period 2015-2016, nearly 39.8% of adults and worldwide, more than 2.1 billion people were classified as obese [3,4].

Table 2 presents the incidence of mortality and its associated comorbidities, including cardiovascular disease, type 2 diabetes (T2D), dyslipidemia, hypertension, low-grade systemic inflammation, depression, hyperlipidemia, and some cancers, which has increased in the obese population relative to the normal weight category and represents a major health and economic burden [5-7]. WHO estimated that overweight and obesity have attributed to 44% of the diabetes cases , 23% of the heart disease cases, and up to 41% of certain cancers worldwide. Globally, more than 2.8 million adults die each year as a

consequence of being overweight or obese [8]. Regardless of race and age, women are more affected by morbid obesity compared to men.

Equally serious, overweight and obesity rates in children parallel those of adults. The incidence of obesity in children has increased to a point where one-third of children are obese or overweight. The prevalence of obesity from 1999-2000 through 2017-2018 increased from 30.5% to 42.4% and affected about 14.4 million (19.3%) children and adolescents. Obesity prevalence was 13.4% among 2-5-year-olds, 20.3% among 6-11-year-olds, and 21.2% among 12-19-year-olds [9]. For children and teens, BMI is age and sex-specific and is referred to as BMI for age. After calculating BMI for a child, the BMI number is plotted on the CDC growth charts to obtain a percentile ranking. Percentiles, which are age and sex-specific, are used to assess the size and growth patterns of children. The growth charts classify the weight status categories into underweight, healthy weight, overweight, and obese (Table 3) [10].

Table 1: WHO classification of adult overweight and obesity

Classification	**BMI (kg/m^2)**	**Risk of comorbidities**
Normal Range	18.5-24.99	Average
Overweight	≥25.0	
Pre-Obese	25.0-29.99	Increased
Obese	≥30.0	
Obese Class I	30.0-34.99	Moderate
Obese Class II	35.0-39.99	Severe
Obese Class III	≥40.0	Very Severe

Treatment for obesity ranges from lifestyle modifications, such as diet and exercise, to drug therapy, and surgical interventions with varying degrees of invasiveness. Such

approaches also differ in effectiveness, health outcomes, and cost. Lifestyle modifications in varying levels of intensity and various combinations have shown low to moderate long-term effectiveness. There are few effective therapeutic products for the treatment of morbid obesity. Weight loss as a result of pharmacotherapy is short term compared to lifestyle modifications, and patients regain most of the lost weight once the therapy has stopped [11]. The rise in the prevalence of obesity resulted in increased attention to the surgical approach as part of the treatment of obesity. The National Institutes of Health, in 1991, established guidelines for surgical therapy of morbid obesity, now known as bariatric surgery.

Table 2: WHO estimated Relative Risk (RR) for the obese subjects developing obesity – related diseases

Greatly Increased (RR > 3)	**Moderately Increased (RR = 2-3)**	**Slightly Increased (RR = 1-2)**
Type 2 Diabetes Dyslipidemia Insulin Resistance Depression Sleep Apnea Breathlessness Gall Bladder disease	Coronary Heart Disease Hypertension Osteoarthritis Hyperuricemia and gout	Cancer (Breast Cancer in postmenopausal women, endometrial cancer, colon cancer) Reproductive Hormonesabnormality Polycystic Ovary Hormone Impaired Fertility Low Back Pain Increased risk for anesthesia complications Fetal defect associated with maternal obesity

Table 3: BMI weight status categories and percentiles

Weight Status Category	**Percentile Range**
Underweight	Less than 5th Percentile
Healthy weight	5th Percentile to less than the 85th Percentile
Overweight	85th to less than the 95th Percentile
Obese	Equal to or greater than the 95th Percentile

INTRODUCTION

Introduction

Bariatric surgery has demonstrated superiority in terms of effectiveness and sustainability of weight loss and resolution of comorbidities associated with obesity when compared to pharmacotherapy and lifestyle modifications [12,13]. Over the past decade, the efficacy of bariatric surgery has led to a noticeable increase in the number of procedures performed in the United States, with approximately 394,431 operations performed in 2018 [14]. One can see remarkable development in the bariatric surgical procedures, based on the technical advances, efficacy data, complication rates, and increased understanding of the physiology underneath their success.

Bariatric surgery procedures can be divided into two general categories: restrictive or malabsorptive, or a combination of the two. Restrictive methods act by limiting the intake of food by reducing the size and capacity of the stomach, slowing gastric emptying, and promoting and prolonging a feeling of satiation. Restrictive methods align with hypotheses that support negative calorie balance and decreased hepatic and pancreatic fat as the main mechanisms responsible for postoperative normalization of glucose metabolism and insulin sensitivity. Malabsorptive methods reduce the size of the stomach and divert food's passage directly to the distal intestine, bypassing the proximal intestine where most absorption occurs and resulting in more rapid delivery to the distal intestine. Malabsorptive methods include not only a calorie restriction model but also align with hypotheses that support enteroendocrine changes that impact the enteroinsular and adipoinsular axes and appetite regulation [15].

Types of Bariatric Surgery

Roux-en-Y Gastric Bypass (RYGB) also known as gastric bypass, sleeve gastrectomy (SG), adjustable gastric band, and biliopancreatic diversion with a duodenal switch are the most common bariatric procedures (Figure 1). Each procedure has its advantages and disadvantages. Even though biliopancreatic diversion (BPD) is performed less frequently due to high complications and severe nutrient deficiencies, the rate of remission is high [16]. Sleeve gastrectomy (SG) (45.9%) and Roux-en-Y gastric bypass (RYGB) (39.6%) are the most common bariatric procedures performed globally [17]. However, 10% to 35% of patients fail to lose sufficient weight or regain weight after RYGB, sometimes with recurrence of co-morbidities [18].

a) **Adjustable gastric banding:** Non-adjustable gastric banding was first reported in 1978 by Wilkinson and Peloso [19], but the first report on the clinical use of the adjustable gastric band was in 1986 by Lubomyr Kuzmak [20]. Adjustable gastric banding is considered to be one of the least invasive procedures. An inflatable gastric band is placed horizontally around the proximal part of the stomach, which is connected to a subcutaneous port. The subcutaneous port creates a pouch by inflating the band, which controls the rate of emptying the pouch and meal capacity. Based on the individual needs, the diameter of the band can be adjusted. This procedure can be done laparoscopically or using an open technique. There are no malabsorptive measures with this procedure. While it is a reversible, adjustable procedure and has the lowest risk of postoperative complications and nutritional deficiencies, it is less successful in achieving weight loss and has the highest rate of re- operation. Moreover, it requires a foreign object to remain in the body, which can probably slip from the position or, in rare cases, erode into the stomach.

b) **Roux-en-Y gastric Bypass:** The first gastric bypass was reported in 1967 by Mason and Ito [21]. This procedure is a combination of both restrictive and malabsorptive methods. In the Roux-en-Y gastric bypass (RYGB), a gastric pouch of about 20-30 ml capacity is created by dividing the upper stomach using surgical staples. The intestine is split to create a proximal biliopancreatic limb of 30 to 45 cm long and a distal Roux limb of about 10 cm long. The Roux limb is anastomosed to the small pouch stomach. The bottom of the biliopancreatic limb is anastomosed to the distal Roux limb. In this way, stomach acids and digestive enzymes mix with food after it has passed through a large part of the Roux limb. The smaller stomach is a restrictive measure, while the bypassed stomach and proximal intestine is a malabsorptive measure. Adjustments of the procedure have been used to increase malabsorption and increase weight loss by lengthening the Roux-en-Y limb to 100–150 cm. This method has excellent results in weight loss and diabetes remission. However, it is more complex than either the Laparoscopic Adjustable Gastric Banding (LAGB) or Sleeve Gastrectomy (SG),potentially. This procedure can be performed laparoscopically or using open techniques.

c) **Sleeve gastrectomy:** Sleeve gastrectomy was first reported by Doug Hess in 1988 [22]. In patients with BMI of more than 60 who pose a greater risk for bariatric surgery, sleeve gastrectomy is considered as a bridging procedure. In a sleeve gastrectomy procedure, about 80% of the stomach along the greater curvature is divided and removed to form a sleeve or a tube-shaped stomach. In 6-12 months, this procedure is converted to either gastric bypass or duodenal switch. However, for some, enough weight loss is achieved with the sleeve gastrectomy alone, and it can be considered the sole treatment for obesity in selective patients. This procedure can be done laparoscopically or using open techniques.

It is a less technically complex procedure: it does not require insertion of any foreign objects into the patient, as in LAGB, or bypass/re-routing of food, as in RYGB.

d) **Biliopancreatic diversion with duodenal switch:** Biliopancreatic diversion was first reported in 1978 by Scopinaro [23] and is now commonly performed by adding the duodenal switch component. It is primarily a malabsorptive procedure involving resection of the stomach along the greater curvature. By removing a larger part of the stomach, a small, tubular pouch is created. The duodenum is then divided just past the outlet of the stomach and roughly three-quarters of the way down the small intestine. The proximal intestine, which remains connected to the pancreas and gall bladder, is reconnected to the distal small intestine. This procedure uses restrictive methods very similar to SG and malabsorptive methods similar to RYGB. It differs from RYGB in that a large portion of the stomach is irreversibly removed, a greater portion of the proximal intestine is bypassed, and bile and pancreatic secretions do not mix with stomach acid and food until much further in the gastrointestinal (GI) tract. This procedure shares many of the same benefits as RYGB, but they are more pronounced in BPD. It is the most effective method for treating diabetes. However, it has the highest complication rate, a greater risk of nutritional deficiencies, and requires intensive follow-up and strict adherence to dietary and lifestyle changes.

Out of all the bariatric procedures, RYGB is considered the "gold standard" of bariatric surgery due to its high rates of diabetes remission and weight loss and low rates of complication [24]. The Roux-en-Y Gastric Bypass accounts for almost 80% of the total number of procedures undertaken in the United States [25]. Hence, in the current situation, the best option left for obese individuals is to undergo bariatric surgery, the gold standard technique for which is the Roux-en-Y gastric bypass (RYGB). These bariatric surgeries

have been shown to benefit the healthcare system by markedly cutting the cost of treatment of comorbid conditions in obese patients. RYGB achieves its key objectives in two ways: (a) cutting down the absorptive surface (forced malabsorption) and (b) restricting the contents of the food intake because of anatomical changes after surgery [26]. The most disconcerting side effects of these procedures include anastomotic leak, strictures, or marginal ulcers. In relatively rare instances, these complications can lead to death in approximately 0.5% of patients; however, severe complications are rare and occur in less than 2% of the patients undergoing these procedures. Despite the continuous improvement in the safety and efficacy of these procedures, the costs remain high [27].

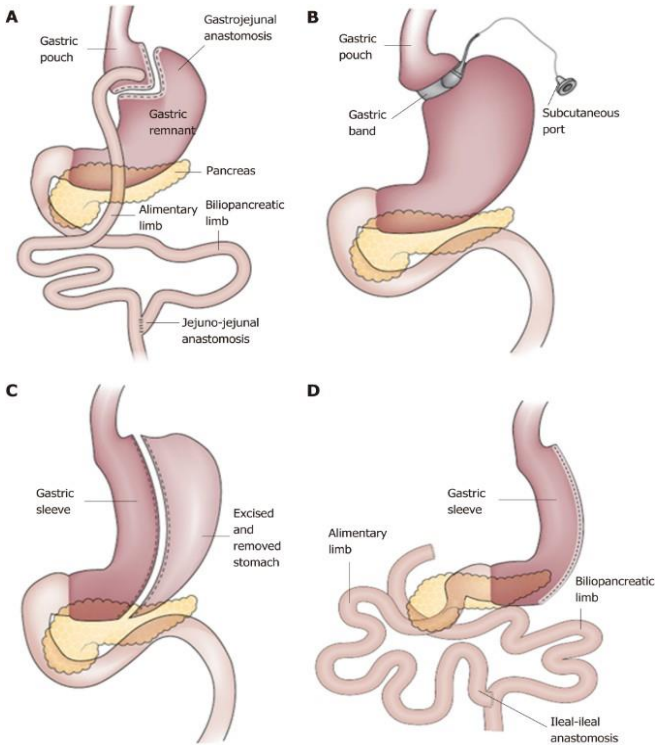

Figure 1: A- Roux-en-Y Gastric bypass, B- Adjustable gastric band, C- Sleeve Gastrectomy, D- Biliopancreatic diversion with duodenal switch [28].

Implications of Roux-en-gastric bypass on Drug Absorption, Metabolism, and Transport

All bariatric surgery procedures alter the anatomy and physiology of the GI tract. These changes in the GI tract can impact a broad range of factors involved in limiting the oral bioavailability of drugs [29]. Overall, the bioavailability of orally administered drugs (F) depends on three main processes: the fraction of the drug absorbed into the intestinal gut wall (f_a), the fraction that escapes gut wall metabolism (f_g), and the fraction that escapes hepatic metabolism (f_h). The observed bioavailability is obtained by multiplying these three fractions. f_a and f_g can be affected in bariatric surgery, and the subsequent weight loss may affect f_g and f_h.

$$F = f_a \times f_g \times f_h \quad (1)$$

As a result of RYGB surgery, there may be implications on the absorption and pharmacokinetic disposition of various drugs administered to patients after the procedure (Table 4) [30,31]. For example, the lower stomach and duodenum are effectively nonfunctional in RYGB patients, and therefore, drugs whose absorption window may be in the stomach to the duodenum region may show altered pharmacokinetic behavior. These physiological and anatomical changes can alter the pharmacokinetics of a given drug by the following mechanisms: increased gastric pH, delayed entry of bile acids, reduced small intestinal surface area available for absorption and a potential bypass of intestinal regions with a high abundance of drug-metabolizing enzymes [31].

Table 4: Physiological alteration after RYGB surgery and its possible impacts on oral drug absorption [31]

Anatomical changes	**Physiological changes Expected**	**Impact on drug pharmacokinetics**
Reduced gastric volume	Alteration of gastric emptying time	Change in the rate of oral absorption[a]
	Increased gastric pH	Change in the extent of oral absorption[b]
	Increased GI tract pH	Change in the rate and extent of oral absorption
Bypass of the duodenum	Reduced surface of absorption	Change in the rate and extent of oral absorption
	Reduced intestinal first-pass metabolism (Mainly CYP3A4, CYP3A5)	Change in the extent of oral absorption
	Reduced intestinal first-pass efflux: P-gp	Change in the extent of oral absorption
	Decreased intestinal transit time	Change in the rate of oral absorption
Dissociation of bile salt delivery	Decreased or delayed absorption of drugs requiring pancreatic secretions or solubilization with bile salts Reduced enterohepatic circulation	Change in the extent of oral absorption
Weight loss	Decreased low-grade inflammation	Change in drug metabolism
	Decreased steatohepatitis and insulin resistance	Change in the extent of oral absorption
	Decreased fat and lean mass	Change in drug distribution

CYP cytochrome P450, P-gp P-glycoprotein

a Measuring Tmax and Cmax can assess change in the rate of oral absorption

b Measuring area under the curve (AUC) can assess change in the extent of oral absorption

Antibiotics

Bariatric surgery continues to be one of the most successful ways of producing long-term weight loss (defined as loss of at least 50 percent of excess weight retained for at least 5 years). Despite improvements in medical weight control, with a substantial improvement in obesity- related co-morbidities and overall mortality [32], long-term follow-up and aggressive lifelong vitamin supplementation are needed to avoid micronutrient deficiencies due to the malabsorption caused by the alteration in GI anatomy [33]. A significant rise in the risk for intra-abdominal infections and urinary tract infections, while a reduction in the risk of infection of the respiratory,skin, and soft tissues is associated with bariatric surgery. Goto et al., performed a self-controlled case series study by using the emergency visits and inpatient databases from California, Florida, and Nebraska. The study reported the frequency of emergency visits and hospitalizations due to any of four types of infections - intra-abdominal infection, urinary tract infection (UTI), respiratory infection, or skin and soft tissue infections after bariatric surgery, compared to a reference period of 13 to 24 months before surgery [34]. With the increased risk of infections post-bariatric surgery, there is a need to use different oral antibiotics in both in-patient and out-patient settings. In addition, given the scarcity of data about the exposure changes of oral antibiotics post-bariatric surgery, there is a need to look into the dose modifications or frequency modifications of oral antibiotics if necessary.

The anatomical and physiological changes of the GIT, changes in gastric emptying time, pH, and a decrease in absorptive surface area of the small intestine along with bypass of many transporters, metabolic enzymes, and efflux pumps used to move the drugs through the intestinal epithelium located in the proximal gut may result in anticipated

reductions in drug absorption. These changes can result in the altered bioavailability of oral antibiotics that use these absorption processes, posing a risk for increased treatment failures [35]. The data demonstrating changes in oral antibiotic bioavailability after RYGB is primarily limited to a small number of pharmacokinetic single-dose studies. In RYGB patients, drugs with known oral bioavailability close to 100 %, such as linezolid, have shown no significant change in pharmacokinetics [36]. However, in patients that have undergone RYGB, antibiotics, such as azithromycin, have shown substantial reductions in systemic drug exposure [37]. The only data documenting clinical results with oral antibiotic use after RYGB were limited to a case report where amoxicillin, nitrofurantoin, and amoxicillin/clavulanate failed to treat a patient for microbiologically susceptible urinary tract infection and eventually required parenteral ceftriaxone therapy [38]. Therefore, more studies are needed to investigate whether altered pharmacokinetics from RYGB lead to a change in treatment outcomes of oral antibiotics.

Gastric bypass circumvents the primary site of absorption for antibiotics like azithromycin, cefuroxime axetil, and metronidazole, i.e., the upper small intestine [39]. It is also possible that this procedure can alter the pharmacokinetics of drugs by altering the expression of transporters and enzymes in that region. Overall, compared with controls, antibiotic plasma concentrations in gastric bypass subjects could be significantly reduced/altered. Even though the clinical significance is currently unclear, patients treated with the medications after bypass surgery may require a dose adjustment and/or closer clinical monitoring for treatment failure.

Azithromycin

Azithromycin is a broad-spectrum macrolide antibiotic used to treat both local and systemic infections, including skin, respiratory, GI, and genital tract infections such as pneumonia, sinusitis, and pharyngitis, tonsillitis infections, and gonococcal and chlamydial infections [40]. Azithromycin remains an integral part of treatment regimens for COPD exacerbations due to its immunomodulating and anti-inflammatory characteristics [41]. It acts by binding to the 23S rRNA of the bacterial 50S ribosomal subunit, preventing the mRNA translation by preventing the next amino acid addition by tRNA, thereby ceasing the protein synthesis of bacteria [42,43].

Azithromycin [9-deoxo-9a-aza-9a-methyl-9a-homoerythromycin, Figure 2] is a part of the azalide subclass and contains a 15-membered ring, with a methyl-substituted nitrogen instead of a carbonyl group at the 9a position on the aglycone ring, which prevents metabolism by the mechanism undergone by other macrolides [44].

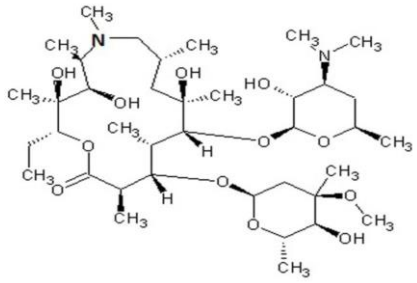

Figure 2: Molecular structure of Azithromycin [45]

Azithromycin has an oral bioavailability of 37 % due to its increased stability at low pH [46]. Azithromycin is lipophilic in nature and is distributed widely in blood and tissues. Upon reaching the bloodstream, azithromycin binds to alpha-1-acid glycoprotein (AGP),

an important plasma binding protein in addition to albumin. The protein binding of azithromycin is nonlinear, decreasing from 51% at 0.02 mcg/ml to 7% at 2mcg/ml. [47]. Concomitant administration of oral azithromycin with food significantly decreases by bioavailability by 50%. The time to maximum concentration is relatively short (1 to 2 h), and the dominant site of azithromycin absorption is assumed to be in the duodenum, the jejunum, or both. Thus, intact drug captured distal to the jejunum would suggest that incomplete absorption is mainly responsible for the poor bioavailability of the oral capsule.

Azithromycin is widely distributed across the body following oral administration, with an apparent steady-state volume of distribution of 31.1 L/kg. Greater amounts of azithromycin have been found in tissues than in plasma or serum. High tissue concentrations are not quantitatively linked to clinical efficacy. Azithromycin is minimally metabolized by CYP3A4 (a weak substrate), and neither induces nor inhibits CYP3A4 activity [48]. It is thought that MRP2 plays a smaller role in the excretion of azithromycin into bile than ABCB1 [49]. Azithromycin is mainly eliminated unchanged in the feces via biliary excretion and transintestinal secretion. Urinary excretion is a minor elimination route: about 6% of an oral dose and 12% of an intravenous dose are recovered unchanged in the urine. The mean terminal elimination half-life of azithromycin is 48 to 96 hours [50].

Cefuroxime Axetil

Cephalosporins are among the most widely prescribed classes of antimicrobial agents since their introduction in the 1970s. Cephalosporins of the second generation, such as cefamandole and cefuroxime, have a more extended spectrum than those of the first generation. Cefuroxime is a cephalosporin of the second generation with broad

antimicrobial activity against gram-positive and gram-negative organisms [51]. Cefuroxime is a bactericidal antibiotic that, like other β-lactam antibiotics, and it inhibits bacterial cell wall synthesis by interfering with the cell wall binding mechanism of transpeptidation, compromising the cell wall to create filaments that are not viable. Cefuroxime leads to lysis of the organism by binding to a protein that plays a role in the formation of the bacterial cell wall.

Chemically, cefuroxime axetil is the 1-(acetyloxy) ethyl ester of cefuroxime, is (RS)-1-hydroxyethyl (6R,7R)-7-[2-(2-furyl) glyoxylamido]-3-(hydroxymethyl)-8-oxo-5-thia-1-azabicyclo [4.2.0] oct2-ene-2-carboxylate,72-(Z)-(O-methyl-oxime), 1-acetate 3-carbamate (Figure 3). Its molecular formula is $C_{20}H_{22}N_4O_{10}S$ and has a molecular weight of 510.48.

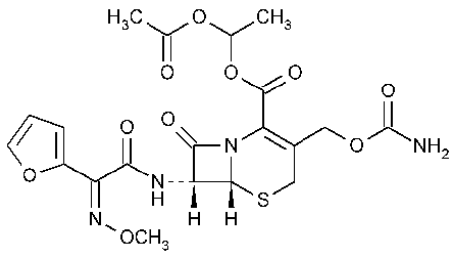

Figure 3: Molecular structure of Cefuroxime axetil [51]

Cefuroxime axetil is lipophilic in nature and it is the ester prodrug of the parenteral agent, cefuroxime. Cefuroxime axetil is primarily absorbed from the gastrointestinal tract following oral administration and rapidly hydrolyzed to cefuroxime by non-specific esterases in the intestinal mucosa and blood (Figure 4) [52]. Cefuroxime axetil oral formulations are recommended in the treatment of respiratory tract infections, intra-abdominal infections, and intensive care units. The bioavailability of the drug is only 37 % upon oral administration, and the absorption of a tablet is higher when taken after food,

i.e., 37 to 52 %. Cefuroxime, a β-lactam antibiotic is a substrate for PEPT1 mediated transport with higher activity in duodenum, and jejunum which serves as a major route of absorption for most of the oral antibiotics [53]. The serum protein binding of cefuroxime is approximately 38-50%. Cefuroxime is distributed throughout the extracellular fluids, and the axetil moiety is metabolized to acetaldehyde and acetic acid [54-56]. Oral administration of cefuroxime and cefuroxime axetil yields high blood concentrations ensuring that pathogenic microorganisms are eradicated. These drugs, even administered at high doses, do not cause adverse effects. The enhanced absorption of the prodrug compared with cefuroxime alone is thought to be due to increased lipophilicity, resulting in more rapid diffusion. The elimination of cefuroxime is essentially renal. Within the first 12 h, about 90% of the quantity absorbed is found in unchanged form. Cefuroxime is excreted by both glomerular filtration and by tubular secretion via OAT [57-58].

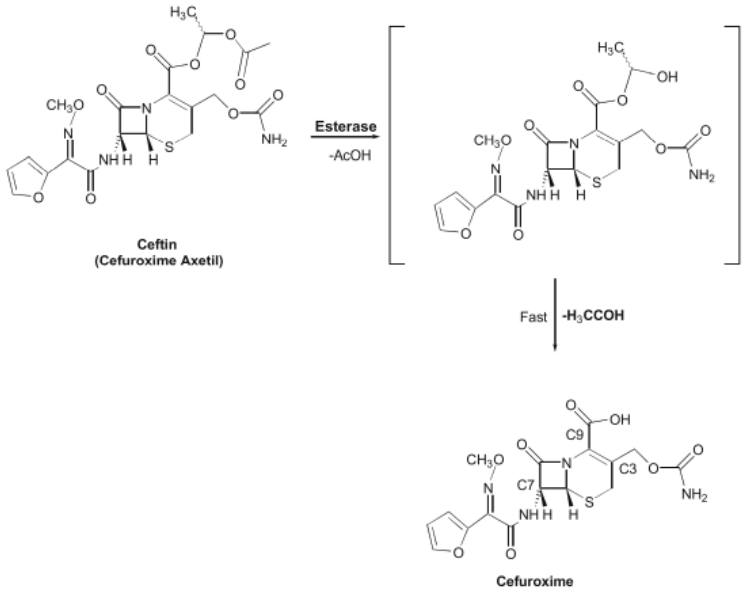

Figure 4: Bioconversion pathway of Cefuroxime axetil to cefuroxime [52]

Metronidazole

Metronidazole (2-methyl-5-nitroimidazole-1-ethanol, Figure 5) is an oral synthetic antiprotozoal and antibacterial agent that belongs to the class of nitroimidazoles. Metronidazole is widely used to treat anaerobic infections and in prophylaxis against infections after elective intestinal surgery. Metronidazole may be administered orally, topically, or intravenously [59]. Metronidazole exhibits a concentration-dependent bactericidal effect by developing free radicals after passive diffusion into cells [60].

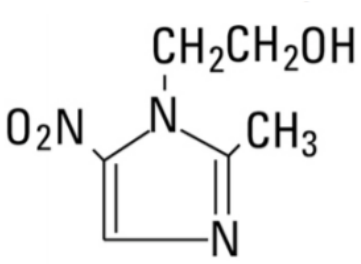

Figure 5: Molecular structure of Metronidazole [61]

Metronidazole is a relatively hydrophilic compound with low plasma protein binding (20%) and high distribution into various tissues and body fluids [62]. Metronidazole is well absorbed after oral administration, with peak concentrations occurring after 1 to 2 h after dosing. The plasma concentrations increase linearly with dose. Metronidazole undergoes hepatic metabolism (~ 85% of the administered dose), resulting in the generation of three metabolites. Metronidazole is metabolized by CYP3A4 and 2A6 to hydroxy metronidazole and oxidized to 1-metronidazole acetic acid. It undergoes UGT-mediated glucuronidation to form a glucuronide metabolite (Figure 6). Both the parent and the hydroxy metabolite possess in vitro bactericidal activity. The enzyme involved in the

oxidation of metronidazole to acetic acid metabolite has not yet been identified, but several studies suggest that CYP2E1 may play an important role in acid metabolite formation [61,63]. Plasma concentrations of the hydroxy metabolite range from 25 to 65% of the metronidazole concentrations observed, while only trace amounts of the acid metabolite were detected shortly after administration. The major route of elimination of both metronidazole and its metabolites (~60-80%) is renal and 6 – 15% is accounted for as fecal excretion. The elimination half-life of metronidazole ranges from 6 to 10 h, whereas the half-life of hydroxy metabolite ranges from 8 to 19 h [64-67].

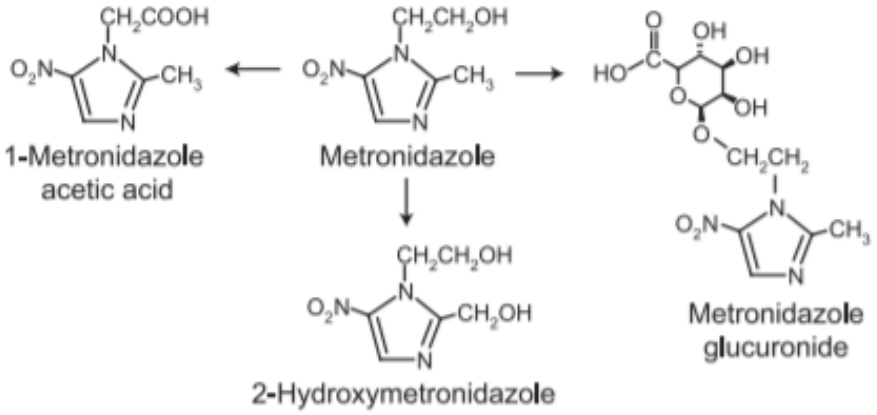

Figure 6: Biotransformation of Metronidazole to its metabolites [68]

Pharmacodynamics of Antibiotics

A pharmacokinetic/pharmacodynamic (PK/PD) analysis is important in antibiotic dosing. Understanding the PK/PD relationship helps optimize the dosing and maximize the efficacy while also preventing the development of resistance against bacteria. The minimum inhibitory concentration (MIC) is considered a principal PD parameter to determine the in vivo efficacy. However, some antibiotics have the same MIC value, which

differs in the bactericidal characteristics. Thus, MIC alone cannot predict the in vivo efficacy of antibiotics.

Antimicrobial killing characteristics are dependent on both the concentration of drug in relation to the MIC and the time that the exposure is maintained. When the effect of concentration predominates over that of time, the antibiotic displays concentration-dependent effects that are significantly associated with an optimal free drug maximum concentration to MIC ratio (fC_{max}/MIC). When the effect of time is greater, then the antibiotic displays time-dependent effects, and bacterial outcomes are associated with free drug concentrations remaining above the MIC for a defined portion of the dosing interval (fT>MIC). Antibiotics that have both the concentration- and time- dependent effects may observe killing that is associated with the free drug are under the curve to MIC ratio (fAUC/MIC). Concentration-dependent killing is characteristic of aminoglycosides, quinolones, macrolides (*e.g.*, azithromycin), ketolides. Time-dependent drugs is a characteristic of β-lactam antibiotics [69].

This classification of antibiotics evolved into three PK/PD indices (i) concentration-dependent antibiotics: the ratio of the maximum plasma concentration to MIC (C_{max}/MIC), (ii) concentration-dependent with time dependency antibiotics: the ratio of the area under the curve to the minimum inhibitory concentration (AUC/MIC), and (iii) time-dependent antibiotics: time for which the drug concentration exceeds the MIC (%T > MIC).

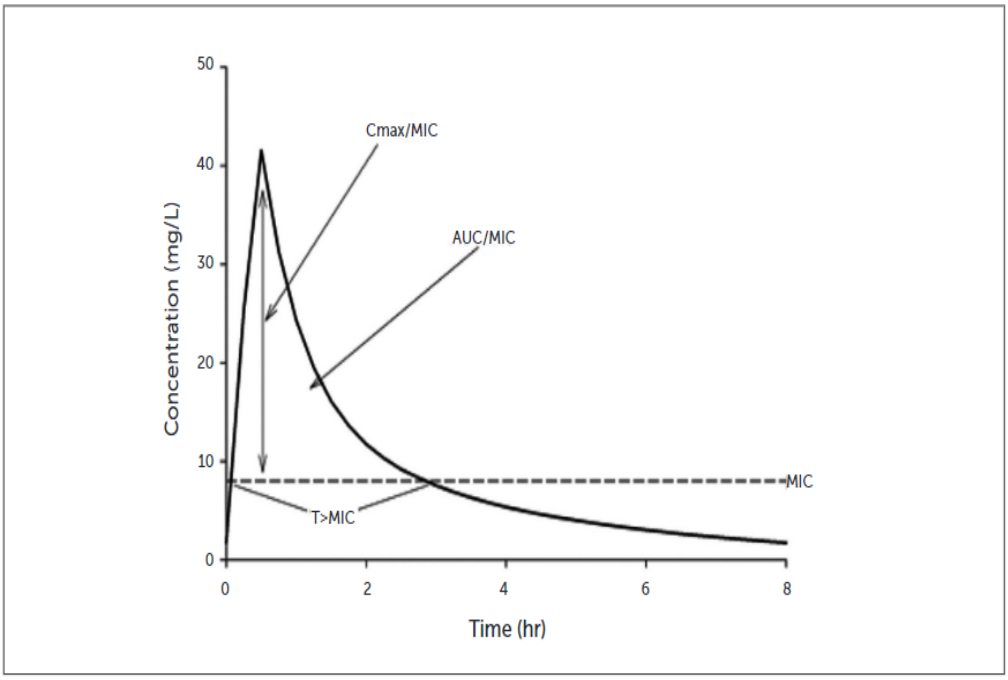

Figure 7: PK/PD indices associated with the efficacy of the antibiotics [69]

MIC: Minimum Inhibitory Concentration; Cmax/MIC: Maximum concentration to MIC ratio; AUC/MIC: Area under the curve to MIC ratio; T>MIC: Time above the MIC

Role of Physiologically Based Pharmacokinetic Modeling and Simulation

Physiologically based pharmacokinetic (PBPK) modeling and simulation approaches have become an integral part of drug discovery and development. The pharmacokinetics of drugs in the target population with varying physiology compared to healthy subjects can be predicted prior to the conduct of clinical trials using a PBPK approach. These models, when used in combination with pharmacodynamic (PD) models, can predict the effect profile and help to optimize dosage regimens to attain the desired exposure in vivo.

Teorell first introduced the concept of physiologically based pharmacokinetic modeling in 1937. Efforts have been made over the past several decades to refine PBPK

models for the application in drug discovery and development [70]. These PBPK models are usually applied from an early stage of discovery to drug development in further stages of research where a large amount of data is available for the drug [71]. The role of PBPK modeling can be categorized in three ways: a) informing regulatory communications, b) making impactful clinical development decisions, and c) promoting the mechanistic understanding of clinical observations. PBPK modeling is one approach that enables the integration of physiological, chemical, and drug-dependent preclinical and clinical information to model drug absorption, distribution, metabolism, and excretion and ultimately simulate untested clinical scenarios [72].

PBPK models are comprised of a series of compartments that represent various physiological organs of the body. These compartments are then connected by the circulating blood system, and these compartments are described by tissue volume and blood flow, which are assumed to be either permeability-rate-limited or perfusion-rate-limited. Blood flow to tissues is the limiting step for perfusion-rate-limited kinetics, which tends to apply to small lipophilic molecules, whereas permeability across cell membranes is the limiting step for permeability limited kinetics. Permeability limited kinetics tends to occur for large hydrophilic molecules. These PBPK models consider the parameters that can affect the pharmacokinetics of drug molecules in the target population, such as age, sex, enzyme expression, race, and disease states. A schematic representation of the PBPK model is shown in Figure 8.

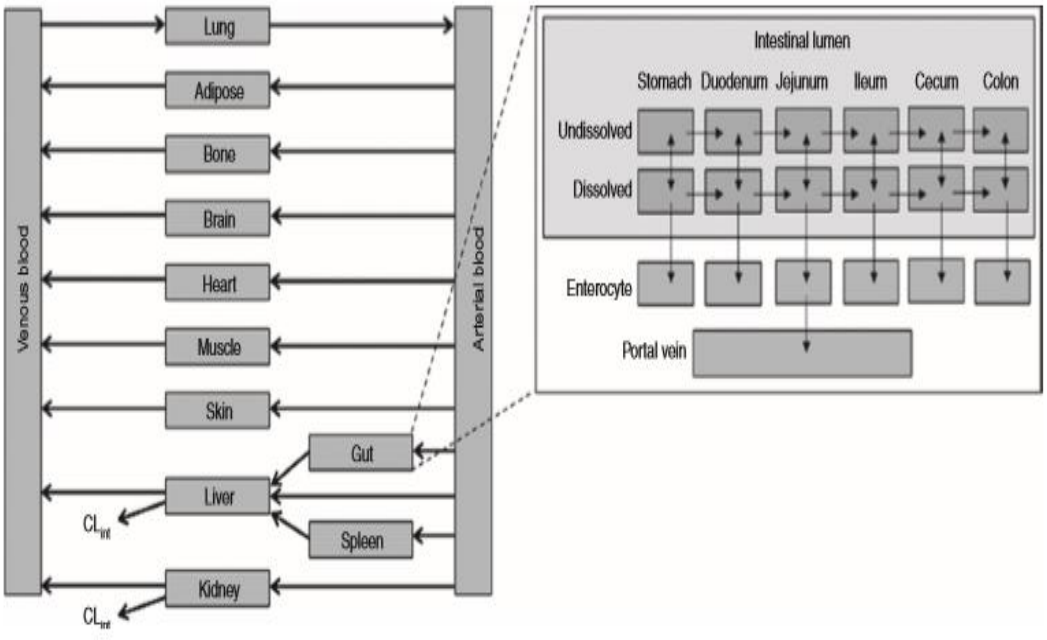

Figure 8: Schematic of a PBPK model. Insert denotes detailed representation of the intestine. CL_{int}, intrinsic clearance; PBPK, physiologically based pharmacokinetics[73].

PBPK modeling naturally uses a "bottom-up" approach where preclinical data collected during the early drug discovery stage are used to predict the pharmacokinetics and pharmacodynamics of drugs in humans. Both the physicochemical and biochemical properties of the drug molecule determine the predictive ability of these models. Prior to the conduct of clinical trials in humans, the PBPK approach can be used to predict the in vivo data through in vitro-in vivo extrapolation models. In the last 10 years, regulatory agencies have accepted PBPK models as a tool for informing clinical study strategy and has become a useful tool over drug development. Sixty percent of all of the PBPK models submitted to regulatory agencies in 2013 were for drug-drug interaction (DDI) assessment [74].

PBPK models can be utilized to extrapolate drug pharmacokinetic behavior in healthy volunteer as well as patient populations that are a challenge to test clinically, such as predicting doses and drug exposure in children and infants and patients suffering from impaired renal or liver function [75]**.** Simcyp®, a population-based simulator, is one of several platforms of PBPK modeling available, which uses the in vitro data to simulate absorption, metabolism, and excretion of the drug, and to predict the systemic exposure of the drug in healthy and diseased populations. This investigation was carried out using the Simcyp simulator.

To date, a total of 18 published studies reported drug exposure changes post RYGB surgery. Of these, 7 examined the effect of gastric bypass surgery on the pharmacokinetics of drugs using the physiologically based pharmacokinetic modeling [76-83]. Only one publication addressed effect of gastric bypass surgery on pharmacokinetics of azithromycin and there is little reference to drug treatment in the international guidelines. The published studies were conducted with a single dose with 24 h sampling and in small number of participants, there are no published studies examining the effect of gastric bypass surgery on the pharmacokinetics of cefuroxime axetil and metronidazole. making it difficult to draw conclusive recommendations about suitable dosing strategies for patients after bariatric surgery. Additionally, most of the reviews presented in the literature recommend that liquid formulations are preferred to solid dosage forms for all drug classes, assuming that some problems related to tablet/capsule absorption may occur post-RYGB surgery. However, none of the reviews or studies published demonstrated differences in bioavailability between tablet and liquid suspension formulations in the gastric bypass surgery population [84].

For this dissertation research, Simcyp was used to develop a PBPK model for oral antibiotics azithromycin, cefuroxime axetil, and metronidazole post gastric bypass surgery. These models were used to evaluate the pharmacokinetics, of azithromycin, cefuroxime axetil, and metronidazole solid formulations like tablets, capsules in comparison to suspensions in post-gastric bypass patients. The exposure-response relationships for the efficacy and safety of these oral antibiotics were assessed using the PD indices like AUC/MIC and $T_{>}$MIC to predict the therapeutic success or failure of antibiotics post gastric bypass surgery.

STUDY RATIONALE

Study Rationale

As previously described, obesity has been declared as one of the major global health concerns by the WHO. Obesity more often is associated with multiple comorbidities, such as cardiovascular disease, type 2 diabetes (T2D), dyslipidemia, hypertension, low-grade systemic inflammation, depression, hyperlipidemia, and some cancers, which collectively pose social, economic as well as psychological implications on patient lives affecting nearly over a third of population today [85]. Both lifestyle modifications and pharmacotherapy have successfully demonstrated short term weight loss. The surgical treatment of obesity results in higher weight loss, and greater reduction in comorbidities, which results in prolonged survival rates as compared to other nonsurgical interventions. Hence, in the current situation, the best option for obese individuals is to undergo bariatric surgery, the gold standard technique for which is the Roux-en-Y gastric bypass (RYGB). RYGB surgery results in significant alterations in the anatomy of the GI tract that could result in potentially significant alterations in the absorption and hence the pharmacokinetic behavior of different drugs that are commonly prescribed to this population, thereby restricting or affecting the overall process of oral drug bioavailability.

Obesity has been associated with increased risk of infection, and patients often require treatment with antimicrobial therapy following bariatric surgery [86]. Given that oral antibiotics represent an important first-line treatment option for a variety of infections, further studies investigating the rates of oral antibiotic failure in patients following bariatric surgery are warranted to better put existing data into clinical context. In addition to altering the anatomy and physiologyof the GI tract, bariatric surgery causes significant changes in

bile acid physiology and the gut microbiome. These changes may influence the ADME of drugs, such as oral antibiotics [87].

However, there are only sparse reports available evaluating the effect of bariatric surgeries on the pharmacokinetics of oral antibiotics. Furthermore, the current available data is insufficient to make clinical recommendations regarding the appropriate surgical adjustment of dose or alternate dosage forms for patients after bariatric surgery. Thus, it is important that patients who require antimicrobial therapy receive appropriate evidence-based dosing of the agents after surgery.

A self-controlled case series study conducted by Goto et al. found a divergent pattern in the risk of four common infectious diseases like skin and soft tissue infections (SSTI) and respiratory infections, intra-abdominal infections, and urinary tract infections (UTI) after bariatric surgery. Azithromycin, cefuroxime axetil, and metronidazole are oral antibiotics that are widely prescribed for outpatient treatment for respiratory infections like community-acquired pneumonia, intra-abdominal infections, and UTIs. Most of the bacterial infections are managed on an outpatient basis; many patients are not directly monitored in the hospital. Early antibiotic dosing is vital as it significantly lowers the mortality rate if antimicrobials are administered within 4-8 h of diagnosis of infection. To maximize clinical effectiveness, early (within 24 h) administration of antimicrobials at appropriate doses is, therefore, necessary [88].

Conducting clinical studies on antibiotic exposure and efficacy post-RYGB surgery is costly and time-consuming, which is the main reason for the lack of published studies in this patient population. Therefore, developing an in-silico model that can accurately predict the drug exposure following RYGB surgery could provide appropriate evidence-

based dosing for antibiotic dosing after surgery. Thus, the pharmacokinetic analysis of antibiotics and the PK/PD analysis using the PD indices like AUC/MIC and $T_{>}$MIC may help provide evidence about the need for dose adjustments when prescribing antibiotics in gastric bypass patients.

This research aimed to use the PBPK modeling platform Simcyp to develop PBPK models for oral antibiotics that characterize the drug disposition in gastric bypass surgical patients, which can inform safe and effective dosing in these patient populations. The goal was to test the hypothesis that a model-based dosing regimen will prevent antibiotic therapeutic failure by maintaining the plasma drug concentrations within an effective range over the course of therapy.

SPECIFIC AIMS

Specific Aims

Specific aim 1: To verify the previously published postsurgical population model using two CYP3A4 substrates, atorvastatin and midazolam

The aim was to verify a previously published post-surgical RYGB population in Simcyp simulator. The population model was developed by altering the physiology of the GI tract in the morbidly obese population which was prebuilt in Simcyp. A physiologically based pharmacokinetic model (PBPK) of atorvastatin was developed and verified in healthy volunteers. Subsequently, the verified substrate profiles for atorvastatin and midazolam available in the Simcyp library were used for postsurgical population model verification by capturing the changes in drug exposure in morbidly obese and post RYGB patients. This validated population model then utilized for the other aspects of the research.

Specific aim 2: To develop and verify physiologically based pharmacokinetic models for azithromycin, cefuroxime axetil, and metronidazole in healthy volunteers

The goal of this aspect of the research was to develop and to verify physiologically based pharmacokinetic models of probe drugs cefuroxime axetil, metronidazole, and azithromycin in healthy volunteers. A PBPK model for each probe drug was developed by incorporating the physicochemical, absorption, distribution, metabolism and elimination properties obtained from literature. These developed PBPK models were then verified by simulating and predicting plasma concentration profiles and exposure metrics (AUC and C_{max}) in healthy volunteers and comparing it to the clinical observed data obtained from literature.

Specific aim 3: To simulate and predict the drug exposure changes for cefuroxime axetil, metronidazole and azithromycin tablets in morbidly obese and post gastric bypass population, characterize the PK/PD relationship using PD indices AUC/MIC and T>MIC

The goal was to simulate and predict the drug exposure changes for probe drugs cefuroxime axetil, metronidazole and azithromycin in morbidly obese and post gastric bypass population when these medications were administered as solid oral dosage forms. These predictions were used to evaluate the changes in bioavailability of these formulations (*e.g*., tablets) in post-gastric bypass patients when compared to controls (morbidly obese). Systemic exposure and exposure time in morbidly obese and gastric bypass were used to characterize the PK/PD relationship to predict the therapeutic success or failure. Systemic drug exposure in morbidly obese and post gastric bypass patients was simulated using the verified PBPK models developed under specific aim 2.

Specific aim 4: To predict the relative bioavailability of orally administered suspension and tablet formulations for azithromycin and cefuroxime axetil in post-gastric bypass population, and characterize the PK/PD relationship using the PD indices AUC/MIC and T>MIC for suspension formulations

The goal of this aspect of the research was to evaluate drug exposure changes for azithromycin and cefuroxime axetil when administered as liquid suspensions in post RYGB patients. These predictions were then used to evaluate the changes in bioavailability in gastric bypass patients for solid dosage forms when compared to liquid dosage forms like suspensions for various clinically recommended doses and characterize the PK/PD relationship of antibiotics for suspension formulations.

SPECIFIC AIM 1

Specific Aim 1

Specific aim 1: To verify the previously published postsurgical population model using atorvastatin and midazolam

Introduction

Oral bioavailability (F) is dependent on the fraction of drug that is absorbed in the intestinal gut wall (f_a), the fraction that escapes gut wall metabolism (f_g) and the fraction that escapes hepatic metabolism (f_h) (Equation 1).

Drug and formulation properties such as disintegration, dissolution, permeability, solubility, and chemical stability highly impact f_a. The physiology of GI tract can also affect fa, which include factors such as gastric emptying time, pH profile, small intestinal transit time, abundance and enzymes and transporters in gut wall. Gastric emptying time can serve as the rate limiting step for drugs that are highly permeable and highly soluble as reduction in size of stomach results in inevitably low absorption from stomach [89]. Altered pH after bariatric surgery might affect the drug dissolutionof drugs having a pKa within the range of GI pH fluctuations. The small intestine is the main siteof absorption, and bioavailability of drugs that are poorly soluble or formulated as extended release might be altered as a portion of small intestine will be bypassed post-surgery [90].

Gut metabolism (f_g) can be an important determinant of absorption and acts to regulate the oral bioavailability of drugs and xenobiotics. Drug metabolizing enzymes like CYP, UDP glucuronosyltransferases, sulfotransferases, and glutathione S-transferases are expressed in the intestinal cells. Both CYP3A4 and 3A5 are present along the GI tract,

where 3A4 is expressed at lower levels in duodenum, at higher levels in jejunum and decreasing towards the ileum. Numerous transporters are present in the gut, such as the multidrug resistance transporter1, also referred to as P-glycoprotein (P-gp), multidrug resistance associated protein 2 and breast cancer related protein. These transporters effect the absorption and extent of gut metabolism through gut efflux. Relative expression pattern of P-gp in the small intestine increases from the proximal to the distal parts of the small intestine [91].

The Simcyp Simulator v19 (Simcyp Limited, Sheffield, UK) population template for the morbidly obese subjects is based on a Northern European Caucasian population and was used to build the Post-surgical RYGB population model. GI physiological parameters based on surgical/population data were implemented into advanced dissolution absorption and metabolism (ADAM) model to create Post Roux-en-Y gastric bypass population template/file. The ADAM model is a mechanistic representation of the GI tract that is implemented into Simcyp simulator. This ADAM model considers the type of formulation, and various physicochemical factors such as disintegration, dissolution, solubility, precipitation, supersaturation occurring in each section of GIT (Figure 9). Development and validation of RYGB population model was previously published by Darwich et al [80].

A goal of the proposed research was to verify and analyze the model performance against the physiologically based pharmacokinetic model of atorvastatin (drug tested in the pilot study by Darwich et al.), and another CYP3A4 substrate, midazolam. Empirical PK models of atorvastatin and midazolam describing the changes in drug exposure pre (morbidly obese) and post RYGB surgery have been published in the literature [92,93].

The model performance was analyzed by comparing the predicted pharmacokinetic data to the observed data obtained from the literature.

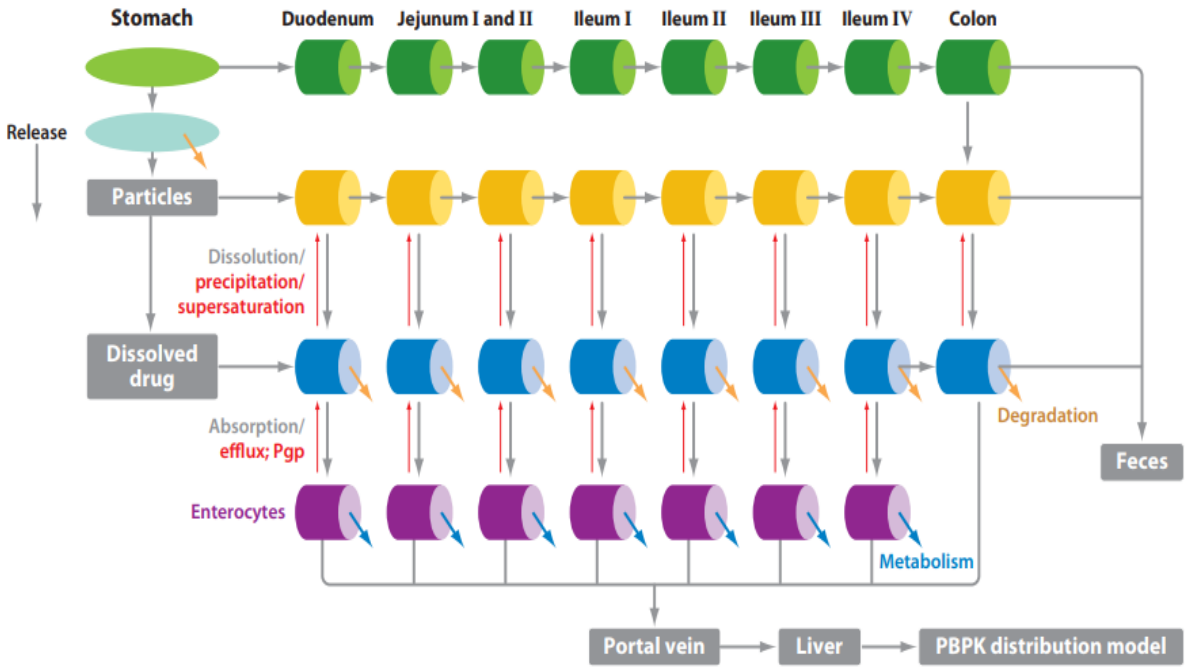

Figure 9: The advanced dissolution, absorption, and metabolism (ADAM) model of events in the gastrointestinal tract (94).

Modeling strategy

Evaluation of post RYGB population model previously developed through mimicking clinical investigations on atorvastatin and midazolam after gastric bypass

A virtual "Post Roux-en-Y gastric bypass" population was created using Advanced Dissolution Absorption and Metabolism (ADAM) model within the Simcyp simulator based on the characteristics of morbidly obese population published by Darwich et al and Chen et al., [80, 81]. The ADAM model describes the oral absorption

through a physiologically based eight segment model of the small and large intestine, including: duodenum, jejunum I & II, Ileum I-IV, and colon. The model defines release of drug from formulation, dissolution, precipitation. degradation, absorption, active transport, and metabolism as the drug moves through the small intestine, which allows for incorporation of population variability and saturation effects.

The post-surgical PBPK model describes absorption using ADAM model with alterations of specific anatomical and physiological parameters that are known to change post-surgery. These parameters include gastric capacity, fluid dynamics, gastric emptying rate, small intestinal bypass, GI pH, bile flow, and changes in regional abundance of drug metabolizing enzymes and transporter p-gp. Whole body physiological changes, such as postsurgical recovery of renal function was also incorporated intothe model (Table 5).

Population implementations of small intestinal bypass and delay in bile inlet were dimensionally estimated as a function of body surface area (BSA) utilizing Equations 2 and 3 as implemented into the Simcyp Simulator ADAM model. The effective human permeability (Peff) was set to zero in the drug template for intestinal segments that are bypassed.

$$\text{Length of duodenum} = 0.205 \cdot \text{BSA}^{0.550} \quad (2)$$

$$\text{Length of jejunum and ileum} = 5.231 \cdot \text{BSA}^{0\,414} \quad (3)$$

Small intestinal transit time post-surgery was implemented into the model utilizing the incorporated Weibull distribution fitted to describe a log normal distribution through

altering the scale factor (β) of small intestinal transit time, keeping the shape factor (α) constant, thus retaining the log normal distribution assumption (Equation 4).

$$f(x)=\frac{\alpha}{\beta}\left(\frac{x}{\beta}\right)^{\alpha-1} e^{-(x/\beta)^{\alpha}} \quad (4)$$

Table 5: Input parameters for population template to mimic the postsurgical conditions (Darwich et al.,[80])

Parameters	**RYGB**
Gastric emptying: liquids (minutes)	7; CV:45%
Gastric capacity (ml)	30
Qsec stomach (l/h)	0.059
Initial volume of stomach acid (ml)	9.9
Gastric pH	6.5
Small intestinal bypass (centimeters and/or segments)	100cm (duodenum and jejunum I) [a]
Bile exclusion (centimeters and segments)	110cm (Stomach and jejunum I)
CYP3A4 abundance (nmol/total gut)	48.3 CV:60%
CYP3A5 abundance (nmol/total gut)	18.0 CV:60%
Mean small intestinal transit time (hours)	[b] 3.0; α=2.6, β=3.7
Renal equation	MDRD

CV, coefficient of variation; MDRD, modification of diet renal disease equation; Qsec, secretion flow; RYGB, Roux-en-Y gastric bypass;

[a]Setting human effective permeability (*P*eff) of compounds close to zero in bypassed segments.

[b] α and β, Weibull scaling factors utilizing assuming a variance of 1.8h used to calculate intestinal transit item using equation 4.

The population recreated using the post-surgical condition from the previously published model was then validated with two substrates: atorvastatin (the substrate studied by Darwich et al., for validation of the Gastric bypass population model) and midazolam. The substrate profile for midazolam was available in Simcyp library and the model was

used without any further modifications. The substrate profile for atorvastatin was not available in the library, so a PBPK model was developed and verified in healthy volunteers.

Development of PBPK model of atorvastatin in healthy subjects

The substrate profile of atorvastatin was created using Simcyp simulator version 19. The substrate's physiochemical parameters and additional parameters relating to absorption, distribution, metabolism, and transport [95-102] are summarized in Table 6. The ADAM model was used to predict the absorption of atorvastatin in Simcyp. Atorvastatin acid is primarily metabolized by CYP3A4 to ortho and para hydroxy atorvastatin acid, with marginal contribution from CYP2C8. Acyl glucuronidation of atorvastatin acid to lactone and UDP mediated metabolism of atorvastatin acid primarily to a minor glucuronide metabolite through UGT1A1 was also considered as a part of model development. Given the rapid absorption of atorvastatin (Tmax $\leq$ 1 h), it was presumed that the plasma Cmax was primarily that of absorbed atorvastatin acid and not that later formed systemically from atorvastatin lactone. In vitro data suggest P-gp mediated efflux and OATP1B1 mediated hepatic uptake of atorvastatin acid.

The developed atorvastatin PBPK model was used to simulate the plasma concentration profile in Healthy Volunteers, which is in-built in the Simcyp population library, and the simulated systemic exposure was compared against the published data [103, 104]. Next, simulations were carried out to predict the changes in atorvastatin systemic exposure in morbidly obese (pre-surgery) subjects and in the developed post-RYGB population, model. Sex, age, weight, height, and matched simulations was carried out corresponding to identified clinical studies.

The healthy population virtual trial #1 include of total 120 subjects (10 trails of 12 subjects each), aged between 24-48 years, fasted, 6 males and 6 females, single oral dose of 40mg. In trial #2, 630 subjects (10 trails of 63 subjects each), aged between 18-55 year, fasted, 51 males and 12 females, single oral dose of 40mg was simulated. The pre- and post-Surgery virtual trail include subjects aged between 29-63 years, fasted, total 120 patients (10 trails of 12 subjects each), 4 female and 2 males for a single oral dose of 20mg, all females for a single oral dose of 40mg and all males for a single oral dose of 80mg. The demographics and the study design is shown in Table 7.

The simulated plasma concentration profiles in healthy, pre, and post-surgery populations were compared with published clinical data [93,103-104] digitized using WebPlotDigitizer (https://automeris.io/WebPlotDigitizer/). Fold error calculation of pharmacokinetic parameters Cmax and AUC and visual predictive checks was performed for all three populations. Fold error was calculated as a ratio of predicted to the observed value of each pharmacokinetic parameters.

Table 6**:** Input parameters to create substrate profile for atorvastatin in Simcyp®

Parameter		
Physicochemical Properties:		
Molecular weight	546 g/mol	[95]
Log P	4.47	[95]
pKa	4.46	[95]
Blood/plasma ratio	0.61	[98]
Fraction unbound in plasma	0.027	[98]
Absorption:		
Absorption Model	ADAM	
Caco-2 (pH 6.4:7.5) (10^{-6} cm/s)	4.9	[97]
	1.23	
Dissolution:		
Aqueous Solubility @ pH 6.0 (mg/ml)		[96]
Distribution:		
Distribution Model	Full PBPK model	
Prediction Method	Method 2 (Rodgers et al.,)	
Kp Scalar	2 (optimized)	
Metabolism/Elimination:		
Clearance Type	Enzyme Kinetics	[99, 100, 101]
CYP3A4: para-OH		
Cl_{INT} (µL min-1 mg-1 protein)	35.5 ± 48.1	
CYP3A4: ortho-OH		
Cl_{INT} (µL min-1 mg-1 protein)	45.8 ± 59.1	
CYP2C8		
Cl_{INT} (µL min-1 mg-1 protein)	10.5	
Additional HLM		
Cl_{INT} (µL min-1 mg-1 protein)	65	
UGT1A1		
Cl_{INT} (µL min-1 mg-1 protein)	5.23	
UGT1A3		
Cl_{INT} (µL min-1 mg-1 protein)	6.2	

Transport :		
P-gp (Apical efflux, small intestine)		[97]
J_{max} (pmol/min)	141±11	
K_m (μM)	115±19	
OATP1B1 (Sinusoidal uptake, Liver)		[102]
J_{max} (pmol/min/10^6 hepatocytes)	25	
K_m (μM)	0.77	
OATP1B3 (Sinusoidal uptake, Liver)		
J_{max} (pmol/mg protein/min)	25	
K_m (μM)	0.73	
OATP2B1		
J_{max} (pmol/mg protein/min)	24.272.84	
K_m (μM)		

ADAM, advanced dissolution, absorption, and metabolism; [a] Optimized to account for acid to lactone conversion in stomach; [b] Optimized to reproduce C_{max}

Table 7: Study design for Simcyp® simulations in healthy population

	Healthy (Lau 2007)	**Healthy (Bullman 2011)**
No. of Trials	10	10
No of subjects in each Trial	12	63
Age of Subjects(years)	24-48	18-55
% of females	50	20
Duration of study (h)	24	24
Dosage regimen	40mg single dose	40mg QD for 7days

Results

PBPK modeling of atorvastatin in healthy population

A PBPK model for atorvastatin was developed and validated in healthy subjects. To evaluate the model's accuracy, the simulated plasma profiles were compared to the published data. As illustrated in Figure 10. the predicted values are within the 95% confidence interval when comparedto observed data. Table 8 shows the observed and predicted pharmacokinetic parameters and calculated fold error for healthy populations. These results demonstrate that the model successfully captured the drug behavior in healthy subjects. Fold errors for AUC and C_{max} ranged from 0.77 to 1.14, indicating that the model successfully predicted the pharmacokinetic parameters compared to observed data.

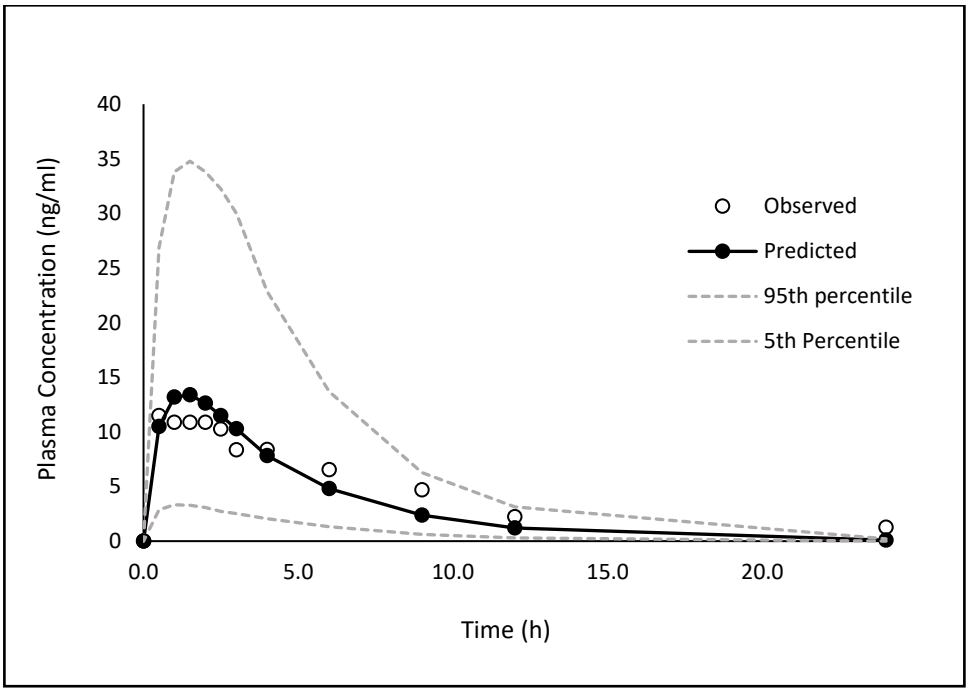

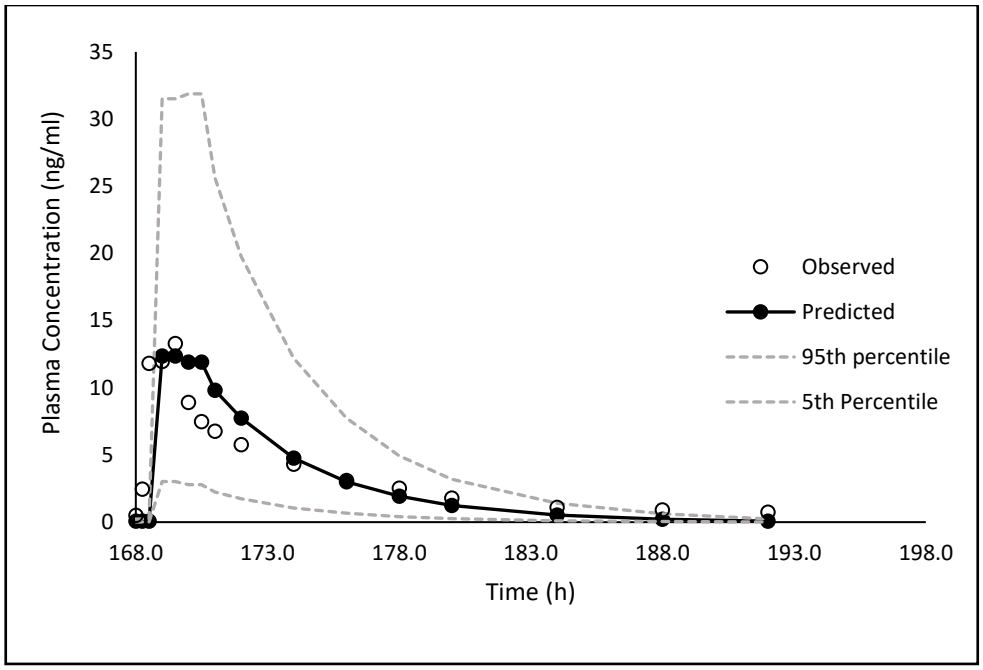

Figure 10: Observed (solid circles) and Predicted (open circles) concentration time profiles of 40mg single oral dose ofatorvastatin in healthy subjects with 5% and 95% confidence predicted interval (grey dashed lines) from Lau et.al., 2007 (top) and Bullman et al., 2011 (bottom)

Table 8**:** Pharmacokinetics of atorvastatin in healthy population: PBPK model predictions vs. published clinical data

	Lau 2007		**Bullman 2011**	
	Cmax (ng.ml)	**AUC (ng.h/ml)**	**Cmax (ng.ml)**	**AUC (ng.h/ml)**
Observed	17.4 ± 8.7	89.0 ± 31.3	14.3	62
Predicted	13.9 ± 10.7	74.4 ± 58.1	12.7 ± 9.9	70.8 ± 53.9
Fold Error (FE)	0.80	0.84	0.89	1.14

Observed- Parameter estimate reported in literature [103,104];
Predicted- Parameter estimate predicted by PBPK model using Simcyp Simulation;
FE- Fold-error- ratio of [predicted]/[observed] values

PBPK modeling of atorvastatin and midazolam in morbidly obese and post RYGB surgery population

Changes in oral drug bioavailability post bariatric surgery were demonstrated for atorvastatin and midazolam following Roux-en-Y gastric bypass [92-93]. Sex, age, height, and weight matched simulations were carried out based on corresponding clinical studies utilizing the post gastric bypass surgery population coupled to a full PBPK distribution model into the Simcyp® Simulator. The results from the comparison of observed versus simulation studies are discussed below

Atorvastatin

In a clinical trial carried out on 12 morbidly obese patients, atorvastatin was administered as an immediate-release (IR) tablet (dose 20-80 mg) in the fasted state where patients were allowed to eat two hours post-administration. The pre- to post-surgical trend in oral exposure in this study displayed high variability where the overall reported trend displayed a median post/pre-surgery AUC ratio of 1.07 (range: 0.59-2.72), albeit being statistically insignificant ($p>0.05$). The median post/pre-surgery AUC ratio was in close agreement to the AUC ratio of 1.12 (range: 0.34 – 2.33) reported by Darwichet al., [80].

Virtual simulations of oral drug exposure of atorvastatin pre- to post-RYGB were conducted in 10 randomized trials, consisting of 12 subjects for 20mg dose, 40mg, and 80mg dose. The demographic data for this aspect of research was summarized in Table 9. Table 10 shows the observed and predicted median AUC of atorvastatin for different doses of 20-80 mg. Figures 11 shows the observed (Darwich et al.,) and simulated post/pre surgery fa and fg ratios of atorvastatin. The model predicted fa and fg are in close agreement to the fa and fg reported by Darwich et al., [80].

Table 9: Study design for Simcyp® simulations of atorvastatin acid in pre and postsurgical population

	20mg	**40mg**	**80mg**
No. of Trials	10	10	10
No of subjects in each Trial	6	4	2
Age of Subjects(years)	29-63	29-63	29-63
% of females	33	100	0
Duration of study (h)	12	12	12
Dosage regimen	20mg single oral dose	40mg single oral dose	80mg single oral dose

Table 10: Observed vs predicted median $AUC_{(0-8)}$ of Atorvastatin acid pre- and post-surgery

Dose	**Median $AUC_{(0-8)}$ (ng.h/ml)**					
	Pre surgery (Morbidly Obese)			**Post-surgery**		
	Observed	**Predicted**	**FE**	**Observed**	**Predicted**	**FE**
20mg	18.5	20.7	1.12	28	25.3	0.9
40mg	100.5	98.3	0.98	64	53.1	0.83
80mg	175	171.96	0.98	84	83.6	0.99

Observed- Parameter estimate reported in literature [93];
Predicted- Parameter estimate predicted by PBPK model using Simcyp Simulation;FE- Fold-error- ratio of [predicted]/[observed] values

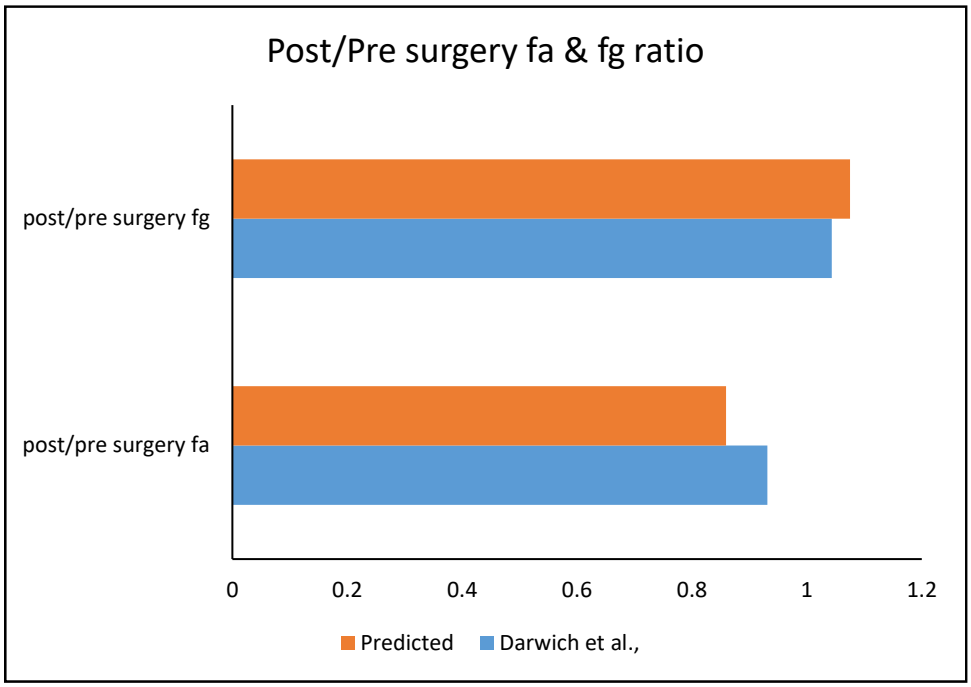

Figure 11: Observed (Darwich et al.,) and predicted post/pre surgery fa (fraction of dose absorbed in the intestine) and fg (fraction escaping gut wall metabolism) ratios

Midazolam

The midazolam compound file, available in the Simcyp® simulator compound library, was adapted to account for changes in oral drug exposure of a 2mg midazolam oral solution post-RYGB surgery. The ADAM model was used to predict the absorption, and a full PBPK model was utilized to describe midazolam distribution. Following RYGB, Chan et al. [92] reported a higher mean peak concentration of midazolam occurring earlier (shorter Tmax) compared to baseline. Plasma concentration profiles were obtained for 12 h after drug administration. Virtual simulations for oral drug exposure of midazolam pre to post RYGB were conducted in 10 randomized trials, consisting of 12 subjects in each trial. The demographic data for this aspect of the research is shown in Table 11.

Table 11: Study design for Simcyp® simulations of midazolam in pre and postsurgical population

	Pre-Surgery	**Post-Surgery**
No. of Trials	10	10
No. of subjects in each trial	12	12
Age of subjects (years)	37 - 55	37 - 55
% of females	75	75
Duration of Study (h)	12	12
Dosing Regimen	2mg oral solution	2mg oral solution

As illustrated in Figures 12 and 13, the predicted systemic concentrations of midazolam over time after administration are well within the 95% confidence interval compared to observed data. Figure 14 compared the simulated plasma concentration profile pre and post RYGB of the 2mg oral solution of midazolam. Table 12 summarizes the observed and predicted pharmacokinetic parameters and calculated fold error pre-and post-surgery. These results show that the model successfully captured the drug behavior in pre and post RYGB surgery population with fold errors for AUC and Cmax ranging from 0.74 to 1.25, which indicates that the model successfully predicted the pharmacokinetic parameters compared to observed data.

The analyses found that the AUC_{0-12} (22 ± 7.8 ng.h/mL) for the postsurgical group was close to that of the morbidly obese group (25 ± 9.5 ng-h/mL), and statistically insignificant ($p > 0.05$). However, the Cmax for the postsurgical group (17.6 ± 4.6 ng/mL) was significantly higher than that for the morbidly obese group (7.2 ± 2.4 ng/mL), and the mean T_{max} was shortened from 0.76 h to 0.21 h. Collectively, these results indicate that a significant increase in absorption rate with no significant change in overall exposure was observed for midazolam post-RYGB surgery.

Table 12: Pharmacokinetic parameters of midazolam 2mg oral solution in pre and postsurgical population: PBPK model predictions vs. published clinical data

	Pre-Surgery (Morbidly Obese)			**Post-surgery**		
	Obs	**Pred**	**FE**	**Obs**	**Pred**	**FE**
Cmax (ng/ml)	9.7 ± 6.8	7.4 ± 2.9	0.74	16.1 ± 6.7	17.6 ± 4.6	1.09
$AUC_{(0\text{-last})}$ (ng.h/ml)	20.8 ± 10.7	25 ± 9.5	1.19	20.3 ± 10.8	22 ± 7.8	1.08
Tmax (h)	0.61 ± 0.22	0.72 ± 0.13	1.25	0.28 ± 0.08	0.21 ± 0.03	0.75

Obs- Parameter estimate reported in literature [92];
Pred- Parameter estimate predicted by PBPK model using Simcyp Simulation;
FE- Fold-error- ratio of [predicted]/[observed] values

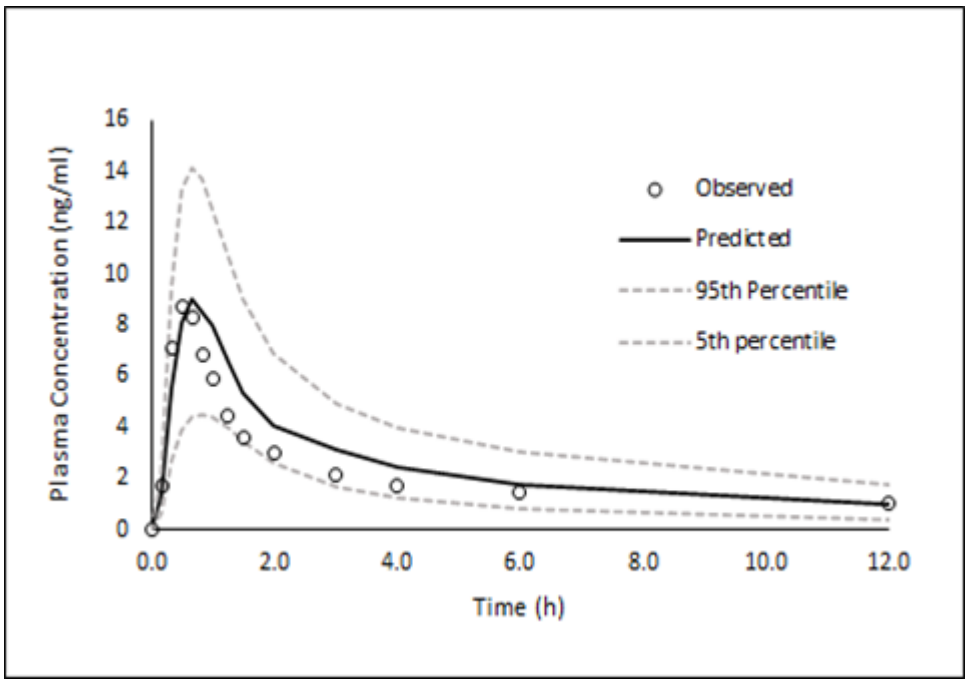

Figure 12: Observed (open circles) and Predicted (solid circles) concentration time profiles of 2mg oral solution of Midazolam in Pre RYGB surgery (Morbidly obese) subjects with 5% and 95% confidence predicted interval (grey dashed lines).

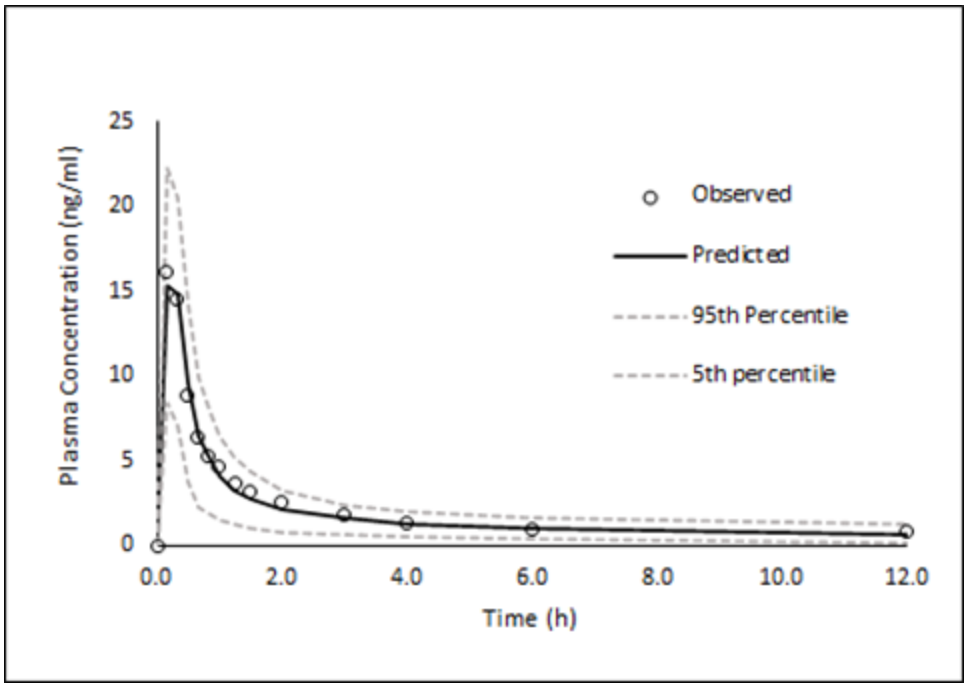

Figure 13: Observed (open circles) and Predicted (solid circles) concentration time profiles of 2mg oral solution of Midazolam in Post RYGB surgery subjects with 5% and 95% confidence predicted interval (grey dashed lines).

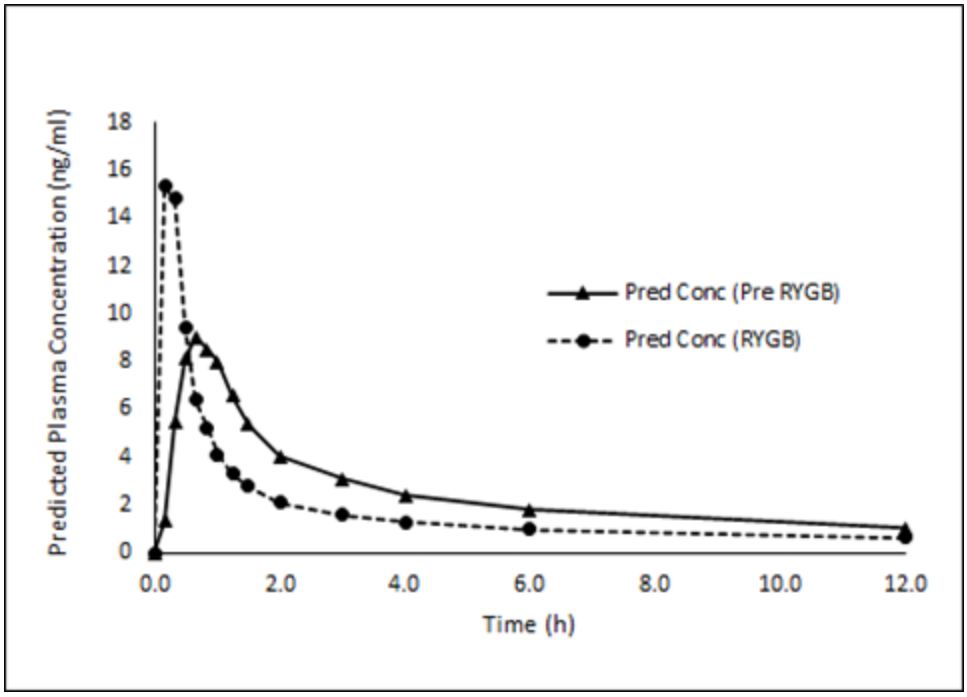

Figure 14: Predicted pre RYGB (solid circles) and post RYGB (solid triangles) concentration time profiles of 2mg oral solution of Midazolam.

Discussion

Because RYGB involves profound alterations to GI anatomy and physiology, it has been suspected that patients undergoing RYGB may be at an increased risk for either adverse reactions or a suboptimal response due to altered pharmacokinetics and pharmacodynamics of orally administered drugs. However, recent studies have shown contrasting results either because of altered bioavailability from decreased absorption or because of rapid transit or decreased first-pass metabolism from bypassing the drug-metabolizing enzymes in the duodenum and proximal jejunum. [105].

Atorvastatin, administered in the acid form, is an HMG-CoA reductase inhibitor with high permeability. Atorvastatin undergoes extensive liver and small intestine metabolism, primarily mediated by CYP3A4, UGT1A1, and UGT1A3. Atorvastatin is a substrate of drug transporters such as P-glycoprotein and OATP1B1 [95]. UGTs play a significant role in the interconversion of atorvastatin acid and the lactone metabolite. The stomach degradation function in Simcyp was used in the atorvastatin model file to illustrate the acid-to-lactone conversion. The plasma peak concentration was considered to be predominantly that of absorbed atorvastatin acid and not that later formed systemically from atorvastatin lactone. Furthermore, as atorvastatin has a low solubility at low pH, for doses of 10 mg or more, the concentration of atorvastatin in the stomach would be greater than the solubility. As only soluble drug would be subject to conversion, it is expected that the gastric conversion of atorvastatin acid to atorvastatin lactone will vary depending on the dose; thus, the less gastric conversion will occur with higher atorvastatin doses. This would result in a non-linear increase in atorvastatin plasma concentration as the dose is increased, as reported in clinical data [96]. Trends in simulated oral drug exposure of atorvastatin pre to post RYGB were consistent with observed data. The area under the

concentration curve (AUC_{0-8} ng.h/ml) ranged from 9 to 315 ng.h/ml vs. 14.4 to 136.3 ng.h/ml pre-surgery (obs vs. pred) and from 17 to 107 ng.h/ml to 17 to 106.6 ng.h/ml post-surgery (obs vs. pred). It was also observed that the interindividual variability in the exposure of atorvastatin was decreased after gastric bypass surgery, which is evident from the decreased coefficient variation of AUC_{0-8} post surgery, i.e., from 121 to 52% vs. 77 to 54% (obs and pred). Bypassing the proximal small intestine reduces the surface area available for absorption. However, because the CYP content is greater in the proximal small intestine [106], bypass of this segment will also cause a relatively large reduction in overall GI, metabolic activity. These two opposing processes may, to different degrees, affect the bioavailability of orally administered drugs, depending on the drug and the individual patient characteristics resulting in high variability of oral drug bioavailability.

Midazolam is a substrate of CYP3A4 with baseline oral bioavailability of ~30%. Therefore, for a CYP3A4 substrate with relatively low oral bioavailability, RYGB appears to increase the rate of absorption, thereby achieving higher peak concentrations. The faster midazolam oral absorption can be explained by faster gastric emptying of stomach due to the reduced size of stomach post-surgery. This increase in peak concentrations could increase the risk of dose-related side effects. It appears that the new RYGB procedure alters the pattern of absorption without significantly changing the overall exposure to the drug. The RYGB procedure bypasses the duodenum and proximal jejunum, leading to a reduction of intestinal CYP3A4-mediated metabolism. The predicted fraction of drug escaping the gut wall metabolism increased from 64% to 82% post-surgery due to decreased gut wall clearance (Clint, G). Due to post-surgical upregulation of hepatic CYP3A4, the intrinsic hepatic clearance increased 1.3-fold in patients post gastric bypass

[107]. Despite the faster rate of absorption of midazolam post gastric bypass surgery, the observed increase in clearance after oral (Cl_{PO}) administration indicated increase in the fraction of drug escaping the intestinal first pass metabolism (fg) which resulted in unaltered bioavailability of midazolam post-surgery. This alteration would result in higher peak concentration after oral administration of midazolam in post-gastric bypass surgery population in comparison to the morbidly obese subjects before surgery. These changes may be of clinical importance. However, the extent and direction of change would depend on the individual patient and the characteristics of the drug administered (e.g., intestinal vs. hepatic first-pass metabolism).

Trends in simulated oral drug exposure of atorvastatin and midazolam pre to post RYGB were consistent with the observed data. The drug exposure of atorvastatin in morbidly obese and post-surgical patients displayed high variability, and higher mean peak concentrations with decreased Tmax were observed for midazolam. However, no significant changes in terms of the extent of absorption were observed for midazolam.

In this aspect of research, the post-surgical population model adopted from the literature was successfully created in Simcyp and verified for two model drugs. Furthermore, PBPK model prediction of systemic exposure in all three populations tested were well within the 95% confidence interval for both atorvastatin and midazolam. Thus, this mechanistic PBPK modeling approach has the potential to serve as a tool in examining the effect of surgical alterations after RYGB on oral bioavailability in the absence of published clinical pharmacokinetic data, thus illustrating the validity of PBPK modeling and simulation in predicting the impact of bariatric surgery on drug exposure.

SPECIFIC AIM 2

Specific Aim 2

Specific aim 2: To develop and verify physiologically based pharmacokinetic model for cefuroxime axetil, metronidazole and azithromycin in healthy volunteers

Introduction

Intra-abdominal infection (IAI) is the second most commonly known source of severe sepsis in the intensive care unit (ICU), a standard disease process managed by surgical practitioners. Despite clinical advancements made over the past decades, it is associated with significant morbidity and death. The definitive treatment for complicated IAI is surgery, but systemic antibiotic therapy is a required addition. One of the main components of managing these infections is adequate antimicrobial therapy directed against the infection's micro-organisms. In this setting, the purpose of antibiotics is to prevent and treat the hematogenous spread of infection and minimize late complications [108].

The Surgical Infection Society (SIS) developed and disseminated guidelines for the management of these infections in 1992, in 2002, and most recently in 2010 as a joint guideline with the Infectious Diseases Society of America (IDSA) [109]. In intra-abdominal infections, cefuroxime is effective against most gram-negative and gram-positive causative aerobes, and metronidazole is effective against anaerobes. Most infections are polymicrobial, with both aerobic and anaerobic bacteria involved.

Community-acquired pneumonia (CAP) is a common condition affecting millions of individuals every year. It is one of the four common infections affecting gastric bypass patients, thereby resulting in a significant increase in number of emergency visits or hospitalizations post-surgery. It is also one of the most prevalent infectious diseases

worldwide that can result in morbidity and mortality. Every year over 5.6 million Americans and 915,900 Americans aged 65 are affected by community-acquired pneumonia (CAP). In the United States, it is the sixth leading cause of death and is responsible for 600,000 hospitalizations of geriatric patients . Many viruses and bacteria cause CAP, but *Streptococcus pneumoniae*, *Haemophilus influenzae* and *Moraxella catarrhalis* remain the bacterial pathogens causing significant morbidity and mortality in adults [110 - 111].

The etiology of CAP has changed over the past few decades: antibiotic-resistant bacteria that were thought to exist only in hospital environments are becoming more prevalent in community environments (*e.g., Staphylococcus aureus*). [112]. Several guideline-recommended clinical alternatives for CAP care are provided by the Infectious Diseases Society of America (IDSA) and the American Thoracic Society (ATS). Although clinical performance or mortality has not been correlated with the selection of agents, the availability of guideline-recommended therapy has been related to improved clinical results. The treatment options for community-acquired pneumonia are shown in Table 13. [113-114].

Table 13: Treatment options for outpatients with Community-acquired pneumoniae [115]

Patient status	**Recommended Antimicrobial Therapy**
No comorbidities or risk factors for MRSA[1] or Pseudomonas aeruginosa	Amoxicillin or doxycycline or macrolide (if local pneumococcal resistance is, 25%)
With comorbidities[2]	Combination therapy with amoxicillin/clavulanate or cephalosporin NAD macrolide or doxycycline or monotherapy with respiratory fluroquinolone

[1]MRSA = methicillin-resistant Staphylococcus aureus.
[2]Comorbidities include chronic heart, lung, liver, or renal disease; diabetes mellitus; alcoholism; malignancy; or asplenia.

Azithromycin is a member of the macrolide class of antibiotics. It is a semi-synthetic erythromycin derivative. Azithromycin is less active than erythromycin against gram-positive bacteria but is significantly more effective against certain gram-negative species. Azithromycin acts by binding to the 50S ribosome subunit and inhibit protein synthesis. Clinically, azithromycin is used for most community-acquired infections, including infections involving the upper and lower respiratory tract, as well as sexually transmitted diseases [116].

Orally administered azithromycin is quickly absorbed and is widely distributed across the body, except to the brain and cerebrospinal fluid. The bioavailability of azithromycin in healthy volunteers is 37% following an oral dose of 500 mg, with a peak serum concentration of 0.4 ug/ml approximately 2-3 h after dosing. Azithromycin also can be administered intravenously, producing plasma concentrations of 3–4 g/ml after a 1-h infusion of 500 mg. As the time to maximum concentration following oral administration is relatively short (1 to 2 h), it is presumed that the dominant site of absorption of azithromycin is in the duodenum, jejunum, or both [117]. Food reduces absorption from capsules but not from tablets or suspensions. Extensive tissue distribution and high drug concentrations within cells (including phagocytes) are the unique pharmacokinetic properties of azithromycin, resulting in significantly higher drug concentrations in tissue or secretions than corresponding serum concentrations [118]. Azithromycin undergoes some hepatic metabolism (demethylation) to inactive metabolites, but biliary excretion is the major route of elimination. Only 12% of the drug is excreted unchanged in the urine. The elimination half-life (t1/2), 40–68 h, is prolonged because of extensive tissue sequestration and binding [119-120].

Cefuroxime is a second-generation cephalosporin antibiotic that has been used to treat various bacterial infections globally for more than three decades. Two forms of cefuroxime are available: cefuroxime sodium (salt) and cefuroxime axetil (ester prodrug). Cefuroxime sodium is suitable for parenteral administration. Cefuroxime axetil (CA) is formulated as an ester prodrug to facilitate its oral absorption by increasing lipophilicity compared to free acid (cefuroxime). CA exhibits enhanced gastric stability due to its higher pKa value [121]. However, CA is primarily absorbed in the proximal region of the GI tract upon oral administration and undergoes rapid hydrolysis to form cefuroxime in the presence of non-specific esterase enzymes in the intestinal mucosa and blood. The ester group is later metabolized to acetic acid and acetaldehyde, which have no inherent activity [122].

Although the ester prodrug (CA) increases lipophilicity of cefuroxime, de-esterification due to esterase enzymes before absorption in the intestinal fluids leads to low permeation across the intestinal mucosa [123]. CA is poorly soluble and exhibits greater bioavailability in the presence of foods rich in lipids due to the lower specificity of esterase enzymes in the intestine toward CA [124]. Cefuroxime axetil is available in tablet form and suspension. Plasma protein binding has been reported as 33-50% with a small volume of distribution of 0.25 to 0.3 L/kg. Peak plasma concentrations are reached 3-3.5 hours after oral administration. The reported elimination half-life of cefuroxime axetil is 1.2-1.9 hours. Cefuroxime is eliminated mainly by the kidney, in an active unchanged form, by glomerular filtration and tubular secretion, and very little of the drug is excreted via the bile [125].

Metronidazole, the antimicrobial prototype of nitroimidazole, is also used to treat anaerobic infections. Metronidazole has remained a reliable medication for the treatment of most anaerobic/microaerophilic infections over many years, thereby setting it apart from most other antimicrobials to which resistance grows much faster [126]. Orally administered metronidazole is almost fully absorbed, with a bioavailability > 90 percent for tablets; absorption is unaffected by infection. After a single dose of 500 mg, the peak plasma drug concentration (Cmax) is approximately 8 to 13 mg/L, with a Tmax of 0.25 to 4h [127]. Oral administration of benzoyl metronidazole suspension formulations, equivalent to 400 mg and 2 g single doses of metronidazole to healthy males, yielded mean serum peak metronidazole concentrations of 4.6 mg/L (400 mg dose) and 17 mg/L (2 g dose) with mean Tmax values of 3.2 to 5.1 h. This formulation has a 20 percent lower bioavailability and produces a lower Cmax (~ 45% lower) than metronidazole [128].

Metronidazole has low protein binding (<20 percent) and is widely distributed. In adults, with a steady-state volume of distribution is 0.51 to 1.1 L/kg. The liver extensively metabolizes metronidazole to five metabolites. Metronidazole and its metabolites are primarily eliminated in urine and feces, with only 12% excreted unchanged in the urine. The total clearance (CL) of metronidazole from serum has been reported to range from 2.1 to 6.4 L/h/kg bodyweight. The elimination half-life for metronidazole ranges from 6 to 10 h, with most studies reporting values in the 8 h range [129].

This aspect of the dissertation research aims to develop and validate the PBPK models for three probe drugs, azithromycin, cefuroxime axetil, and metronidazole, in healthy volunteers.

Modeling Strategy

Development of PBPK model of azithromycin in healthy subjects

The substrate profile of azithromycin was created using Simcyp simulator version 19 by incorporating all the physicochemical properties and parameters relating to absorption, distribution, metabolism, elimination, and transport [130-136]. All the input parameters for azithromycin substrate profile were obtained from literature and summarized in Table 14. The ADAM model was used to predict the oral absorption of azithromycin. The blood to plasma ratio was assumed to be 1. The intrinsic solubility was predicted using the Simcyp Prediction Toolbox based on melting point (˚C), log P, and molecular weight. The whole body (Full) PBPK model was chosen, and steady-state volume of distribution (Vss) of azithromycin was estimated by the Rodger's estimation method (Method 2) available in software. Simcyp's retrograde model was used to calculate the biliary clearance of azithromycin as biliary excretion is the major route of elimination. Estimates of renal clearance and P-gp mediated transporter kinetics were obtained from the literature.

The developed azithromycin substrate profile using the listed parameters (Table 14) was then used to simulate the plasma concentration profile after IV and oral administration in a healthy volunteer population, which is provided in the in the Simcyp population library. A virtual clinical trial with a population size of 80 (10 trials of 8 male subjects), aged between 18 and 43 years, was carried out with IV infusion of 1g and 2g administered over 2 hours under fasting conditions. The simulated plasma concentration profile was compared against published clinical data [134] digitized using WebPlotDigitizer (https://automeris.io/WebPlotDigitizer/). C_{max} and AUC and visual predictive checks were

performed. Fold error was calculated as a ratio of predicted to the observed value of each pharmacokinetic parameter. Once the model was verified IV administration, verification was continued for oral administration of azithromycin.

Table 14: Input parameters to create substrate profile for azithromycin in Simcyp®

Parameter		Reference
Physicochemical Properties:		
Molecular weight	749.12 g/mol	[130]
Log P	4.02	[130]
pKa	8.5	[130]
Blood/plasma ratio	1	Assumed
Fraction unbound in plasma	0.69 (Bound to Alpha-1 acid glycoprotein)	[131]
Absorption:		
Absorption Model	ADAM	
P_{eff}Caco-2 (pH 6.4:7.5) (10-6 cm/s)	3.59	[132]
Dissolution:		
Intrinsic Solubility ((mg/ml)	0.029	Predicted
Melting Point (˚C)	114.76 ± 0.095	[133]
Distribution:		
Distribution Model	Full PBPK model	
Prediction Method	Method 2 (Rodgers et al.,)	
Metabolism/Elimination:		
Clearance Type	Enzyme Kinetics	
Biliary Intrinsic clearance ($\mu l/min/10^6$)	9.25 Calculated using Simcyp's retrograde method, using the IV and renal clearance	
Cl_{IV} (L/h)	46.5	[134]
Cl_R (L/h)	8.67	[135]

Transport: P-gp (Apical efflux, small intestine) Jmax (nmol/min) Km (μM)	 9.07 11.3	 [136]

log P, log octano 1-water partition coefficient; pKa, acid dissociation constant; ADAM , advanced dissolution absorption and metabolism ; Peff, effective human jejunal permeability; $Cl_{IV,}$ IV clearance; CLr, renal clearance

A virtual clinical trial with a population size of 120 (10 trials of 12 subjects), 8 males and 4 females, aged between 22 and 39 years, under fed condition, was carried out with a single 500mg dose of azithromycin. Another virtual trial with a population size of 120 (10 trials of 12 subjects), 6 males and 6 females, aged between 30 and 45 years, under fasting conditions, was carried out with a 3-day regimen (500mg Once daily for 3 days) and 5-day regimen (500mg on day1, 250mg from day 2 to 5). Finally, a virtual clinical trial with a population size of 240 (10 trials with 24 male subjects), aged between 21 and 31 years, under fasting condition was carried out with a single dose of 500mg azithromycin suspension. The simulated plasma concentration profile was compared against published clinical data [137-139] digitized using WebPlotDigitizer (https://automeris.io/WebPlotDigitizer/). Fold error calculation of pharmacokinetic parameters Cmax and AUC and visual predictive checks were performed. Demographic data for the reference clinical studies for the IV, solid oral, and oral suspension formulations are summarized in Table 15.

Table 15: Study design for azithromycin Simcyp® simulations in healthy population

	IV Dose		Oral Tablet			Oral Suspension
	1g	**2g**	**500mg**	**3-Day Regimen**	**5-Day Regimen**	
No. of Trials	10	10	10	10	10	10
No of subjects in each Trial	8	8	12	12	12	24
Age of Subjects(years)	18-43	18-43	22-39	30-45	30-45	21-31
% of females	0	0	33	50	50	0
Duration of study (h)	240	240	96	288	288	72
Dosage regimen	1mg IV inf for 2h	2mg IV Inf for 2h	500mg single dose	500mg once daily for 3 days	500mg day 1, 250mg day 2-5	500mg Single dose

Development of PBPK model of cefuroxime axetil in healthy subjects

A substrate profile of prodrug cefuroxime axetil (CA) and its active form cefuroxime was built using Simcyp simulator version 19. Physicochemical properties and properties relating to absorption, distribution, metabolism, elimination, transport was obtained from the literature [140-147] [Table 16]. The ADAM model was used to predict the absorption of cefuroxime axetil. The whole body (Full) PBPK model was chosen and the steady-state volume of distribution (Vss) of CA was predicted by the Rodger's estimation method (Method 2) available in software. Cefuroxime axetil is hydrolyzed by non-specific esterases in the intestinal cells. To account for the formation of active drug (cefuroxime) in the intestine, intestinal esterase CES 2 mediated hydrolysis was incorporated in the model and the kinetic parameters were obtained from the literature. PEPT-1 mediated uptake kinetic parameters obtained from the literature were also incorporated in the model.

Table 16: Input parameters to create substrate profile for Cefuroxime axetil in Simcyp®

Parameter	Cefuroxime Axetil	Cefuroxime
Physicochemical Properties:		
Molecular weight	540.48 g/mol [140]	424.4 [146]
Log P	0.55 [140]	-0.75 [146]
pKa	10.52 [140]	3.15 [146]
Blood/plasma ratio	0.55 [140]	0.55 [Fitted]
Fraction unbound in plasma	0.33 [140]	0.7 [146]
Absorption:		
Absorption Model	ADAM	ADAM
P_{eff}Caco-2 (pH 6.4:7.5) (10-6 cm/s)	3.6 [141]	1.7 [141]
Dissolution:		
Solubility ((mg/ml) @pH 6.8	2.49 [142]	NA
Distribution:		
Distribution Model	Full PBPK model	Full PBPK model
Prediction Method	Method 2 (Rodgers et al.,)	Method 2 (Rodgers et al.,)
Metabolism/Elimination:		
Clearance Type	Enzyme Kinetics [143]	
Intestinal Esterases (CES2)		
Vmax (pmol/min)	500	
Km (µM)	31.5	
Cl_R (L/h)	10.62 [144]	12.25 [144]
Transport:		
PEPT-1 (Uptake, small intestine)		
Jmax (pmol/min)	40	
Km (µM)	7 [145]	NA
MRP4	NA	
Vmax (Pmol/min)		14.4
Km (µM)		248 [147]

log P, log octano 1-water partition coefficient; pKa, acid dissociation constant; ADAM , advanced dissolution absorption and metabolism ; Peff, effective human jejunal permeability; $Cl_{IV,}$ IV clearance; CLr, renal clearance.

The PBPK model of cefuroxime axetil and the active drug cefuroxime was verified against the clinical data obtained from literature in a healthy population, in-built in the Simcyp population library. Sex, age, weight, and subject number-matched simulations were performed corresponding to the identified clinical trials. A virtual clinical trial with a population size of 120 (10 trials of 12 subjects), 7 males and 5 females, aged between 18 and 45 years, under fasting conditions were carried out for 500 mg single oral dose of cefuroxime axetil. A second virtual trial with a population size of 240 (10 trials with 24 male subjects), aged between 19 and 38 years, under fed conditions were carried out for 250mg oral tablet and suspension twice daily for 5 days.

The simulated plasma concentration profile was compared against published clinical data [148-149] digitized using WebPlotDigitizer (https://automeris.io/WebPlotDigitizer/). In addition, fold error calculation of pharmacokinetic parameters Cmax and AUC and visual predictive checks were performed. Demographic data for the reference clinical studies for oral tablet and oral suspension formulations are summarized in Table 17.

Table 17: Study design for cefuroxime axetil Simcyp® simulations in healthy population

	500mg QD Tab	**250mg BID Tab**	**250mg BID Suspension**
No. of Trials	10	10	10
No of subjects in each Trial	12	24	24
Age of Subjects(years)	18-45	19-38	19-38
% of females	42	0	0
Duration of study (h)	24	96	96
Dosage regimen	500mg Single dose	250mg Twice daily	250mg Twice daily

Development of PBPK model of metronidazole in healthy subjects

A substrate profile of metronidazole was built in Simcyp simulator version 19. The developed PBPK model was then verified by comparing the predicted plasma concentration profile in a healthy population against the published clinical data. The physicochemical properties and parameters related to absorption, distribution, metabolism, and elimination were obtained from the literature [150-155]. The ADAM model was used to predict the absorption of metronidazole. The whole body (Full) PBPK model was chosen and the steady-state volume of distribution (Vss) of metronidazole was predicted by the Rodger's estimation method (Method 2) available in software. Simcyp's retrograde model was used to calculate the intrinsic hepatic clearance of metronidazole. Metronidazole is a substrate of CYP2A6, 2E1. 3A4 and also undergoes glucuronidation. The hepatic metabolism of metronidazole was attributed to these isoforms and UGT. Oral clearance and fraction of drug excreted unchanged in urine were obtained from the literature. 30-40% of active re-absorption through enterohepatic recirculation was implemented in the model. The input parameters for the metronidazole substrate profile were summarized in Table 18.

Table 18: Input parameters to create substrate profile for metronidazole in Simcyp®

Parameter		Reference
Physicochemical Properties:		
Molecular weight	171.16 g/mol	[150]
Log P	0.75	[150]
pKa	2.62	[150]
Blood/plasma ratio	1	[151]
Fraction unbound in plasma	0.9	[151]
Absorption:		
Absorption Model	ADAM	
P_{eff} (10^{-4} cm/s)	3.96	[150]
Dissolution:		
Solubility (mg/ml) @pH 6.8	13	[150]
Distribution:		
Distribution Model	Full PBPK model	
Prediction Method	Method 2 (Rodgers et al.,)	
Metabolism/Elimination:	Intrinsic hepatic clearance was calculated using the Simcyp retrograde model	[152,153]
Clearance Type	Enzyme Kinetics	
CYP3A4	fm – 0.27	
CYP2A6	fm - 0.25	
CYP2E1	fm - 0.24	
UGT1A1	fm - 0.1	[154]
Enterohepatic recirculation	30-40%	[155]
Cl_R (L/h)	0.45	

log P, log octano 1-water partition coefficient; pKa, acid dissociation constant; ADAM, advanced dissolution absorption and metabolism; Peff, effective human jejunal permeability; $Cl_{IV,}$ IV clearance; CLr, renal clearance.

The developed PBPK model of metronidazole was verified against the clinical data obtained from published studies after administration of intravenous, oral tablet, and oral suspension formulations to healthy subjects. A healthy population in-built in the Simcyp library was used for verification of the model. In addition, sex, age, and number-matched simulations were performed corresponding to the identified clinical trials.

In trial #1, for verification of IV plasma concentration profile after 500mg Q8H and 1500mg QD, a virtual trial with a population size of 180 (10 trials with 18 male subjects), aged 18 to 40 years, under fasting conditions were carried out. In trial #2, for verification of the systemic profile after oral administration of a tablet formulation, one virtual trial with a population size of 90 (10 trials with 9 subjects), 8 males and 1 female, aged 21 to 23 years, under fasting conditions was carried out for a single dose of 500mg and second virtual trial with a population size of 100 (10 trials with 10 male subjects), aged 23 to 35 years, under fasting conditions were carried out for 400mg single dose of metronidazole. In trial # 3, for verification of oral suspension formulation plasma profile, a virtual trial with a population size of 240 (10 trials with 24 male subjects) aged between 18 and 60 years, under fasting conditions were carried out for a single dose equivalent to 500mg of metronidazole.

The simulated plasma concentration profile was compared against published clinical data [156-159] digitized using WebPlotDigitizer (https://automeris.io/WebPlotDigitizer/). In addition, fold error calculation of pharmacokinetic parameters Cmax and AUC and visual predictive checks were performed. Demographic data for the reference clinical trials for IV, oral tablet, and oral suspension formulations are summarized in Table 19.

Table 19: Study design for metronidazole Simcyp® simulations in healthy population

	IV Dose		Oral Tablet		Oral Suspension
	500mg Q8H	**1500mg QD**	**500mg**	**400mg**	**500mg**
No. of Trials	10	10	10	10	10
No of subjects in each Trial	18	18	9	10	24
Age of Subjects(years)	18-40	18-40	21-23	23-35	18-60
% of females	0	0	12	0	0
Duration of study (h)	74	74	24	48	36
Dosage regimen	500mg IV inf for 1h Q8H	1500mg IV Inf for 1h	500mg single dose	400mg single dose	500mg Single dose

Results

PBPK modeling of azithromycin in healthy volunteer population

The accuracy of the developed PBPK model of azithromycin was evaluated by comparing the simulated plasma concentration profile against the published clinical data. As illustrated in Figures 15 to 19, the predicted values are within the 95% confidence interval compared to published data. In addition, Table 20 reports the observed and predicted pharmacokinetic parameters along with the calculated fold error in a healthy volunteer population. These results show that the model successfully captured the drug behavior in healthy subjects with fold errors for AUC and Cmax ranging from 0.85 to 1.03, which indicates that the model successfully predicted the pharmacokinetic parameters compared to observed data.

a)

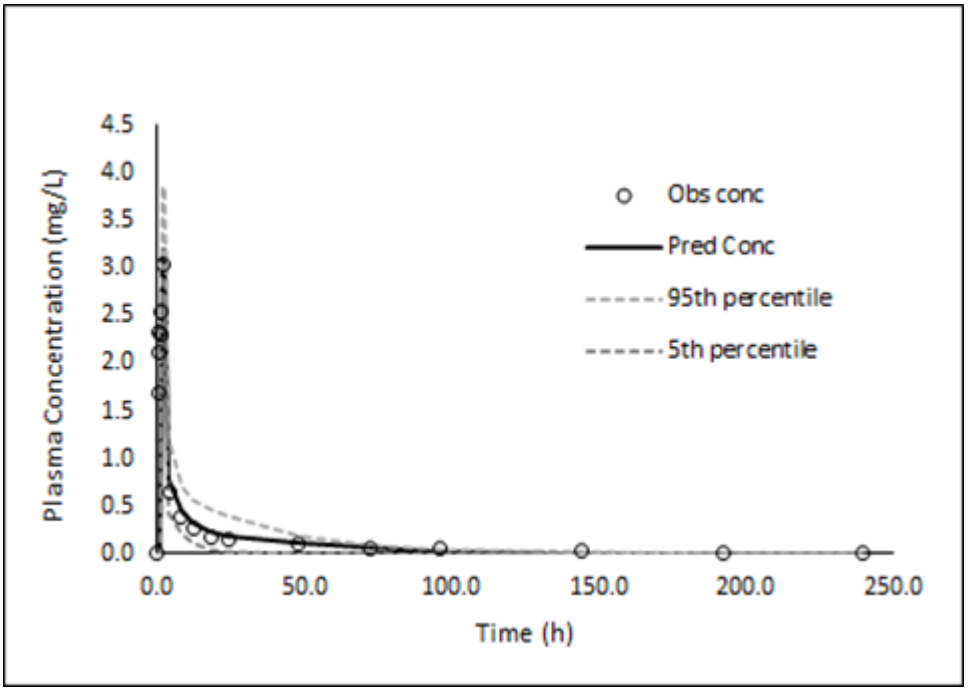
Plasma Concentration (mg/L)
4.5
4.0
3.5
3.0
2.5
2.0
1.5
1.0
0.5
0.0
0.0
50.0
100.0
150.0
200.0
250.0
Time (h)
Obs conc
Pred Conc
95th percentile
5th percentile

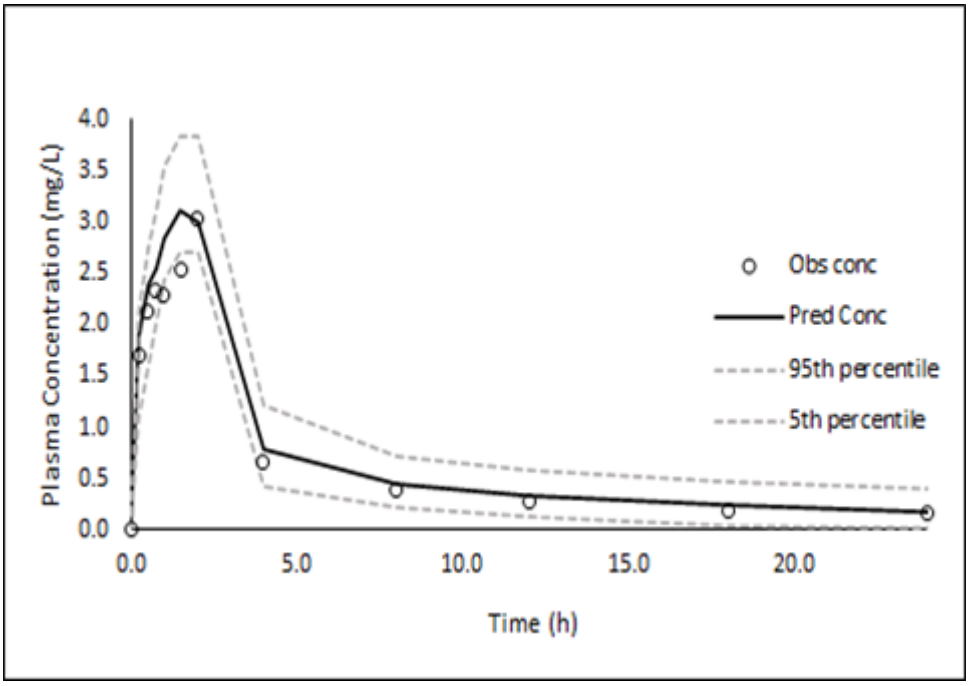
Plasma Concentration (mg/L)
4.0
3.5
3.0
2.5
2.0
1.5
1.0
0.5
0.0
0.0
5.0
10.0
15.0
20.0
Time (h)
Obs conc
Pred Conc
95th percentile
5th percentile

b)

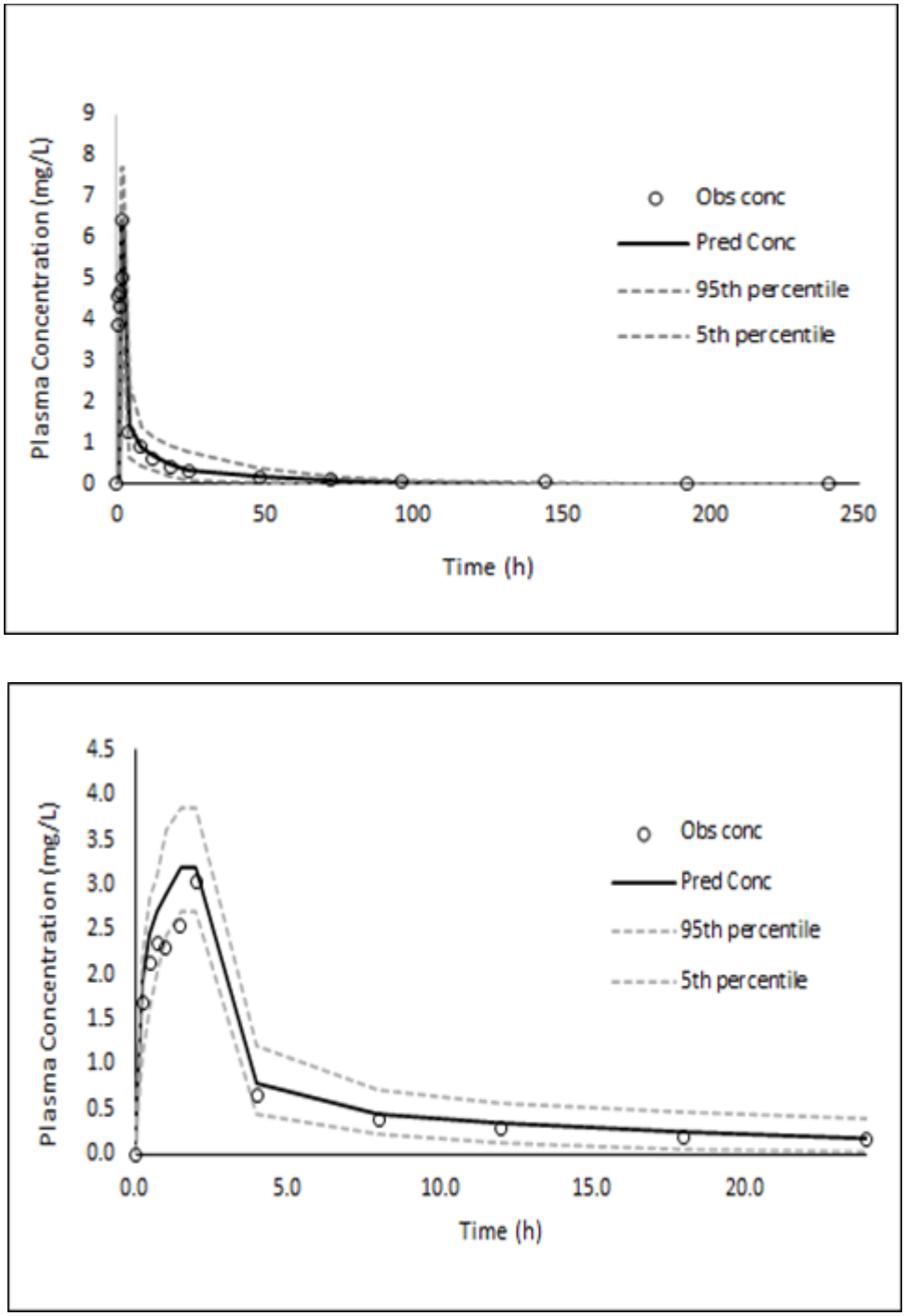

Figure 15: Observed (Open circles) and predicted (solid line) concentration time profiles of azithromycin a) 1g 240hr (top), 24hr blowup (bottom), b) 2g 240hr (top), 24hr blowup (bottom) IV infusion in healthy subjects with 5% and 95% confidence predicted interval (grey dashed lines) from Luke et.al., 1996

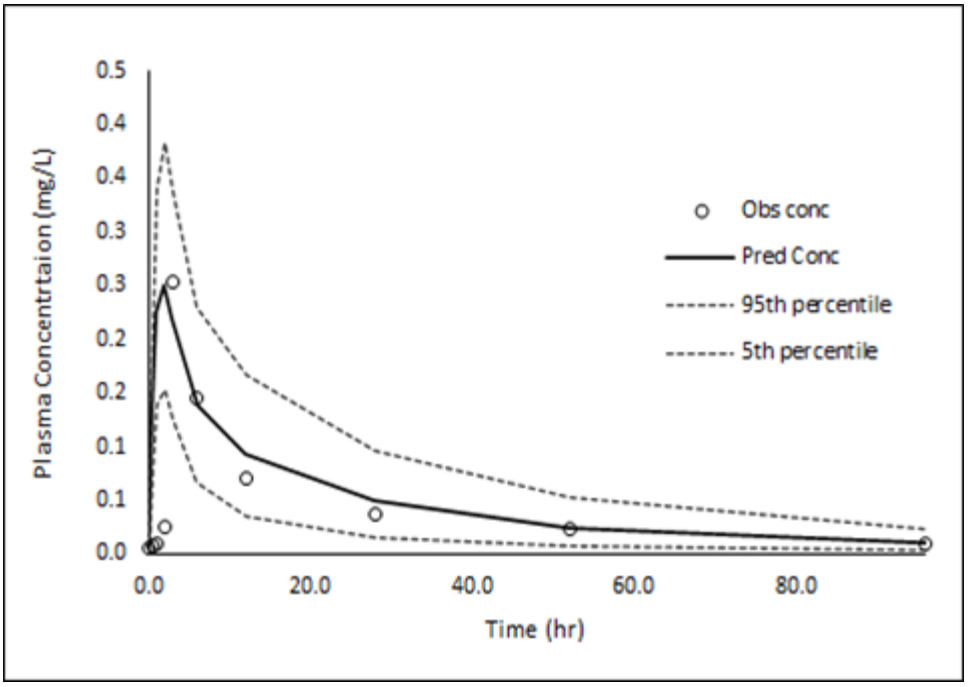

Figure 16: Observed (Open circles) and predicted (solid line) concentration time profiles of 500mg single oral dose of azithromycin in healthy subjects with 5% and 95% confidence predicted interval (grey dashed lines) from Beringer et.al., 2005

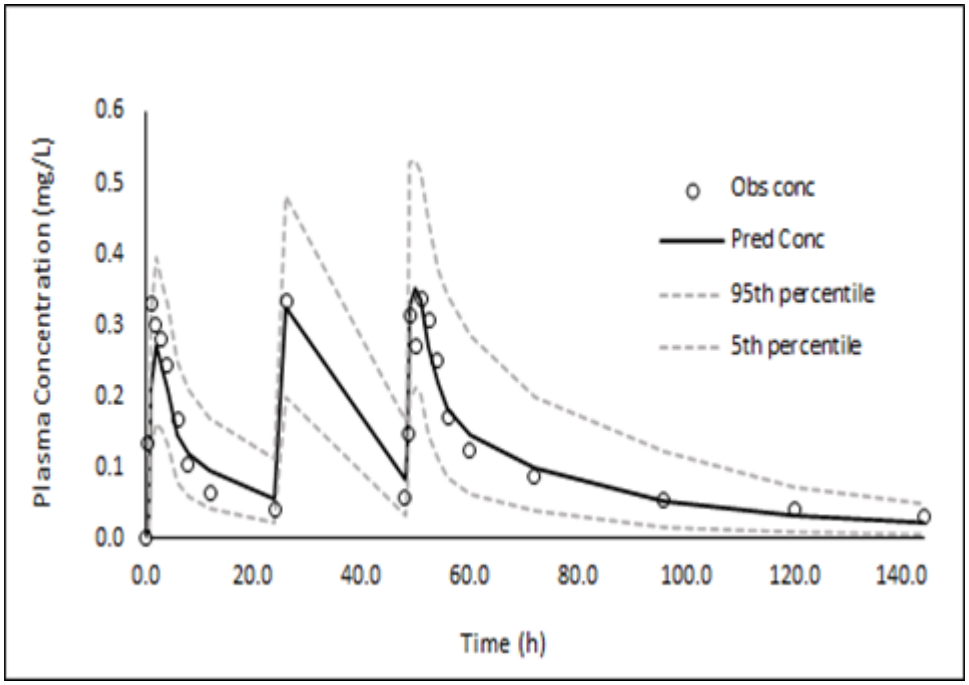

Figure 17: Observed (Open circles) and predicted (solid line) concentration time profiles of 500mg QD dose of azithromycin (3-day regimen) in healthy subjects with 5% and 95% confidence predicted interval (grey dashed lines) from Amsden et.al., 1999

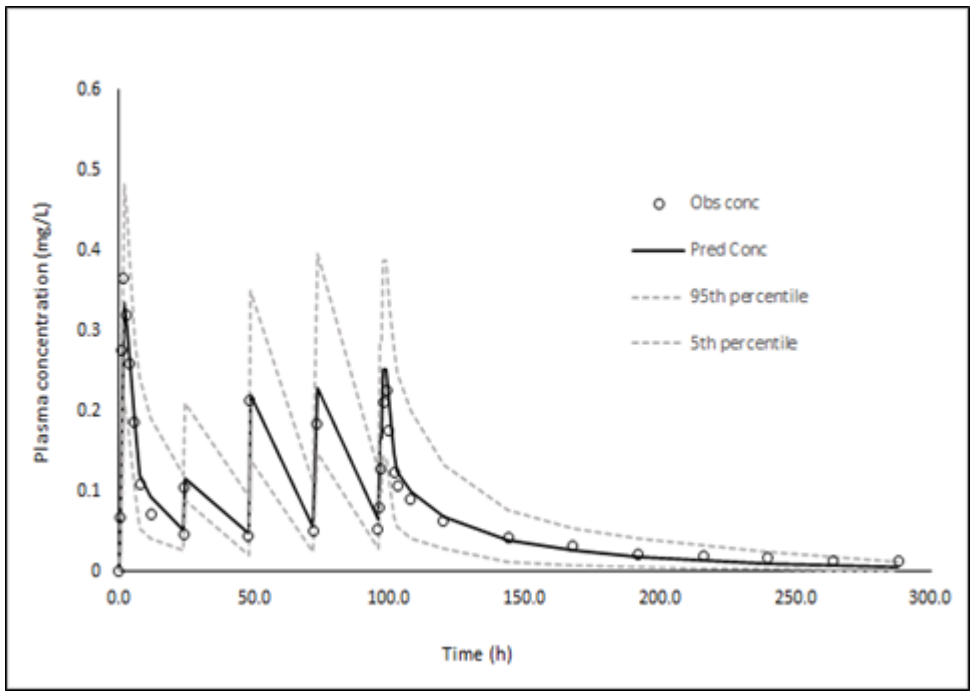

Figure 18: Observed (Open circles) and predicted (solid line) concentration time profiles of 5-day regimen (every 24 hr dosing) of azithromycin in healthy subjects with 5% and 95% confidence predicted interval (grey dashed lines) from Amsden et.al., 1999

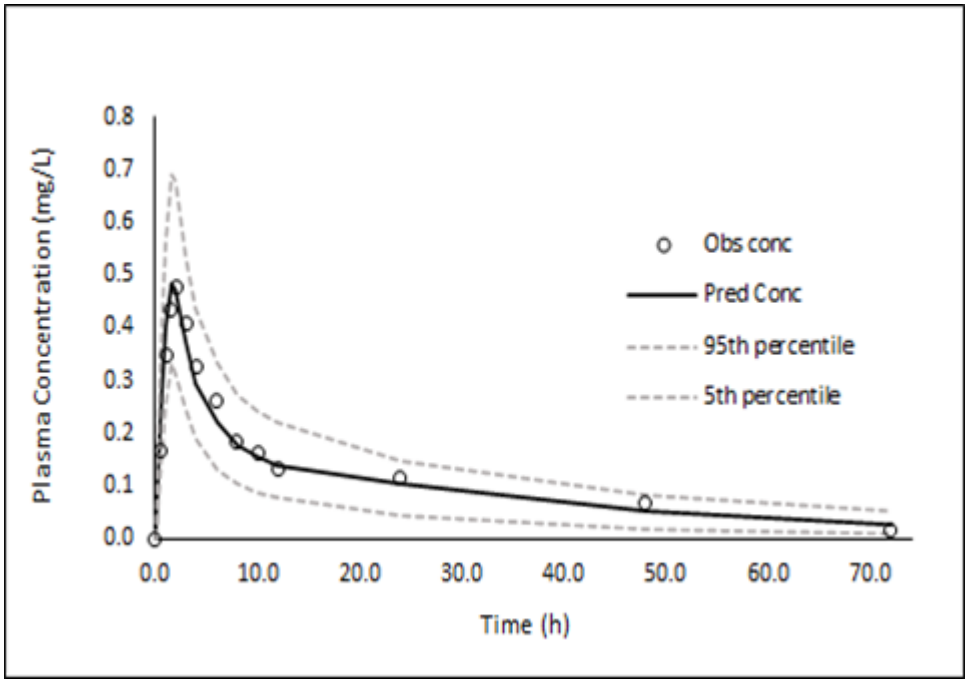

Figure 19: Observed (Open circles) and predicted (solid line) concentration time profiles of 500mg single oral dose of azithromycin Suspension in healthy subjects with 5% and 95% confidence predicted interval (grey dashed lines) from Zakeri et.al., 2010

Table 20: Pharmacokinetics of azithromycin in healthy population: PBPK model predictions vs. published clinical data

Azithromycin Dose	**Parameter**	**Observed (Mean ± SD)**	**Predicted (Mean ± SD)**	**Fold Error**
1g IV Infusion for 2h	Cmax (mg/L)	3.1 ± 0.4	3.2 ± 0.4	1.03
	AUC (mg.h/L)	23 ± 4	23.3 ± 4.9	1.01
2g IV Infusion for 2h	Cmax (mg/L)	6.9 ± 2.0	6.4 ± 0.8	0.94
	AUC (mg.h/L)	46 ± 9	46.5± 9.8	1.01
500mg single oral tablet	Cmax (mg/L)	0.30 ± 0.34	0.26 ± 0.07	0.86
	AUC (mg.h/L)	4.4 ± 1.9	4.4 ± 1.8	1.01
3-day regimen (500mg for 3 days)	AUC (mg.h/L)	19.4 ± 7.9	17.2 ± 3.5	0.89
5-day regimen (500mg day 1, 250mg day 2-5)	AUC (mg.h/L)	15.9 ± 4.8	14.5 ± 3.1	0.91
500mg suspension single dose	Cmax (mg/L)	0.49 ± 0.13	0.49 ± 0.11	1.01
	AUC (mg.h/ml)	7.57± 2.63	6.45 ± 2.11	0.85

Observed- Parameter estimate reported in literature [134, 137-139];
Predicted- Parameter estimate predicted by PBPK model using Simcyp Simulation;FE- Fold-error- ratio of [predicted]/[observed] values

PBPK modeling of cefuroxime after oral cefuroxime axetil in healthy population

The model predicted plasma concentration profiles of cefuroxime axetil after an oral administration of a tablet formulation (500mg single dose and 250mg twice daily) and an oral suspension (500mg single dose) in healthy subjects were compared to clinically observed data. As demonstrated in Figures 20-22, PBPK simulations were in close agreement with the observed values. Table 21 presents the observed and predicted pharmacokinetic parameters and calculated fold error for healthy populations. The calculated fold errors for AUC and Cmax ranging from 0.84 to 1.36, indicating that the model successfully predicted the pharmacokinetic parameters compared to observed data.

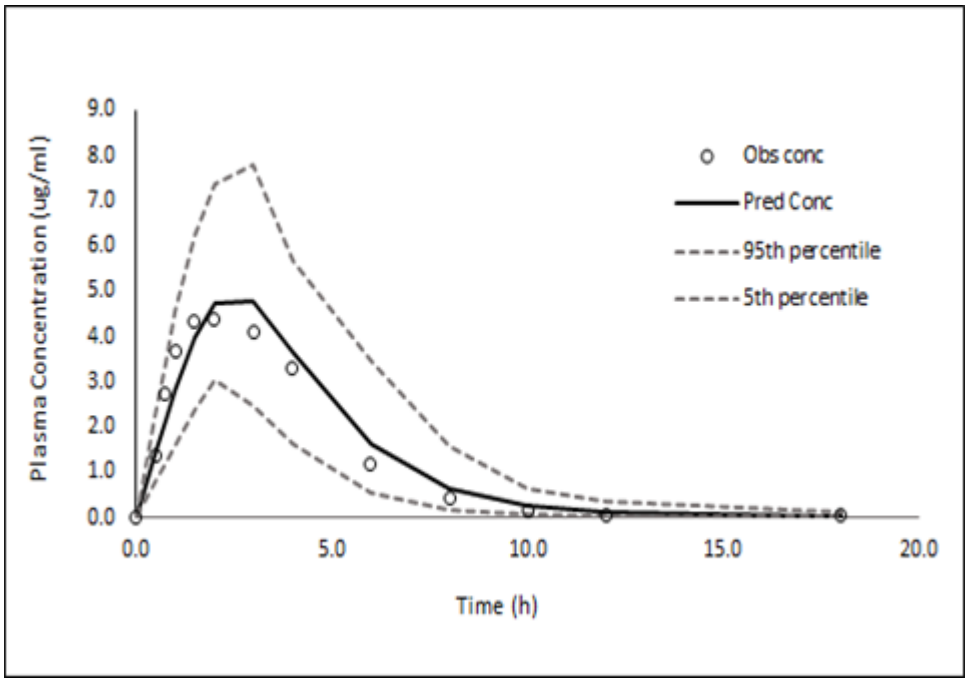

Figure 20: Observed (Open circles) and predicted (solid line) concentration time profiles of cefuroxime following 500mg single oral dose of cefuroxime axetil in healthy subjects with 5% and 95% confidence predicted interval (grey dashed lines) from Nix et.al., 1997

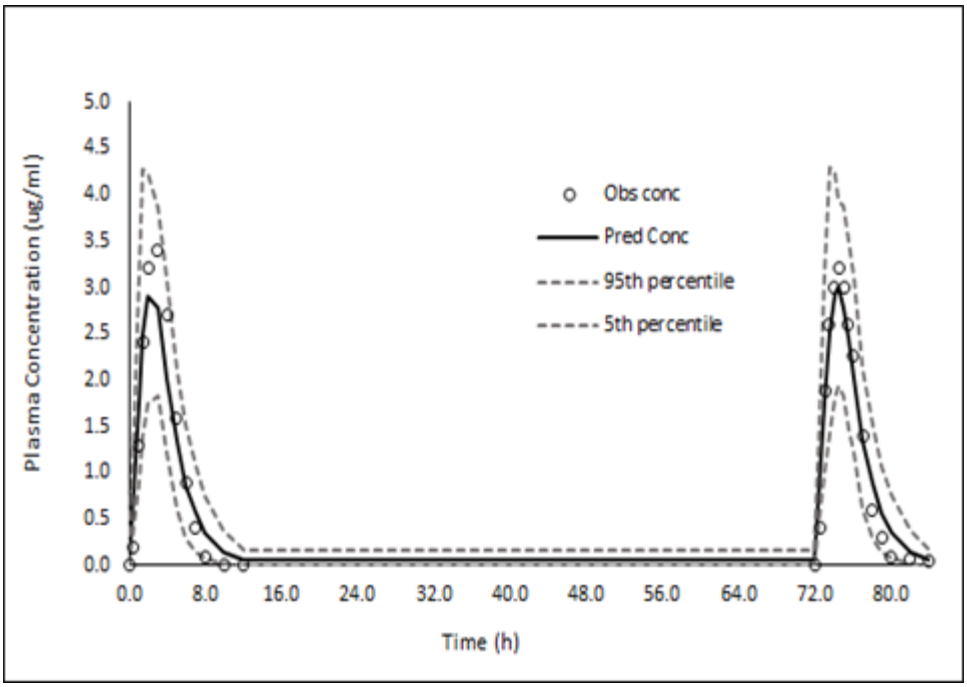

Figure 21: Observed (Open circles) and predicted (solid line) concentration time profiles of cefuroxime following 250mg twice daily oral dose of cefuroxime axetil in healthy subjects with 5% and 95% confidence predicted interval (grey dashed lines) from Donn et.al., 1994

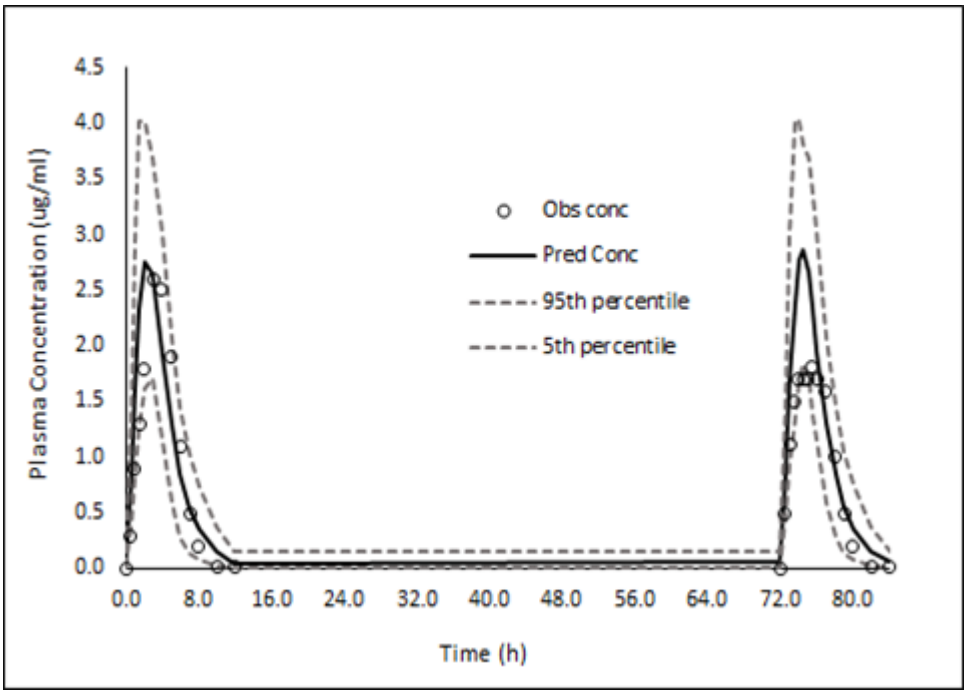

Figure 22: Observed (Open circles) and predicted (solid line) concentration time profiles of cefuroxime following 250mg twice daily oral dose of cefuroxime axetil suspension in healthy subjects with 5% and 95% confidence predicted interval (grey dashed lines) from Donn et.al., 1994

Table 21: Pharmacokinetics of Cefuroxime after oral Cefuroxime axetil in healthy population: PBPK model predictions vs. published clinical data

Dose	Parameter	Observed(Mean ± SD)	Predicted (Mean ± SD)	Fold Error
500mg single oral dose	Cmax (µg/ml)	5.3 ± 19.6	5.5 ± 1.7	1.04
	AUC (µg.h/ml)	19.6 ± 27.6	23.3 ± 6.0	1.19
250mg BID	Cmax (µg/ml)	3.8 ± 0.9	3.2 ± 0.7	0.84
	AUC (µg.h/ml)	12.7 ± 2.0	12.7 ± 2.7	1.00
250mg BID suspension	Cmax (µg/ml)	2.2 ± 0.4	3.0 ± 0.75	1.36
	AUC (µg.h/ml)	11.3 ± 1.9	12.1 ± 2.7	1.08

Observed- Parameter estimate reported in literature [148-149];
Predicted- Parameter estimate predicted by PBPK model using Simcyp Simulation;FE- Fold-error- ratio of [predicted]/[observed] values

PBPK modeling of metronidazole in healthy population

The performance of the PBPK model for metronidazole was assessed by comparing the predicted plasma profile against the clinical data. As illustrated in Figures 23 – 27, the metronidazole model captured the drug behavior in healthy subjects. The predicted plasma profiles are within the 95% confidence interval in comparison to the observed plasma profile. Table 22 compares the observed and predicted pharmacokinetic parameters (Cmax, AUC). The fold errors for these parameters ranged from 0.81 to 1.16, indicating that the model successfully predicted the pharmacokinetic parameters compared to observed.

Table 22: Pharmacokinetics of metronidazole in healthy population: PBPK model predictions vs. published clinical data

Metronidazole Dose	**Parameter**	**Observed (Mean ± SD)**	**Predicted (Mean ± SD)**	**Fold Error**
500mg IV Inf for 1h Q8H	Cmax (µg/ml)	22.2 ± 5.0	21.6 ± 7.0	0.97
	AUC (µg.h/ml)	356 ± 68	372.5 ± 8.0	1.05
1500mg IV Inf for 1h	Cmax (µg/ml)	37.7 ± 10.0	39.8 ± 7.1	1.06
	AUC (µg.h/ml)	338 ± 105	393.4 ± 5.2	1.16
500mg single oral tablet	Cmax (µg/ml)	9.0 ± 0.5	8.8 ± 1.4	0.98
	AUC (µg.h/ml)	122.2 ± 10.3	115.1 ± 46.6	0.94
400mg single oral tablet	Cmax (µg/ml)	8.5 ± 2.3	6.9 ± 1.1	0.81
	AUC (µg.h/ml)	82 ± 17	88.6 ± 37.6	1.08
500mg suspension single dose	Cmax (µg/ml)	6.1 ± 1.5	6.0 ± 1.6	0.99
	AUC (µg.h/ml)	101.1 ± 23.9	91.0 ± 40.4	0.90

Observed- Parameter estimate reported in literature [156-159];
Predicted- Parameter estimate predicted by PBPK model using Simcyp Simulation;FE- Fold-error- ratio of [predicted]/[observed] values

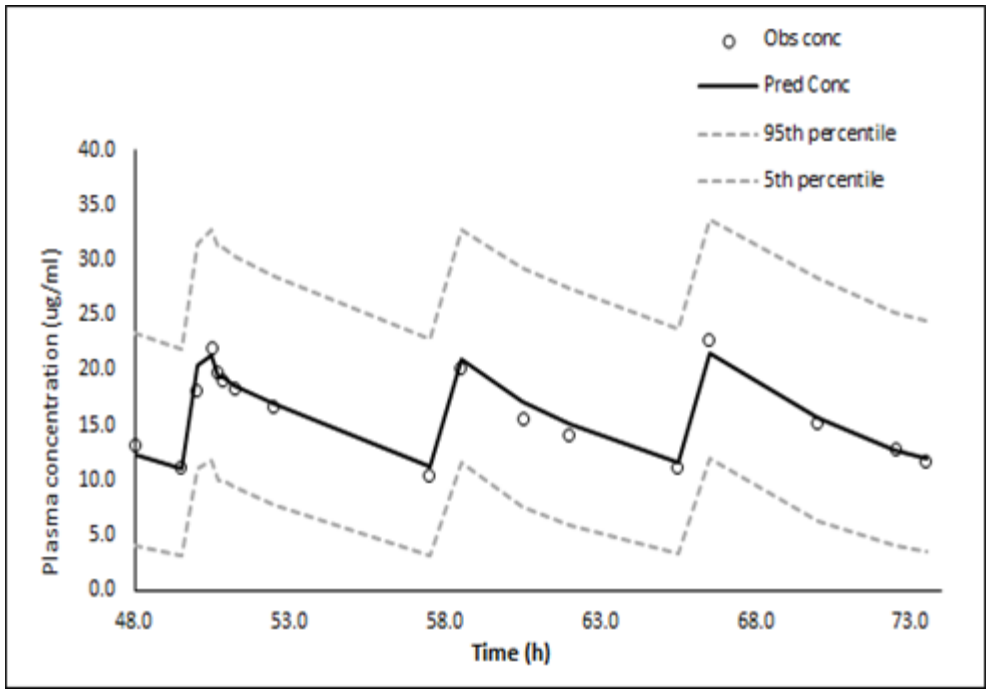

Figure 23: Observed (Open circles) and predicted (solid line) concentration time profiles of metronidazole 500mg IV infusion Q8H in healthy subjects with 5% and 95% confidence predicted interval (grey dashed lines) from Sprandel et.al., 2004

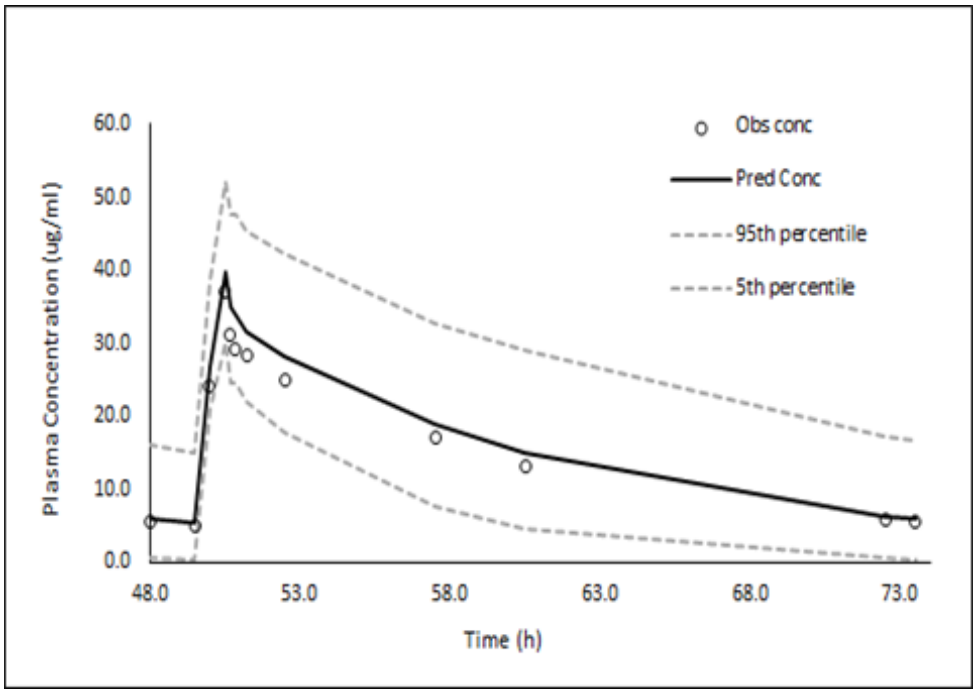

Figure 24: Observed (Open circles) and predicted (solid line) concentration time profiles of metronidazole 1500mg IV infusion QD in healthy subjects with 5% and 95% confidence predicted interval (grey dashed lines) from Sprandel et.al., 2004

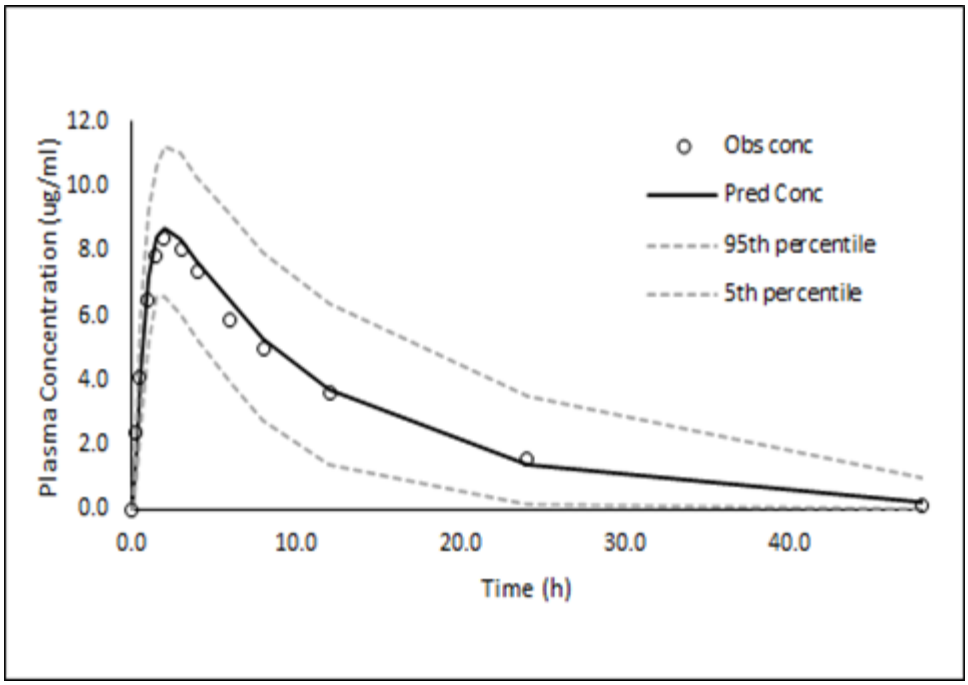

Figure 25: Observed (Open circles) and predicted (solid line) concentration time profiles of oral dose of metronidazole 500mg single dose in healthy subjects with 5% and 95% confidence predicted interval (grey dashed lines) from Jykri et.al., 1983

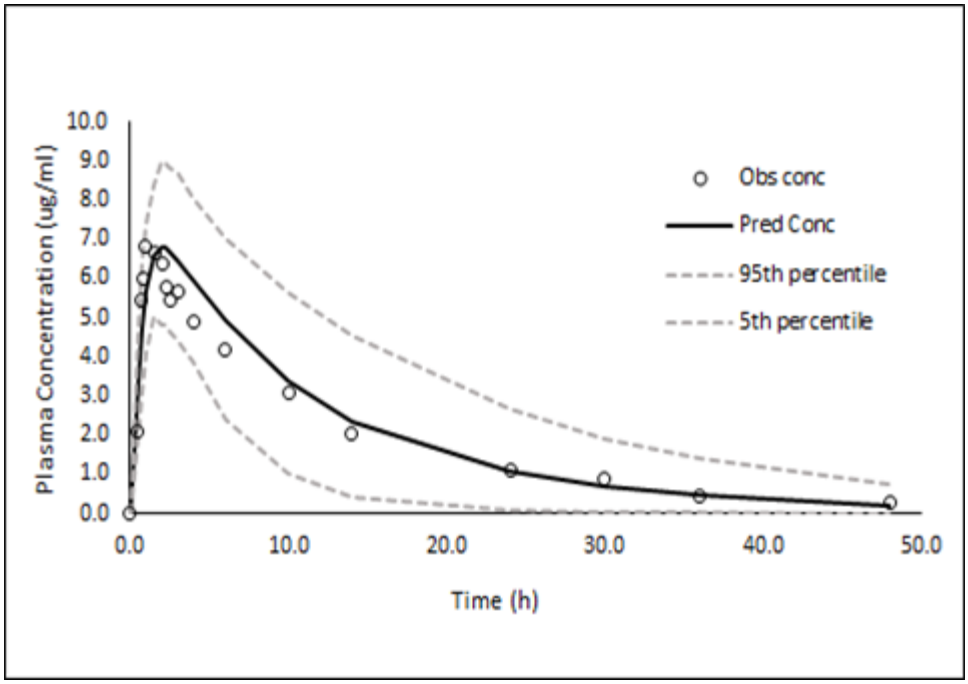

Figure 26: Observed (Open circles) and predicted (solid line) concentration time profiles of oral dose of metronidazole 400mg single dose in healthy subjects with 5% and 95% confidence predicted interval (grey dashed lines) from Houghton et.al., 1982

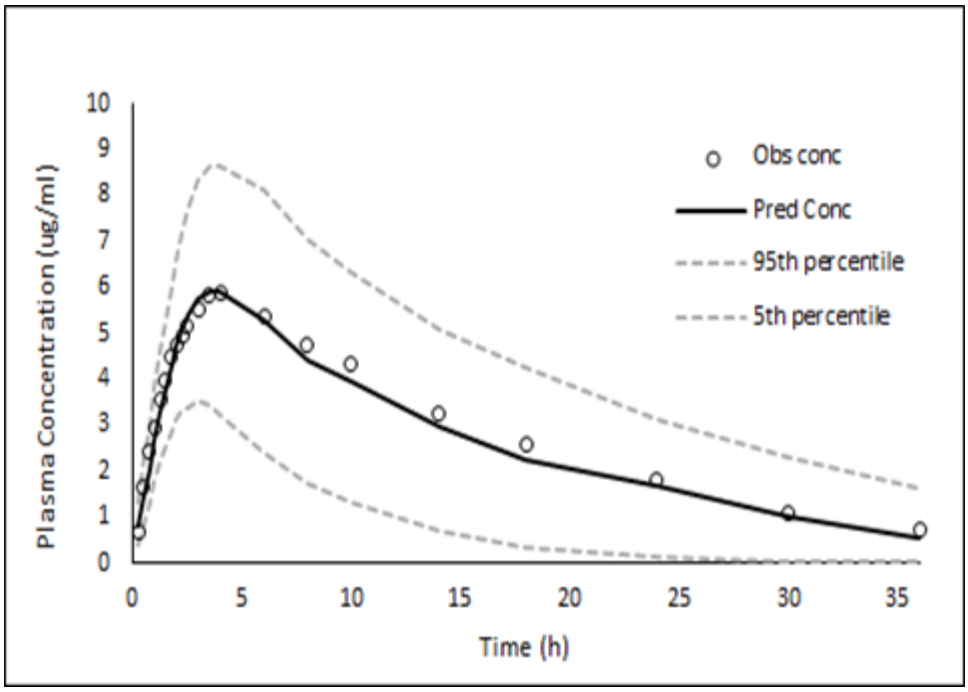

Figure 27: Observed (Open circles) and predicted (solid line) concentration time profiles of metronidazole suspension of 400mg single dose in healthy subjects with 5% and 95% confidence predicted interval (grey dashed lines) from Idkaidek et.al., 2000

Discussion

In recent years, physiological-based pharmacokinetic (PBPK) modeling has emerged as a promising approach to assess drug behavior in virtual populations by combining the key drug and system parameters to obtain insight into the drug characteristics [160]**.** During the process of drug development, PBPK modeling can be used to predict plasma drug concentrations in humans based on preclinical data. Furthermore, the dynamic flux of enzyme production and degradation can be used to estimate parent and metabolite concentrations at any given time after therapy is initiated, which is a major advantage of PBPK modeling. This part of the research aimed to develop

and verify the systemic exposure of three probe antibiotics: azithromycin, cefuroxime axetil, metronidazole in healthy subjects.

Whole-body PBPK models for azithromycin and metronidazole were developed and used to predict systemic drug exposure after intravenous and oral administration in healthy adults. Cefuroxime axetil is an ester prodrug of cefuroxime. So, the developed PBPK model was verified or applied to predict oral pharmacokinetics cefuroxime after administration of the prodrug in healthy adults. This approach of whole PBPK modeling integrated drug-specific parameters such as log P, pKa, permeability, solubility, and other in vitro parameters such as blood to plasma ratio, plasma protein binding.

Whole body-based PBPK models simulate the pharmacokinetic profiles based on drug-related physicochemical properties, such as clearance, the volume of distribution, and relevant physiological parameters like organ volumes, tissue compositions, and blood flow rates. In general, the intravenous profile is determined by the distribution and elimination of the drug. These PBPK models estimate the tissue partition coefficient (Kps) values from physicochemical properties used as input into mechanistic tissue composition equations [161,162]. These published tissue composition equations provide accurate estimates of Vss in humans.

Azithromycin is a macrolide antibiotic with unique pharmacokinetic properties characterized by extensive distribution to tissues and fluids and active uptake by various cells such as white blood cells and fibroblasts. This allows it to be administered for short periods while maintaining high infection site concentrations for much more extended periods. A total of 1500mg of immediate-release azithromycin administered in divided doses over 3 or 5 days (e.g., 500mg once daily for 3 days or 500mg on day 1 followed by

250mg on day 2-5) is the recommended regimen to treat most infections [163]. Accordingly, an intravenous profile of azithromycin was simulated for doses of 1g and 2g in male subjects.

Azithromycin is a high solubility drug with a reported bioavailability of ~37%. In vitro studies suggest that azithromycin is a substrate of P-gp, and P-gp efflux could also limit the oral bioavailability [164]. For azithromycin, biliary elimination is a major route of elimination. The biliary clearance of azithromycin was calculated using the retrograde model available in the Simcyp simulator, which back calculates the intrinsic hepatic clearance/biliary clearance and any additional clearance. The retrograde model estimates the biliary clearance from total intravenous clearance and renal clearance used as input [165]. The predicted AUC and Cmax for 1g and 2g IV infusion of azithromycin were in close agreement with the observed values with fold errors ranging from 0.94-1.03 (Table 20).

Once the PBPK model was verified for intravenous dosing, the model underwent additional evaluation for oral dosing testing different regimens (500mg QD, 500mg Q3D, 500mg day 1 and 250mg day 2-5 and 500mg suspension single dose) in healthy subjects. These simulations relied on the Simcyp ADAM model to estimate the rate and extent of absorption. The predicted Cmax following 500mg single dose of azithromycin is 0.26 ± 0.07 mg/L and was in close agreement with an observed value of 0.30 ± 0.34 mg/L, and the predicted AUC was 4.4 ±1.8 mg.h/L which also was in close agreement with observed AUC of 4.4 ± 1.9 mg.h/L. Additional simulations were conducted to predict the exposure levels of azithromycin for two multiple dose regimens (3-day and 5-day regimens). The model simulated systemic exposure levels of azithromycin for the two regimens were

similar, and 3-day dosing did not provide higher exposure levels than the 5-day regimen. The predicted estimates of pharmacokinetic parameters (AUC and Cmax) for both 3-day and 5-day regimens were in close agreement with observed values with fold errors ranging from 0.89-0.91.

The PBPK model was next extended to predict the pharmacokinetics after an administration of an oral suspension formulation (500mg dose). The predicted Cmax after was 0.49 ± 0.13 mg/L and was in close agreement with observed values. Likewise, the simulated AUC (6.45 ± 2.11 mg.h/L) compared favorably with published clinical observations. Thus, the oral pharmacokinetics of azithromycin for different regimens of tablet and suspension formulations were successfully predicted using the developed whole-body PBPK model, supporting its application to assess the pharmacokinetics of azithromycin in special populations such as gastric bypass surgical populations.

Cefuroxime axetil is an oral cephalosporin that is rapidly hydrolyzed in the gastrointestinal tract to the active parent compound, cefuroxime which is then absorbed into the systemic circulation. Cefuroxime axetil is indicated to treat various infections caused by susceptible bacteria, primarily for upper respiratory infections. The usual course of therapy of cefuroxime axetil for most infections is 250mg twice daily for 7 days with a range of 5-10 days [166]. Cefuroxime axetil has a bioavailability of ~36%. CA is a substrate for the peptide transporter PEPT1, which is highly expressed in the intestinal membrane of enterocytes and is the primary route of absorption. The distribution of CA is variable, and elimination is mainly through the renal route. PBPK model simulations were performed to predict the exposure levels after administration of a single oral dose (500mg tablet) under

fasting conditions, and multiple dosing of both a tablet formulation (250mg twice daily for 5 days) and an oral suspension 250mg twice daily for 5 days) under fed conditions.

The predicted systemic parameters were in close agreement with clinically observed values, which was confirmed following a visual predictive check of the plasma profiles and by calculating fold errors. A pharmacokinetic study conducted by Nix et.al., following a single oral dose of 500mg cefuroxime axetil tablet reported the C_{max} of 5.24 ± 19.6 µg/ml and AUC of 19.6 ± 27.6 µg.h/ml; the PBPK model- predicted values were consistent with the clinical data (C_{max} of 5.45 ± 1.64 µg/ml and AUC of 23.38 ± 5.98 µg.h/ml).

A similar trend was observed following an oral dose of 250mg twice daily tablet and suspension in healthy subjects where the observed and predicted parameters were comparable with fold errors ranging from 0.84-1.36. Upon comparing the mean plasma concentration profile and AUC after an oral tablet and suspension for 5 days, the results suggest that the pharmacokinetics of cefuroxime are not altered after repeated dosing of cefuroxime axetil. Thus, the oral pharmacokinetics of cefuroxime axetil following an oral tablet and suspension dose were successfully predicted compared to the observed values using the whole body PBPK model. This verified PBPK model of cefuroxime axetil can be used or extended to predict the drug exposure changes in special populations.

Metronidazole, an antiprotozoal agent, is a relatively hydrophilic compound with low protein binding [167]. Elimination occurs predominantly via biotransformation (~85% of the dose), and a small fraction (~ 10-15% of the dose) is excreted unchanged in the urine. Metronidazole displays linear PK in over the dose range from 0.2 - 2g [167-168]. The usual adult oral dosage of metronidazole is 500mg every 6 or 8 hours, and the usual duration of therapy is 7 to 10 days. PBPK model simulations were initially performed to

predict the steady-state pharmacokinetics of metronidazole following an intravenous infusion (500mg Q8H and 1500mg Q24H). The PBPK model predicted AUC for the 500mg Q8H (372.5±8.04 µg.h/ml) and 1500mg Q24H (393.39±5.20 µg.h/ml) dosing regimens were in close agreement with literature clinical values reported AUC.

Next, model simulations were used to evaluate metronidazole exposure after oral administration of both tablet (400 and 500 mg, single dose) and suspension (500mg) formulations. The predicted AUC for the 500mg and 400mg oral tablet (115.11±46.58 µg.h/ml, 88.59±37.63 µg.h/ml) were in close agreement with the observed values. Likewise, the PBPK model-simulated AUC for the oral suspension captured the clinical data. Thus, the PBPK model of metronidazole was successfully developed, and the model was able to predict the pharmacokinetics following different doses of metronidazole compared to the clinical data. This verified PBPK model of metronidazole can be applied to predict the pharmacokinetics in special populations.

In this aspect of the research, the whole body PBPK models of azithromycin, cefuroxime axetil, and metronidazole were successfully developed and verified in healthy subjects for various dosing regimens and doses following intravenous and oral tablet and suspension doses. In addition, the predictions of mean peak plasma concentrations and area under plasma concentration curves were well within the calculated 95% confidence interval. Thus, these PBPK models can provide a mechanistic structure from which to extrapolate the pharmacokinetics of these oral antibiotics to different populations, such as gastric bypass patients, where there is currently a lack of published clinical studies examining the effect of surgical alterations of the GI tract on drug disposition and the potential impact on safe and effective antibiotic dosing in this special patient population.

SPECIFIC AIM 3

Specific Aim 3

Specific Aim 3: To simulate and predict the drug exposure changes for cefuroxime axetil, metronidazole and azithromycin tablets in morbidly obese and post gastric bypass population, characterize the PK/PD relationship using PD indices AUC/MIC and T>MIC

Introduction

Obesity is a well-established public health concern, and its prevalence continues to increase worldwide [169]. Bariatric surgery has emerged as the most effective treatment for obesity [170] by providing weight loss to decrease comorbidities, such as type 2 diabetes mellitus, dyslipidemia, and an increased risk for infections post-surgery [171]. Patients post-bariatric surgery have an increased risk of intra-abdominal infections, UTIs, respiratory infections and SSTIs [34,86]. Commonly administered oral antibiotics for intra-abdominal infections and community acquired pneumoniae include cefuroxime plus metronidazole, and cefuroxime plus azithromycin, respectively.

Due to changes in the GI tract post-bariatric surgery, oral absorption of antibiotics can be altered, which may impact therapeutic efficacy. In addition to affecting gastric emptying time and intestinal motility, bariatric surgery modifies available surface area for absorption and may affect the intestinal drug metabolism, making antibiotic drug bioavailability difficult to predict [172 – 173]. Furthermore, obesity itself affects several pharmacological parameters, such that oral antibiotic absorption may change as patients lose weight [169]. Previous studies report that obesity itself has effects on antibiotic dosing requirements [174]. Excess body fat has also been shown to increase the volume of

distribution and increases adipose tissue and clearance of antibiotics from the systemic circulation because of increased kidney mass and glomerular filtration, potentially decreasing their efficacy [175].

Several studies demonstrated decreased oral antibiotic absorption following RYGB; however, associated therapeutic outcomes were not consistent. Given the scarcity of data on rates of oral antibiotic failure and the limited generalizability of the studies conducted to date, close monitoring is required to investigate the rates of antibiotic failure or to allow for dose modifications on a case-by-case basis. A limited number of studies have assessed oral beta-lactams pharmacokinetics post-bariatric surgery; and all included a single dose administration of antibiotic in the fasting state. Among these studies, amoxicillin and ampicillin studies reported a slower rate of drug absorption and lower bioavailability post-bariatric surgery [83, 176-177]. Two studies investigated the pharmacokinetics of oral penicillin after bariatric surgery. Miskowiak et al. [178] reported no significant difference in systemic exposure, whereas Terry et al. [179] reported a substantial increase in plasma concentration post-surgery. Other investigators evaluated the pharmacokinetics of oral fluoroquinolones post RYGB, and they concluded that no dose modification was required post-surgery [180,181]. Additional studies investigated the pharmacokinetics of macrolides in fasting subjects post-surgery using a single dose study design [37, 182]. The results suggested the need for dose modification and monitoring for treatment failure in the case of azithromycin. Overall, the limited data from these studies suggest that patients taking oral beta-lactams and macrolides should be closely monitored following bariatric surgery due to unpredictable absorption, although oral fluoroquinolones and linezolid may

not be affected. To date, there are no studies available in the literature reporting the treatment failure/exposure changes for cefuroxime axetil and metronidazole.

After administration of a drug, it undergoes absorption, distribution, metabolism and excretion processes, which are characterized by various PK parameters. Once the drug reaches the site of action at the desired concentration, it produces the desirable effect. In antimicrobial therapy, the effect is produced on the bacterial pathogen responsible for infection. The complex interplay among the drug and dose administered, its mechanism of action (MOA), the concentration at the infection site, and the severity of infection determines antibiotic treatment success. Pharmacokinetics (PK) and pharmacodynamics (PD) help elucidate the relationship between drug concentrations in biological fluids such as plasma, serum, and urine and the associated pharmacological effect [183]. PK-PD approaches can streamline the process of drug development and help make crucial decisions which include but are not limited to clinical trial design and the optimum dosing strategies, all of which can be extremely costly and critical to the compound being produced if incorrect decisions are taken.

The major indicator of the effect of the antibiotics is the MIC or minimum inhibitory concentration, which provides information on the susceptibility of pathogen against the antibiotic. The MIC is an in vitro measure of the antibiotic effect against a bacterium. The quantitative relationship between a pharmacokinetic parameter and a microbiological parameter is known as a PK/PD index. The best PK/PD index correlated with efficacy for antimicrobials with time-dependent killing for β-lactam antibiotics, such as penicillin, cephalosporins, carbapenems and monobactams, is the duration of time that active antibiotic concentrations exceeded the MIC. The PK/PD indexes for antimicrobials with

concentration-dependent killing such as macrolides, aminoglycosides, metronidazole, clindamycin, or linezolid is Cmax/MIC or the AUC/MIC ratios. For all the three PK parameters, their relationship with the MIC of the infecting pathogen is the key to the effect.

An ideal antibiotic optimization requires a good knowledge of the mechanisms involved in the effect of the antibiotics, the antibiotic's concentration in the patients' body, and the pathogen. PK/PD analysis integrates all the information about the pharmacokinetics and pharmacodynamics and evaluates the dosing required to enhance the possibility of success of the antibiotics therapy, as well as minimize the side effects and the emergence of resistance. Predicting the time course of drug effects under different physiological conditions is an essential quantitative aspect for determining the dose post gastric bypass surgery, which might affect the oral bioavailability of antibiotics.

This aspect of the dissertation aims to characterize the alterations in drug exposure when orally administering solid dosage forms (*i.e.,* tablet formulations) for cefuroxime axetil, metronidazole, and azithromycin. Different dosing regimens (dose, dosing frequency) post gastric bypass surgery were analyzed to predict the efficacy of the study drugs using the PD metrics such as AUC/MIC and $T_{>}$MIC.

Modeling Strategy

PBPK modeling of azithromycin, cefuroxime axetil, metronidazole in morbidly obese and post gastric bypass populations

Azithromycin

The developed and verified azithromycin PBPK model presented in specific aim 2 was adapted to account for changes in drug exposure after oral administration (500mg tablet) to subjects pre- and post-RYGB surgery. An ADAM model was used to predict the absorption, and a full PBPK model was utilized to describe the distribution of azithromycin. Following RYGB, Padwal et al. [37] reported a lower mean azithromycin peak concentration occurring earlier (shorter Tmax) compared to baseline (pre-surgery). Plasma concentration profiles were obtained for 24 hours after 500mg single dose administration. Virtual simulations for oral drug exposure of azithromycin pre- and post-RYGB were conducted in 10 randomized trials, consisting of 14 subjects in each trial. Sex, age, and number matched simulations were performed. The demographic data for pre- and post-RYGB surgery simulations for 500mg single tablet was shown in Table 23.

The simulated plasma concentration profiles in pre- and post-surgery populations were compared with published clinical data [37] digitized using WebPlotDigitizer (https://automeris.io/WebPlotDigitizer/). Fold error (FE) calculation of pharmacokinetic parameters Cmax and AUC and visual predictive checks were performed for all the populations. FE was calculated as a ratio of predicted to the observed value of each pharmacokinetic parameter.

Once it was demonstrated that the model successfully captured the exposure changes of azithromycin single dose compared to the observed data, the simulations were extended to predict the exposure changes of azithromycin tablet at steady state following two different dosing regimens. A single dose pharmacokinetic study of oral azithromycin single dose (*i.e.*, 500mg) evaluating drug exposure in pre-and post- RYGB surgery is available in the literature [37]. As the 3- and 5-day oral regimens have not been evaluated in a clinical study of patients pre- and post-RYGB surgery, a comparison to clinical data could not be performed. The study design used for predictions after 3- and 5-day regimens of oral azithromycin are shown in Table 24.

Table 23: Study design for Simcyp® simulations of oral azithromycin in pre- and post-surgical population [37]

	Pre (Morbidly Obese) and Post-surgery
No. of Trials	10
No. of subjects in each trial	14
Age of subjects (years)	18 – 60
% of females	100
Duration of Study (h)	24
Dosing Regimen	500mg tab single dose

Table 24: Study design for Simcyp® simulations of oral azithromycin (steady state) in pre- and post-surgical population

	Pre (Morbidly Obese) and Post-surgery	
	3-Day Regimen	**5-Day regimen**
No. of Trials	5	5
No of subjects in each Trial	10	10
Age of Subjects(years)	18-60	18-60
% of females	50	50
Duration of study (h)	288	288
Dosage regimen	500mg daily for 3 days	500mg x1 Day 1 250mg daily days 2 to 5

Cefuroxime axetil

The developed and verified PBPK model of prodrug cefuroxime axetil and its active form, cefuroxime, presented in specific aim 2, was used to predict the exposure changes for the following oral dosing regimens of a tablet formulation to pre- (morbidly obese) and post-RYGB patient populations. Several dosing regimens were evaluated: single dose (500mg), 500mg twice daily for 5 days, and 250mg tablet twice daily for 5 days. The Simcyp ADAM model, a more sophisticated absorption model, was adopted to predict the absorption, and a full PBPK model was used to predict the cefuroxime axetil and cefuroxime distribution. Each simulation was performed on 120 virtual subjects (10 trials × 12 subjects). The age, sex, dose, and dosing interval in pre- and post-surgical subjects were identical to the healthy subjects trail. The demographic data for pre-and post-surgical trials were shown in Table 25. As there are no published clinical data available to evaluate

exposure changes of cefuroxime axetil following RYGB, no comparison was made to the observed data.

Table 25: Study design for Simcyp® simulations of oral cefuroxime axetil in pre and postsurgical population

	Pre (Morbidly Obese) and Post-surgery		
	500mg	**500mg BID**	**250mg BID**
No. of Trials	10	10	10
No of subjects in each Trial	12	12	12
Age of Subjects(years)	18-45	18-45	18-45
% of females	50	50	50
Duration of study (h)	24	96	96
Dosage regimen	500mg single dose	500mg BID for 5 days	250mg BID for 5 days

Metronidazole

The PBPK model of metronidazole developed and verified under specific aim 2 was utilized to predict the exposure changes of metronidazole following single (500mg) and multiple (500mg tablet Q8H for 7 days) oral dosing of a tablet formulation in both pre-and post-surgical population. Once again, the ADAM model was used to predict the absorption, and a full PBPK model was used to predict the distribution of metronidazole. Each simulation was replicated in 5 trials with 10 subjects in each trial. Model-simulated systemic exposure estimates were predicted and the ratio of post- to pre-surgery for these estimates were calculated. No comparison was made to observed data as there are no

published clinical studies regarding exposure changes of metronidazole post-RYGB. The demographic data for pre-and post-surgical simulations were shown in Table 26.

Table 26: Study design for Simcyp® simulations of metronidazole in pre and postsurgical population

	Pre (Morbidly Obese) and post-surgery	
	500mg	**500mg Q8H**
No. of Trials	5	5
No of subjects in each Trial	10	10
Age of Subjects(years)	20-50	20-50
% of females	50	50
Duration of study (h)	24	168
Dosage regimen	500mg single dose	500mg Q8H for 7 days

PK/PD Integration

For antibiotics with concentration-dependent time killing, the effect *in vivo* depends on achieving highest concentrations above the infecting pathogen's MIC to ensure maximal killing. For most antibiotics there is a high correlation between the peak concentration or AUC ratioed to the MIC. Azithromycin is an antimicrobial with a concentration-dependent with time dependency killing, which allows for prolonged persistent effects, that protect against regrowth when active drug concentration falls below the MIC. For azithromycin the ratio of unbound AUC (over 24 hrs, AUC24) to MIC correlates well with *in vivo* efficacy. Target AUC24/MIC ratios required for clinical success vary among antibiotic classes, and the value is >5 for macrolides like azithromycin against *H. influenzae*, and >25 against *M. catarrhalis* [184]. Azithromycin is active against gram-positive bacteria and

gram-negative bacteria including *Haemophilus influenzae*, *Moraxella catarrhalis*, and *Mycoplasma pneumoniae*. The MIC_{90} values for these organisms were obtained from SENTRY Antimicrobial surveillance data [https://sentry-mvp.jmilabs.com/app/sentry-public] and published literature [185] and were utilized to determine an AUC/MIC for relevant pathogens including *H. influenzae* and *M. catarrhalis.*

Cefuroxime has a broad spectrum of antimicrobial activity. The MIC_{90} values for oral cefuroxime were also obtained from SENTRY Antimicrobial surveillance data [https://sentry-mvp.jmilabs.com/app/sentry-public] and the literature [186]. Cefuroxime is active against many gram-positive bacteria like *S. pneumoniae* (MIC_{90} of ≤0.012 mg/L (Penicillin susceptible), 4 mg/L (Intermediate). Cefuroxime also shows good activity against several gram-negative bacteria like *H. influenzae* (MIC_{90} 1.0 mg/L), and *M. catarrhalis* (MIC_{90} 2.0 mg/L). Additionally, the drug is also against *E. coli*, with mean MIC_{90} values of 4 and 8 mg/L. The MIC_{90} value for the most resistant strains of *E. coli* ranges from 8 to 32 mg/L. A recent study by Gascon et al [187] reported that for *E.coli* the MIC_{90} of 4 mg/L (CLSI - Clinical and Laboratory Standards Institute) and 8 mg/L (EUCAST – European Committee on Antimicrobial Susceptibility Testing) [188-189] resulted in invariably zero %T>MIC and MIC_{90} of >0.5mg/L resulted in more than 90% of strains reached the target %T>MIC with clinical response above 90%. Gascon et al. reported that most microbiology laboratories analyze the *in vitro* susceptibility with automates systems, which use a straight range of concentrations, around a clinical breakpoint which could be a limitation in the clinical outcome. Accordingly, an MIC_{90} of >0.5mg/L was used for E.coli in this study for PK/PD analysis.

PK/PD analysis suggests that the time cefuroxime concentrations are above the MIC_{90} is the most predictive parameter. A %T> MIC of 50 to 70 % of the dosing interval correlates well with the efficacy assuring therapeutic success [69]. Most of studies reporting PK/PD analysis of oral cefuroxime identified that %T>MIC of 50 to 70% attains near maximal bactericidal activity, especially for *H. influenzae,* and a target of 40% is required to inhibit the growth of bacteria. Thus, a PD target of 50 to 70% of the time interval above MIC was considered as optimal effect [189]. Estimates of the amount of time that plasma levels exceed MIC values were obtained from plasma concentration time profile to determine the %T>MIC for different dosing regimens as demonstrated in the below equation:

$$\%\mathrm{T} > \mathrm{MIC} = [t_2 - t_1] \times \frac{100}{\mathcal{T}} \qquad (5)$$

Where the t_1 and t_2 corresponds to the time at which the drug concentration reaches the MIC in the ascending (absorption) and descending (elimination) phases of the plasma concentration-time profile, where τ represents the dosing interval, which is 12hr for all the simulations in pre- and post-surgical populations[187].

Results

Azithromycin

The PBPK model predicted the clinically observed mean plasma concentration profile after a single oral dose of 500mg tablet in pre- surgical population (Figure 28) and post-surgery (Figure 29). The graphs show that model predicted exposure values were within the 95% confidence interval compared to observed data. Figure 30 compares the predicted plasma concentration profile of azithromycin in pre- and post-RYGB. Table 27

compares the observed and predicted pharmacokinetic parameters (C_{max}, AUC) and calculated fold error pre-and post-surgery.

Collectively, the results show that the PBPK model successfully captured the pharmacokinetic profile of azithromycin in pre- and post-RYGB populations. Fold errors for AUC and Cmax ranging from 0.88 to 1.22 and are close to one, which indicates that the model successfully predicted the pharmacokinetic parameters compared to observed data. The predicted AUC_{0-24} for the post-surgical group was 33% lower (1.69 ± 0.51 mg.h/L vs. 2.52 ± 0.63 mg.h/L) than the pre-surgical (morbidly obese) group, and this was in close agreement with the published clinical study that reported 32% lower AUC in RYGB subjects compared to morbidly obese. Azithromycin C_{max} for the post-surgical group (0.23 ± 0.05 mg/L) was 30% lower than that for the morbidly obese group (0.33 ± 0.06 mg/L). A significant decrease in extent of absorption was observed for a single dose of azithromycin post-surgery.

Table 27: Pharmacokinetic parameters of azithromycin following 500mg tablet in pre and postsurgical population: PBPK model predictions vs. published clinical data

	Pre-Surgery (Morbidly Obese)			**Post-surgery**		
	Obs	**Pred**	**FE**	**Obs**	**Pred**	**FE**
Cmax (mg/L)	0.36 ± 0.2	0.33 ± 0.06	0.91	0.26 ± 0.1	0.23 ± 0.05	0.88
AUC(0-last)(mg.h/L)	2.07 ± 0.8	2.52 ± 0.6	1.22	1.41 ± 0.5	1.69 ± 0.5	1.20
Tmax (h)	2.4 ± 1.2	2.3 ± 0.4	0.96	2.1 ± 0.1	2.2 ± 0.5	1.01

Obs- Parameter estimate reported in literature [37];

Pred- Parameter estimate predicted by PBPK model using Simcyp Simulation;FE- Fold-error- ratio of [predicted]/[observed] values

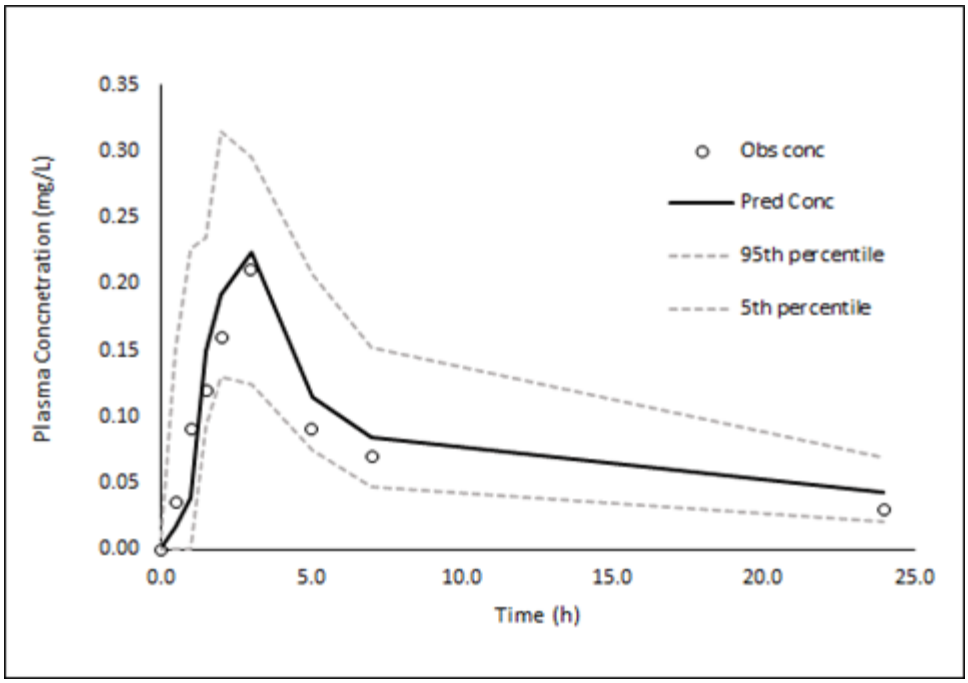

Figure 28: Observed (open circles) and Predicted (solid line) concentration time profiles of 500mg oral azithromycin Pre RYGB surgery (Morbidly obese) subjects with 5% and 95% confidence predicted interval (grey dashed lines).

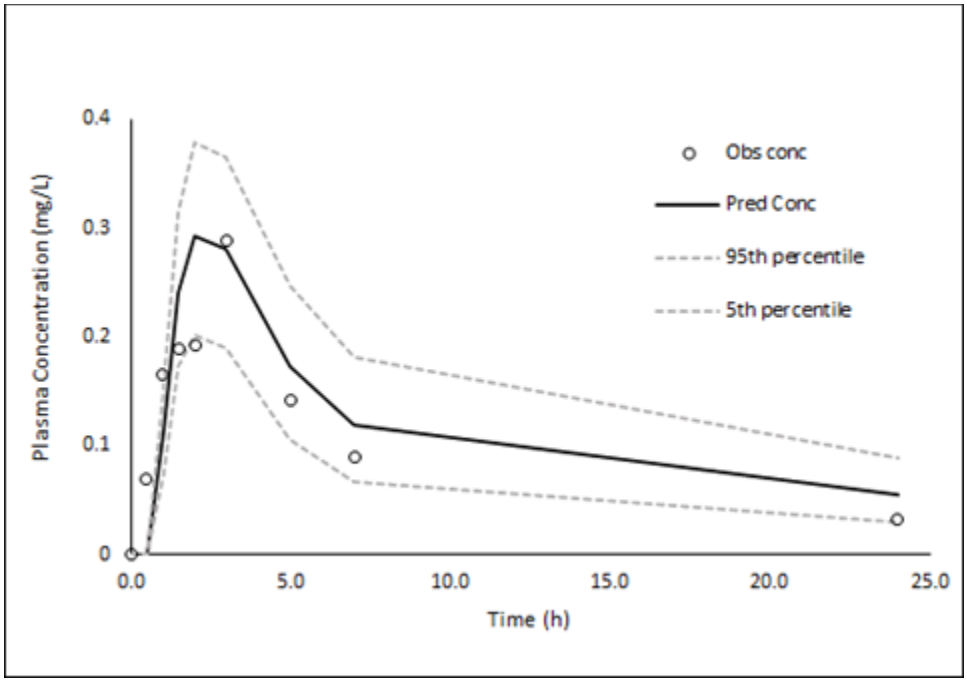

Figure 29: Observed (open circles) and Predicted (solid line) concentration time profiles of 500mg oral azithromycin Post RYGB surgery subjects with 5% and 95% confidence predicted interval (grey dashed lines).

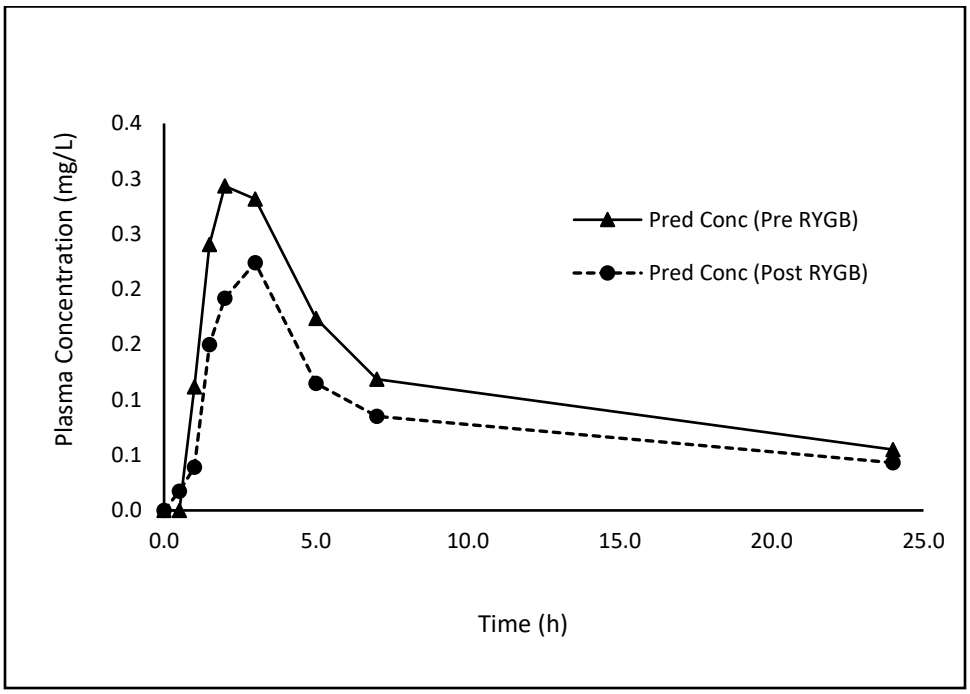

Figure 30: Predicted pre RYGB (solid triangles) and post RYGB (solid circles) concentration time profiles of 500mg oral azithromycin tablet.

The PBPK model was then used to predict the steady state plasma concentration profile of azithromycin resulting from two dosing regimens (500mg once daily for 3 days; 500mg on day 1, 250mg on days 2- 5) in pre-and post-surgery populations, The results are depicted in Figure 31 and 32. Table 28 provides the model-predicted pharmacokinetic parameters of azithromycin following these two dosing regimens in both populations. The predicted steady state AUC after surgery was 30% lower (22.54 ± 4.20 mg-h/L vs 15.71 ± 5.36 mg-h/L) compared to clinically observed data in the pre-surgical (morbidly obese) group for the three-day regimen. Likewise, azithromycin C_{max} for the post-surgical population (0.28 ± 0.07 mg/L) was 28% lower than that for the morbidly obese group (0.39 ± 0.12 mg/L). Similar results were seen for the 5-day regimen, where the model predicted AUC for post-surgery was 28% lower (19.98 ± 3.79 mg-h/L vs 14.47 ± 3.42 mg-h/L lower

than the pre-surgical group. Furthermore, the C_{max} for the postsurgical group (0.28 ± 0.06 mg/L) was 26% lower than that for the morbidly obese group (0.38 ± 0.11 mg/L). A statistically significant ($p < 0.05$) decrease in PBPK model-predicted overall exposure was observed at a steady state of azithromycin post-surgery.

In order to follow PK/PD-based estimates on the clinical efficacy of azithromycin, $AUC_{(24h, SS)}$/MIC ratios were calculated for relevant pathogens of respiratory, skin, and soft tissue infections. Tables 29 and 30 present the MIC values obtained from SENTRY Antimicrobial surveillance data [https://sentry-mvp.jmilabs.com/app/sentry-public] and other studies from literature [185]. $AUC_{(24h, SS)}$/MIC ratios calculated for different pathogens in pre- (morbidly obese) and post-surgical populations for 3-day and 5-day oral regimens. $AUC_{24, SS}$/MIC ratio calculations suggest that the azithromycin concentrations are subinhibitory (below the threshold ratio of 5) for *H. influenzae* – intermediate (moderately susceptible) in both pre- and post-surgical populations , and for the susceptible (isolates with no bacterial resistance or at clinically significant level) group $AUC_{24, SS}$/MIC ratio was above the threshold for pre-surgical group and sub-inhibitory for post-surgical group. For *M. catarrhalis,* although the $AUC_{24, SS}$/MIC was 2-fold lower in post-surgical group, it was above the threshold concentration of 25 indicating the efficacy in both pre- and post-surgical groups.

Table 28: Pharmacokinetic parameters of azithromycin at steady state in pre and postsurgical population

	500mg QD for 3days			500mg day 1, 250mg day 2 - 5		
	Pre-surgery (Morbidly Obese)	**Post-surgery**	**Ratio**	**Pre-surgery (Morbidly Obese)**	**Post-surgery**	**Ratio**
Cmax (mg/L)	0.39 ± 0.12	0.28 ± 0.07	0.72	0.38 ± 0.11	0.3 ± 0.06	0.74
AUC $_{(0\text{-last})}$ (mg.h/L)	22.54 ± 4.2	15.71 ± 5.36	0.70	19.98 ± 3.79	14.47 ± 3.42	0.72

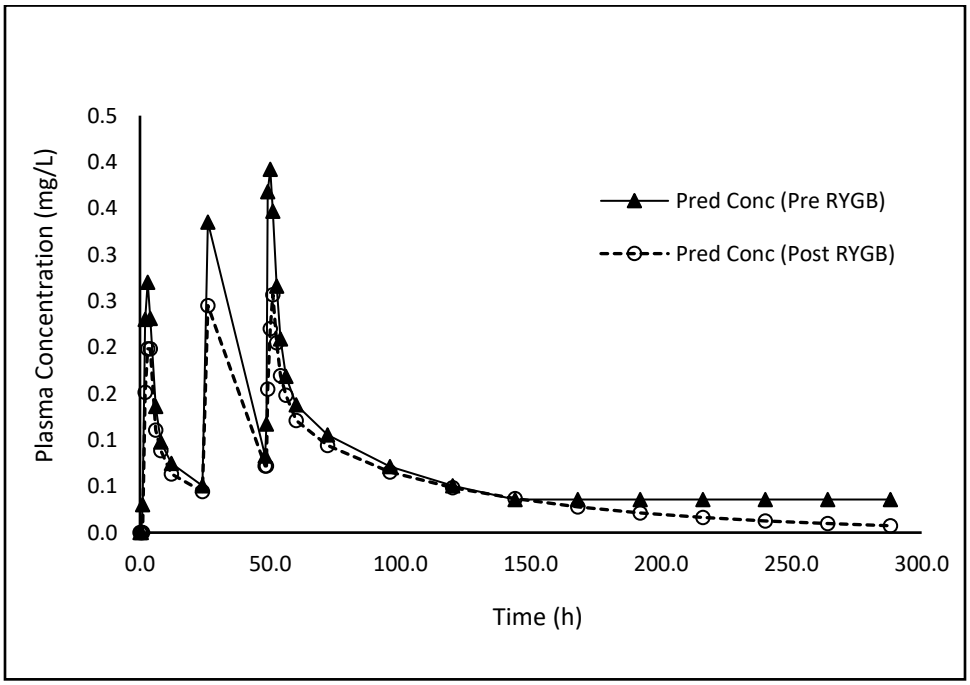

Figure 31: Predicted pre RYGB (solid triangles) and Post RYGB (solid circles) concentration time profiles of oral 500mg azithromycin tablet for 3 days.

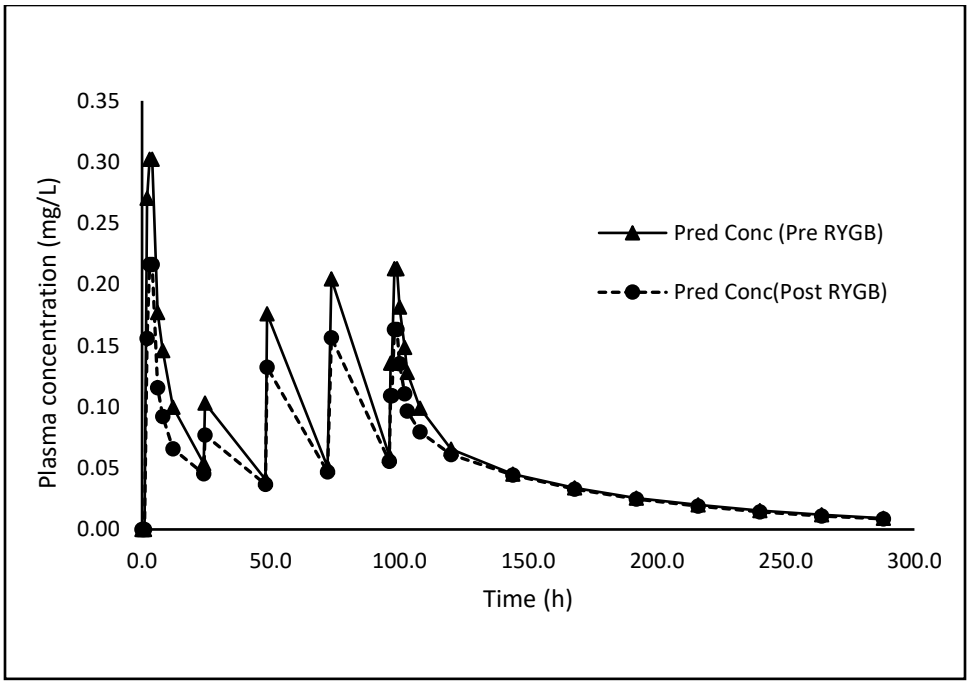

Figure 32: Predicted pre RYGB (solid triangles) and Post RYGB (solid circles) concentration time profiles of oral 500mg azithromycin tablet (5-day regimen).

Table 29: Azithromycin $AUC_{(24h, SS)}$/MIC ratios for relevant pathogens in pre (morbidly obese) and post-surgical population 3-day regimen (500mg daily for 3 days)

MIC	**AUC 24 (mg.h/L), Day 3**		**AUC24h, ss/MIC ratio calculated for the indicated MIC**	
	Pre-surgery	**Post-surgery**	**Pre-surgery**	**Post-surgery**
1 mg/L (*H. influenzae*)	4.25	2.38	4.25	2.38
0.5 mg/L (*H. influenzae*)	4.25	2.38	8.50	4.76
0.06 mg/L (*M. catarrhalis*)	4.25	2.38	70.8	39.7

$AUC_{24,SS}$ – area under the concentration curve over 24hr in steady state
MIC – minimum inhibitory concentration, at which 90% of the isolates are inhibited

Table 30: Azithromycin $AUC_{(24h, SS)}$/MIC ratios for relevant pathogens in pre (morbidly obese) and post-surgical population 5-day regimen (500mg day 1 and 250mg day 2 to day 5)

MIC	**AUC_{24} (mg.h/L)**		**AUC_{24} (mg.h/L)**		**AUC/MIC**		**AUC/MIC**	
	Pre-surgery		**Post-surgery**		**Pre-surgery**		**Post-surgery**	
	Day 1	**Day 5**	**Day 1**	**Day 5**	**Day 1**	**Day 5**	**Day 1**	**Day 5**
1 mg/L (*H. influenzae*)	4.25	3.2	2.45	2.2	4.25	3.2	2.45	2.2
0.5 mg/L (*H. influenzae*)	4.25	3.2	2.45	2.2	8.5	6.4	4.9	4.4
0.06 mg/L (*M. catarrhalis*)	4.25	3.2	2.45	2.2	70.83	53.33	40.83	36.67

$AUC_{24,SS}$ – area under the concentration curve over 24hr in steady state
MIC – minimum inhibitory concentration, at which 90% of the isolates are inhibited

Cefuroxime axetil

The developed and verified PBPK model of the prodrug cefuroxime axetil was used to predict the exposure changes of cefuroxime (active moiety) after single oral dose administration (500mg) and at a steady state (500mg and 250mg dosed twice daily). The model predicted mean plasma concentration profiles these dosing regimens are presented in Figures 33 through 35. Table 31 provides the PBPK model-predicted pharmacokinetic parameters of cefuroxime in the pre- and post-RYGB populations. Following administration of a single 500 mg oral dose of cefuroxime axetil, the predicted $AUC_{0\text{-}24h}$ for postsurgical patients was 40% higher (17.46 ± 4.29 vs. 12.53 ± 2.95 µg-h/ml, $p < 0.05$) than the pre-surgical (morbidly obese) group. No significant difference in cefuroxime Cmax was observed for the postsurgical group (3.59 ± 1.29 µg/ml) compared to morbidly obese group (3.21 ± 0.99 µg/ml).

Moreover, following multiple dosing (500 mg twice daily) to steady state, the model-simulated AUC for the postsurgical group was 42% higher (17.04 ±5.45 µg.h/ml vs. 12.04 ± 3.02 µg.h/ml) and the Cmax was 20% higher (3.86 ±1.53 µg/ml vs. 3.21 ± 0.99 µg/ml) for the post-surgery population compared to morbidly obese subjects. A similar trend was observed for 250mg dosing simulations, where the post-surgical AUC was 42% (9.53 ± 1.72 µg.h/ml vs 6.71 ± 1.42 µg.h/ml) higher than the pre-surgical group and the Cmax was 18% (2.63 ± 0.88 µg/ml vs 2.22 ± 0.48 µg/ml) higher following RYGB. These differences in Cmax and AUC0-24h were statistically significant ($p < 0.05$).

The dose-effect relationship for oral cefuroxime was evaluated by calculating the %T>MIC for relevant pathogens. Table 32 presents the MIC_{90} values and %T>MIC for different pathogens in pre-surgical (morbidly obese) and post-surgical populations. For

antimicrobials like cefuroxime, the %T>MIC of 50 -70% has been identified for near-maximal bactericidal activity, whereas a target of 40% has been proposed as the threshold for achieving bacteriostasis [189]. Table 32 illustrates that that the standard dosing regimens (500mg or 250 mg q12h) achieved the recommended target of ≥50%T>MIC for *S. pneumonia*, in both pre-and post-surgical populations. For *H.influenza*, the target was achieved for 500mg PO q12h regimen but not for 250mg PO q12h.

For *E.coli*, the MIC_{90} of >0.5mg/L reported by Gascon was used to assess the target achievement as the target attainment was invariably zero for the MIC_{90} value from SENTRY Antimicrobial surveillance data [https://sentry-mvp.jmilabs.com/app/sentry-public] and CLSI [188] and the cumulative fraction response was higher than 90% for target MIC_{90} of >0.5 mg/L. With MIC_{90} of >0.5mg/L, the target was reached for the 500 mg dose in pre- and post-surgical subjects, whereas 250mg PO q12h reached the target only in pre-surgical subjects.

Table 31: Pharmacokinetic parameters of cefuroxime after oral cefuroxime axetil in pre and postsurgical population

	500mg Single Dose			**500mg BID for 4 days[#]**			**250mg BID for 4 days[#]**		
	Pre-surgery (Morbidly Obese)	**Post-surgery**	**Ratio**	**Pre-surgery (Morbidly Obese)**	**Post-surgery**	**Ratio**	**Pre-surgery (Morbidly Obese)**	**Post-surgery**	**Ratio**
Cmax (µg/ml)	3.2 ± 1.0	3.6 ± 1.3	1.12	3.2 ± 1.0	2.86 ± 1.5	1.20	2.2 ± 0.48	2.6 ± 0.9	1.18
AUC (µg.h/ml)	12.5 ± 3.0	17.5 ± 5.1	1.40	12.0 ± 3.0	17.0 ± 5.4	1.42	6.7 ± 1.4	9.5 ± 1.7	1.42
Tmax (h)`	3.0 ± 0.5	2.4 ± 0.5	0.8	3.0 ± 0.5	2.4 ± 0.5	0.8	2.0 ± 0.4	2.3 ± 0.5	1.13

[#] Day 4 predicted Cmax and AUC

Table 32: Calculated $\%T_{> MIC90}$ for cefuroxime after oral cefuroxime axetil tablet in pre-surgery (morbidly obese) and post-surgery (gastric bypass) for relevant pathogens

Pathogen	MIC_{90} (mg/L)	%T>MIC (Pre-surgery)		T>MIC (Post-surgery)	
		500mg BID	250mg BID	500mg BID	250mg BID
Gram-negative bacteria					
Escherichia coli	0.5	54.2	41.7	64.8	50.0
H. influenzae	1	50.0	29.2	50.0	45.8
Gram Positive bacteria					
S. pneumoniae (Penicillin Susceptible)	≤ 0.012	100	100	100	100

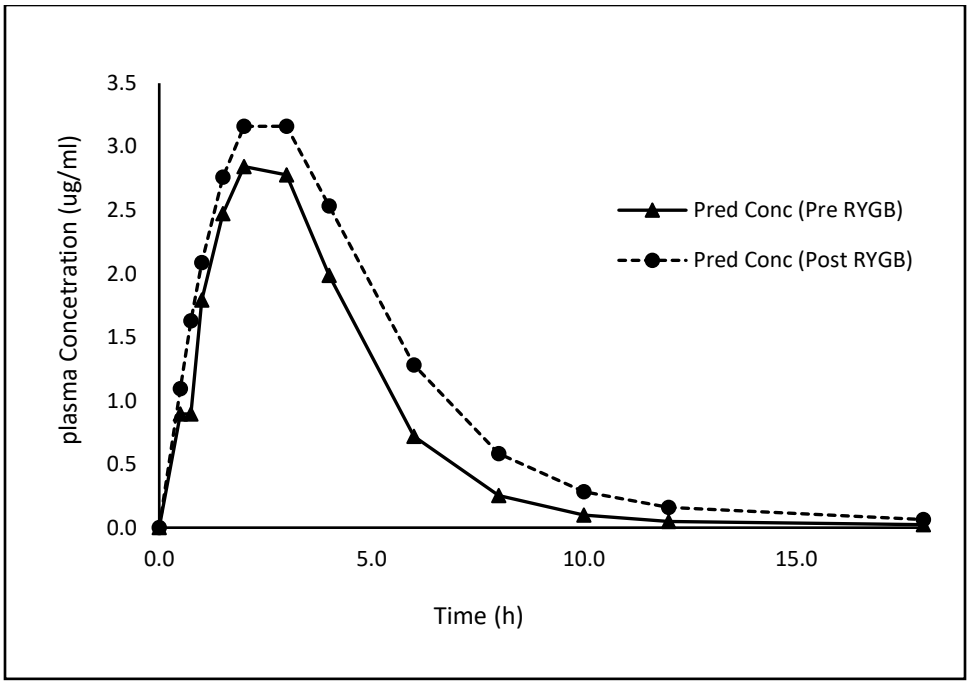

Figure 33: Predicted pre RYGB (solid triangles) and Post RYGB (solid circles) concentration time profiles of cefuroxime after an oral 500mg cefuroxime axetil tablet.

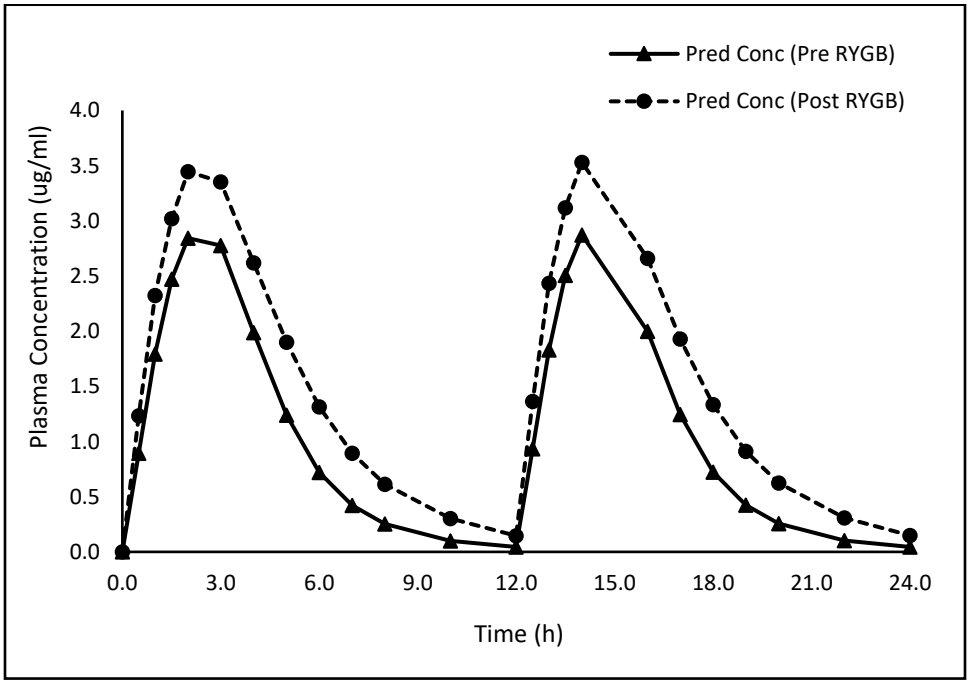

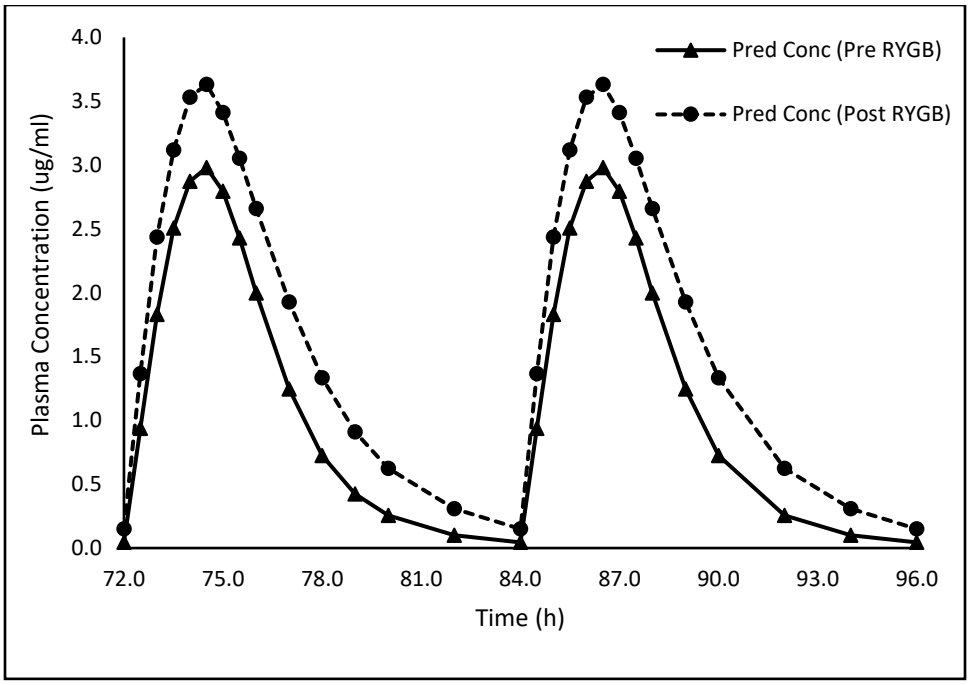

Figure 34: Predicted pre RYGB (solid triangles) and post RYGB (solid circles) concentration time profiles of cefuroxime after an oral 500mg BID cefuroxime axetil tablet Day 1 (top) and Day 4 (bottom).

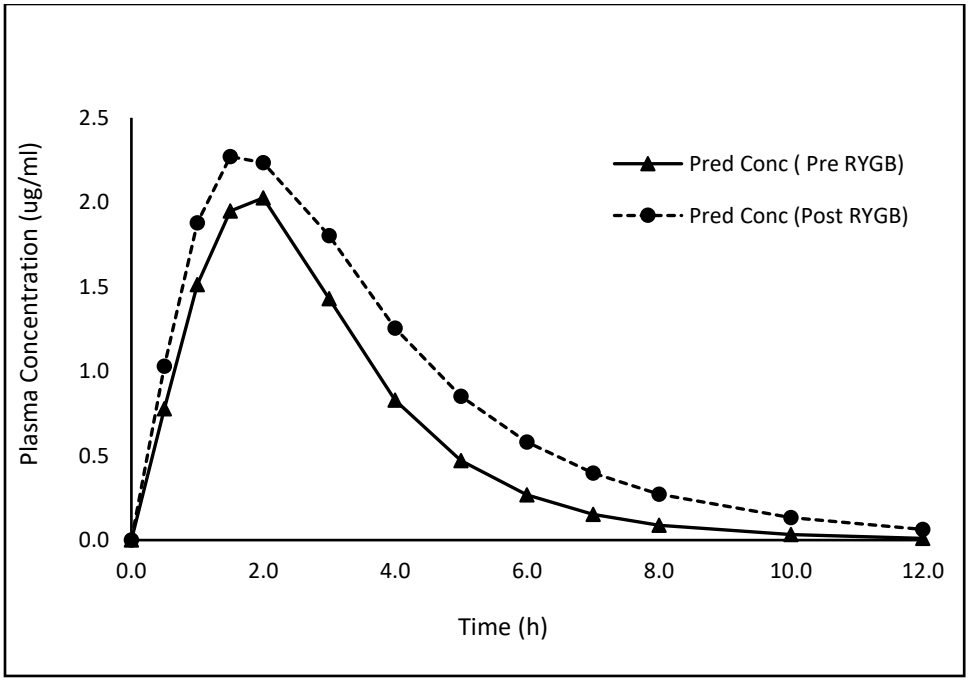

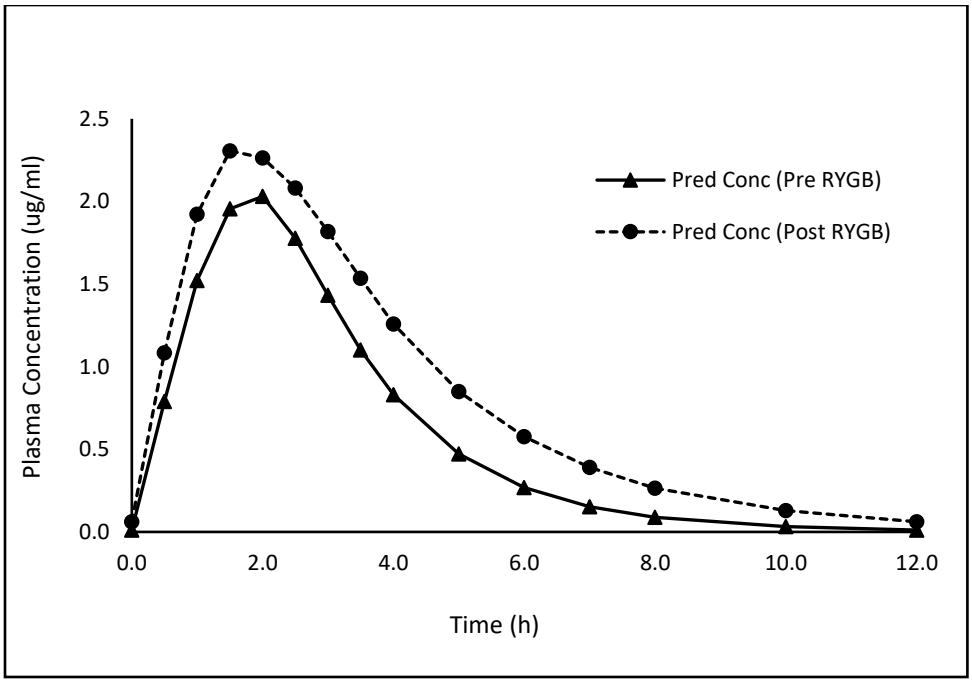

Figure 35: Predicted pre RYGB (solid triangles) and Post RYGB (solid circles) concentration time profiles of cefuroxime after an oral 250mg BID cefuroxime axetil tablet Day 1 (top) and Day 4 (bottom).

Metronidazole

The predicted mean plasma concentration profiles of metronidazole following 500 mg dosing (single dose and 3 times a day for 3 days) in pre-and-post-RYGB are depicted in Figures 36 and 37. The PBPK model developed and verified under specific aim 2 was used for the simulations. Table 33 shows the predicted pharmacokinetic parameters of metronidazole following RYGB for single dose administration and at steady state. The predicted AUC and Cmax estimates were comparable between the pre- (morbidly obese) and post-surgical groups, although the rate of absorption was faster (shorter Tmax) in the post-surgical population.

Table 33: Pharmacokinetic parameters of metronidazole in pre and postsurgical population

	500mg Single Dose			500mg Q8H		
	Pre-surgery (Morbidly Obese)	**Post-surgery**	**Ratio**	**Pre-surgery (Morbidly Obese)**	**Post-surgery**	**Ratio**
Cmax (µg/ml)	5.7 ± 1.0	6.0 ± 1.6	1.06	11.2 ± 3.4	11.6 ± 4.0	1.04
AUC (µg.h/ml)	66.5 ± 28.0	70.7 ± 31.5	1.06	543.5 ± 30.9	581.6 ± 30.9	1.01
Tmax (h)	2.1 ± 0.4	1.5 ± 0.2	1.37	1.6 ± 0.3	1.3 ± 0.1	0.78

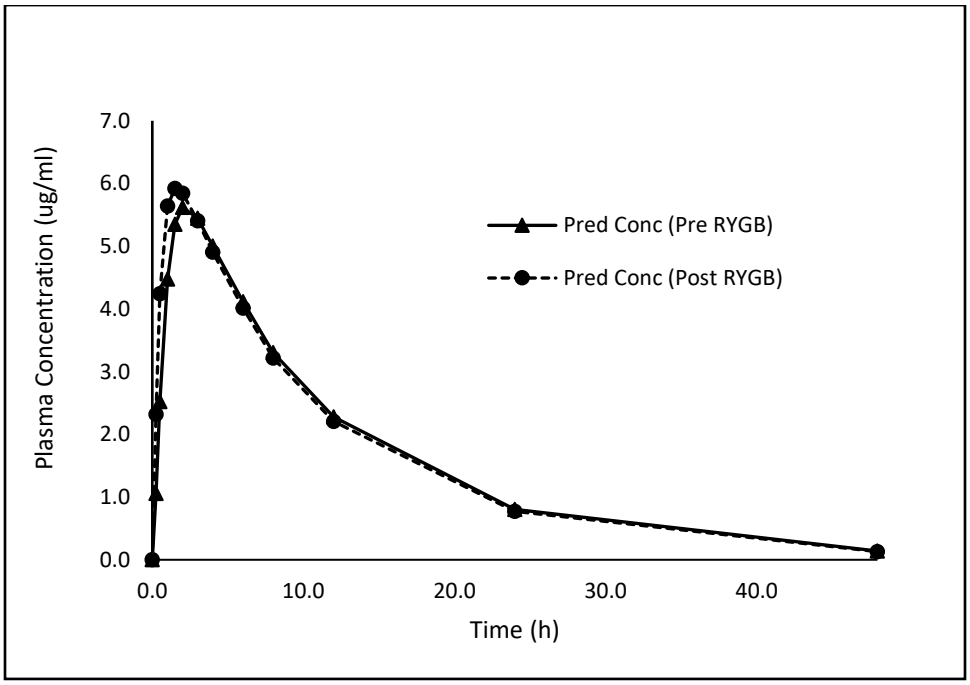

Figure 36: Predicted pre RYGB (solid triangles) and Post RYGB (solid circles) concentration time profiles of oral 500mg metronidazole tablet.

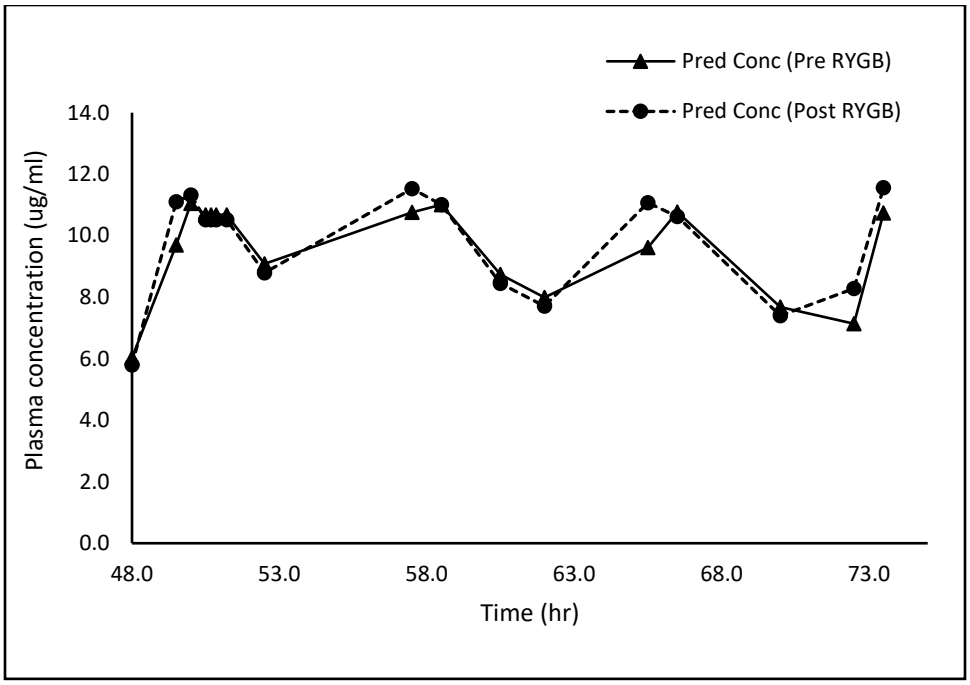

Figure 37: Predicted pre RYGB (solid triangles) and Post RYGB (solid circles) concentration time profiles of oral 500mg metronidazole tablet Q8H.

Discussion

Over the past decade, the use of *in silico* methods to model drug absorption and disposition has improved the ability to predict the effects of patient demographics such as age, sex, and race, disease, and drug-drug interactions on systemic drug exposure, resulting in advances in personalized medicine and reducing some of the challenges of conducting clinical studies [73]. However, PBPK modeling has also recently been used to evaluate the effects of gastric bypass on absorption and the overall bioavailability of drugs [76,77,79]. The post-operative changes in morbidly obese patients are multifactorial. PBPK models offer an advantage over standard compartment models in determining the necessary dosing modifications to ensure safe and efficacious drug therapy after patients undergo gastric bypass surgery by considering both the physiological parameters and the drug

characteristics. By accounting for the combined effects of various physiological factors and drug characteristics on pharmacokinetics, PBPK models have the advantage over traditional compartmental models in predicting necessary dose adjustments in gastric bypass patients. This aspect of research aimed to simulate the alterations in absorption and disposition of oral antibiotics administered as solid dosage forms post-RYGB surgery compared to the morbidly obese or pre-surgical population.

RYGB alters the physiology of GIT, resulting in significant weight loss over time. Correspondingly, alterations in drug absorption, distribution, metabolism, and excretion might be anticipated in these patients after undergoing RYGB surgery, particularly for oral drug dosing, and dosing adjustments may be necessary. In general, the pharmacokinetics and resulting systemic exposure of orally administered drugs are altered post gastric bypass surgery; there can often be an increase in C_{max} and shorter T_{max}, with less consistent results on total exposure (AUC), which can be similar, lower, or higher after surgery.

An important consideration for pharmacodynamic evaluation is that the efficacy of an antimicrobial agent is dependent on the relationship between the MIC of the pathogen and drug exposure. For antimicrobials with concentration dependent time kill activity, efficacy is correlated with Cmax- or AUC to MIC ratio. Alternatively, for medications with time dependent kill activity, %T > MIC correlates well with efficacy. Alterations is systemic drug exposure post-bariatric surgery can impact therapeutic efficacy of an antimicrobial agent, thereby requiring dose adjustments in these patient population. Most published research on bariatric surgery patients compare the pharmacokinetics before and after surgery, although some studies compare the pharmacokinetics post-surgery to non-obese individuals. The proper comparison should be pre- and post-surgery, as comparison

to non-obese or healthy subjects could result in large inter and intra- individual variability. Overall, very few studies have been performed to study the impact of bariatric survey on antimicrobial efficacy.

The anatomical changes along the gastrointestinal tract following RYGB surgery can influence or alter the pharmacokinetic parameters of oral drugs. For example, the large size of the absorption surface is related to faster absorption, but when the transit of the drug through the intestine is too fast, the possibility of drug absorption is reduced. The PBPK models developed and tested in this research, based on the Simcyp ADAM absorption module and appropriate population parameters, successfully simulated clinically observed plasma concentrations and pharmacokinetic parameters of azithromycin following oral administration of a tablet formulation in pre-surgical and RYGB subjects. Model predictions suggested reduced bioavailability of azithromycin after surgery with a mean post/pre-AUC ratio of 0.67 ($p < 0.05$), which was associated with a mean decrease in the projected fraction of dose absorbed (fa) from 0.71±0.03 to 0.56±0.04 and a corresponding increase in oral clearance (Cl/F) from 174.43±63.60 L/h to 262.63±99.46 L/h. The predictions pre-and post-surgery were in close agreement with the clinically observed data. Similar findings were obtained for multiple dose simulations, where the AUC ratio (post/pre surgery) was ~ 0.7 with associated decreases in fa (0.71±0.03 to 0.59±0.04). This decrease in fraction of dose absorbed is likely due to bypassing the upper gut post-RYGB surgery, which is the maximal site of absorption for azithromycin. A reduced fa would lead to reduced bioavailability and increased oral clearance (Cl/F). As a result, total systemic exposure of azithromycin decreased

significantly post RYGB compared to morbidly obese subjects after a single oral dose and at steady state.

In line with these observations, PK/PD calculations support the hypothesis that azithromycin concentrations in gastric bypass patients after surgery might be suboptimal for treating bacterial infections. $AUC_{24,SS}$/MIC ratio is generally considered the major determinant of in vivo efficacy for antibiotics like azithromycin. A reported plasma $AUC_{24,SS}$/MIC threshold of >5 is necessary for maximal clinical efficacy and bacterial killing of azithromycin [184]. PBPK model simulation predict that $AUC_{24,SS}$/MIC values above 5 were achieved for *M.catarrhalis* in both morbidly obese (Pre-surgery) subjects and gastric bypass subjects for both 3-day and 5-day regimens. However, the $AUC_{24,SS}$/MIC ratio was below the threshold value of 5 for both 3-day and 5-day regimens in both morbidly obese and gastric bypass subjects for *H. influenzae* (intermediate pathogen), although the threshold was reached for susceptible *H.influenze* in the pre-surgical population.

Overall, the $AUC_{24,SS}$/MIC results suggests that the azithromycin exposure is subinhibitory against *H.influenze* in gastric bypass subjects for the standard dosing regimens. Hence, higher azithromycin doses might be warranted over the currently employed regimens when treating infections caused by *H. influenzae* in gastric bypass subjects, although no dose modifications seem necessary for infections caused by *M. catarrhalis.* Furthermore, given the long elimination half-life (48 – 96 hrs) of azithromycin several reports have indicated that prolonged exposure of bacterial organisms to sub inhibitory antibiotic drug levels below MIC might trigger the development of macrolide resistance [190].

Cefuroxime axetil is a Biopharmaceutical Classification System (BCS) class II drug with low solubility and high permeability. It is a substrate of the PEPT-1 peptide transporter and that pathway is the primary route of absorption. The PEPT-1 peptide transporter is highly expressed in the upper gut, with expression decreasing towards the lower gut. Cefuroxime elimination is primarily through the renal route. PBPK model simulations predicted a 40 to 42% increase ($p < 0.05$) in mean cefuroxime exposure (AUC) post-RYGB surgery compared to pre-RYGB.

This increased drug exposure can be attributed to improved bioavailability via PEPT-1 active transport resulting from changes in GI anatomy and physiology after surgery. Cefuroxime axetil undergoes hydrolysis by non-specific esterases to cefuroxime in the intestinal lumen. The prodrug that avoids intestinal degradation undergoes PEPT-1 mediated uptake into the intestinal mucosa, where is then then hydrolyzed to cefuroxime [54]. The cefuroxime formed in the intestine mucosa has low permeability at the basolateral membrane. Thus, cefuroxime moves out of the intestinal mucosa into the systemic circulation at a slower rate [191]. Gastric bypass circumvents the upper gut (duodenum and proximal jejunum) region with reduced stomach capacity. When cefuroxime axetil enters the distal jejunum in gastric bypass patients, the degradation rate would be reduced since this segment this region has a higher pH. As a result, a higher fraction of cefuroxime axetil will be available for intestinal uptake in the jejunum where PEPT-1 transporter expression is higher. Thus, enhanced PEPT-1 uptake and subsequent hydrolysis leads to a higher fraction of cefuroxime reaching the systemic circulation. This could explain the higher exposure of cefuroxime in gastric bypass subjects.

The PD results, notably %T>MIC for *S. pneumoniae*, reflect that the plasma concentration of cefuroxime after oral administration is sufficient to treat infections caused by these pathogens and no dose modifications were necessary in pre-surgical and gastric bypass subjects in the treatment of infections caused by these organisms. No activity was found for *E. coli*, when MIC_{90} value from SENTRY Antimicrobial surveillance data was used. A study by Gascon et., al reported that the probability of target attainment was invariably zero for the MIC_{90} from CLSI [188] and SENTRY Antimicrobial surveillance data. The study also stated that, as most microbiological laboratories analyze the in vitro susceptibility with automated systems with straight range of concentrations, the technique introduces variability in MIC measurement due to inter-strain differences, intra-laboratory variability and inter-laboratory variability. Thus, the current or proposed clinical MICs can be a limitation in clinical routine. The study also reported that with MIC_{90} value of > 0.5 mg/L where 90% of the strains reached the target cefuroxime plasma concentrations seem to be sufficient to treat infections caused by *E.coli* . With MIC_{90} of 0.5mg/L no dose modifications seem necessary post gastric bypass surgery for treating infections caused by E.coli. For *H. influenzae,* cefuroxime concentrations reached the target %T>MIC for both the dosing regimens in post-surgical group whereas the target was reached for only 500mg BID regimen in pre-surgical group which suggests that 500mg BID regimen is preferred to 250mg BID regimen in pre-surgical populations.

Metronidazole is a Biopharmaceutical Classification System (BCS) class I drug with high solubility and high permeability. Metronidazole displays a bioavailability of over 95% in healthy volunteers. Metronidazole undergoes hepatic metabolism, and both the metronidazole and its metabolites are excreted renally (~60-80%). Gastric bypass

circumvents the upper gut, the main site of metronidazole absorption and a region with high intestinal CYP content. Thus, it is hypothesized that metronidazole exposure would be altered post gastric bypass surgery. However, PBPK model predictions found no significant difference in C_{max} and AUC post gastric bypass surgery compared to the pre-surgical population, with post-surgery mean peak plasma concentrations occurring earlier (shorter Tmax) in RYGB subjects. The drug was nearly completely absorbed both pre- and post-surgery, with predicted fa values of fa from 0.97 ± 0.05 an 0.95 ± 0.07. Likewise, no difference in systemic exposure levels was predicted for multiple dose simulations. Metronidazole is only 27% metabolized by CYP3A4 (both liver and gut), and a lower fraction of the drug would undergo gut metabolism through CYP3A4 or other CYP enzymes. The post-surgical upregulation of hepatic CYP3A4 and other CYP enzymes could compensate for reduction is presystemic gut metabolism in the upper gut region following surgery. This would result in no differences in metronidazole systemic exposure in gastric bypass surgical subjects.

In this aspect of research, PBPK modeling successfully predicted the exposure changes of azithromycin, cefuroxime axetil, and metronidazole post-RYGB compared to pre-surgical or morbidly obese population following single oral dose and at steady state. No dose modifications are suggested for metronidazole post-RYGB surgery. Azithromycin AUC was reduced by one-third post gastric bypass surgery compared to morbidly obese. This reduced systemic exposure of azithromycin means that the potential for treatment failure exists for patients treated with the standard drug regimen after undergoing bypass surgery. Based on the $AUC_{24h, SS}$/MIC values, a dose modification of azithromycin in gastric bypass patients seems necessary for infections caused by *H.influenze*.

For cefuroxime axetil, where model-predicted increased exposure in gastric bypass subjects, PK/PD analysis suggests that no dose modifications seem necessary for infections caused by *S. pneumoniae* and *E.coli*. For infections caused by *H. influenzae*, 500mg BID regimen is preferred to 250mg BID regimen in both pre- and post-surgical subjects. For *M. catarrhalis* target %T>MIC was not attained for both 500mg and 250mg BID regimens which poses the need for dose modifications in treating infections caused by this pathogen. No change in the exposure was observed with metronidazole, so no PK/PD analysis was performed. With these predictions, this research demonstrated that the mechanistic PBPK modeling approach could serve as a tool in examining the effect of physiological alteration following RYGB on the bioavailability of oral antibiotics in the absence of clinical data and to optimization of oral drug therapy post-RYGB.

SPECIFIC AIM 4

Specific Aim 4

Specific aim 4: To predict the relative bioavailability of azithromycin and cefuroxime axetil suspensions in post-gastric bypass population

Introduction

Obesity is a significant risk factor for multiple chronic health conditions and is often managed with behavioral modifications and drugs. However, these treatments often prove to have only limited and short-term effects [192]. As a result, bariatric procedures are becoming more popular as a long-term weight-loss strategy [193]. Following bariatric surgery, structural and physiological alterations in the GIT may affect the pharmacokinetics, specifically the absorption, of drugs taken by the patient. Nutritional deficiencies in post-bariatric surgery patients have been examined and reported in a reasonable manner [194]. However, there is surprisingly scarce information available on changes in oral drug absorption following bariatric surgery. Furthermore, rather than large, randomized studies, current information is typically obtained from case reports and studies with a small number of participants. This scarcity of information limits the ability of medical professionals to produce clear recommendations on what changes, if any should be made to the dosing regimen of drugs following bariatric surgery, so this critical subject is often overlooked.

Drug absorption from the GI tract is divided into various phases, each of which may be altered following bariatric surgery. For solid, immediate-release (IR) oral drug products, the initial step disintegration and subsequent release of the drug into the stomach [195]. Gastric motility, which is often important to the disintegration of the drug, maybe

impaired following bariatric surgeries. The drug must dissolve in the GI fluids after it is released from the drug product. Dissolution, like disintegration, is influenced by several physiological factors in the stomach, all of which are subject to changes as a result of bariatric surgery: dissolution may be slowed by impaired gastric motility, as the drug is poorly mixed with stomach contents and its transfer to the duodenum is delayed. Furthermore, the reduced gastric volume following bariatric surgery reduces the amount of fluid remaining in the stomach to dissolve the drug. Moreover, the solubility of many drugs is influenced by gastric pH [196], which is significantly increased following bariatric surgery. As a result, the solubility of basic drugs may be reduced after bariatric surgery, while acidic drug solubility may improve.

The GI alterations post-RYGB pose potential concerns for solid oral IR drug formulations that must disintegrate and dissolve in the stomach effectively. On the other hand, gastric processes have a lesser role in drug release from controlled-release oral dose forms and even less so in liquid formulations (syrup, solution, etc.). As a result, individuals who have had bariatric surgery may find it helpful to transition from oral solid IR drug formulations to other dosage forms more resistant to gastrointestinal alterations that could impact the rate and extent of absorption. Indeed, a recent review of the literature found a strong trend of moving post-surgery patients from solid to liquid formulations across numerous therapeutic classes [197].

Azithromycin has shown good stability at low pH, and azithromycin is absorbed mainly in the duodenum, jejunum, or both. Cefuroxime axetil disintegrates and is released in the stomach after being taken orally, and it is rapidly hydrolyzed to cefuroxime and delivered into the systemic circulation following intestinal uptake of prodrug. On the other

hand, cefuroxime axetil suspension gets released in the upper small intestine. Because the processes of disintegration and dissolution of tablets are directly dependent on the fluid content, pH, and motility of GIT, it is hypothesized that any physiological changes in the GI tract following gastric bypass surgery may interfere with the rate and extent of absorption of azithromycin and cefuroxime axetil, especially when given in tablet form.

The majority of previous studies recommend prescribing an oral solution for all drug classes, presuming that tablet absorption issues may arise after gastric bypass surgery. Azithromycin AUC reduced by one-third in gastric bypass patients for tablet formulations. whereas cefuroxime axetil exposure (AUC) increased after gastric bypass. The bioavailability of cefuroxime axetil oral suspension is only 40-45% when compared to the 60% bioavailability of tablets, therefore the oral suspension and tablets cannot have substituted each other on a mg-to-mg basis [198]. With suspension formulations having lower bioavailability compared to tablet formulation of cefuroxime axetil, it is important to identify any changes in the bioavailability of the suspension formulation post gastric bypass. Therefore, this aspect of the research aimed to evaluate the effect of RYGB on the bioavailability of azithromycin and cefuroxime axetil suspension in comparison to tablet formulation and to perform the PK/PD analysis by calculating $AUC_{24h,SS}$/MIC for azithromycin and $\%T_{>MIC}$ for cefuroxime axetil.

Modeling strategy

The azithromycin PBPK model developed and verified following 500mg suspension under specific aim 2 was extended to predict the bioavailability of azithromycin suspension following doses of 500mg single dose: 3-day and 5-day regimens in post-surgical

population. An ADAM model was used to predict the absorption, and the full PBPK model was used to predict the distribution of azithromycin. A virtual clinical trial with a population size of 240 (10 trials with 24 male subjects), aged between 21 and 31 years, under fasting condition was carried out with 500mg single dose, 3-day (500mg QD for 3 days) and 5-day (500mg day 1 and 250mg day 2-5) regimens of azithromycin suspension. Demographic data for all the simulations in post-surgical populations were shown in Table 34.

Likewise, PBPK modeling was used to predict exposure changes of cefuroxime after administration of a cefuroxime axetil suspension in the post-surgical population. An ADAM model and a full PBPK model were used to predict the absorption and distribution of cefuroxime. A virtual clinical trial of 350 (10 trials with 35 subjects), 50% females, aged 18 to 55 years, under fasting conditions were carried for a suspension dose of 500mg BID and 250mg BID for 5 days. Demographic data for all the simulations in post-surgical populations were shown in Table 34.

Table 34: Study design for Simcyp® simulations of azithromycin and cefuroxime axetil suspension formulations in postsurgical population

	Azithromycin Suspension			**Cefuroxime axetil Suspension**	
	500mg Single Dose Suspn	**3-Day Regimen (Suspn)**	**5-Day regimen (Suspn)**	**500mg BID Suspn**	**250mg BID Suspn**
No. of Trials	5	5	5	10	10
No of subjects in each Trial	24	24	24	35	35
Age (years)	21-31	21-31	21-31	18-55	18-55
% of females	0	0	0	50	50
Duration of study (h)	24	288	288	96	96
Dosage regimen	500mg Single Dose	500mg daily for 3 days	500mg Day 1 250mg day 2-5	500mg BID for 5 Days	250mg BID for 5 Days

PK/PD Integration

The MIC_{90} values for the relevant organisms for azithromycin and cefuroxime axetil were obtained from SENTRY Antimicrobial surveillance data [https://sentry-mvp.jmilabs.com/app/sentry-public] and other studies available in the literature [184 - 187]. AUC/MIC for relevant pathogens were calculated as the area under the concentration-time curve over 24 h at steady state divided by the MIC for standard 3-day and 5-day regimen of azithromycin in pre- (morbidly obese) and post-surgical (gastric bypass) subjects for suspension formulations and compared to AUC/MIC of tablet formulation. The $\%T_{>MIC}$ for cefuroxime axetil was calculated using equation 5 for standard regimens of 500mg q12h and 250mg q12h in pre-surgical and post-surgical subjects. The %T>MIC of suspension formulation was compared to tablet formulation to interpret the superiority of suspensions to tablets.

Results

The model predicted mean plasma concentration profile of azithromycin suspension following 500mg single dose, 3-day, and 5-day regimens in post-gastric bypass subjects was depicted in Figures 38-40. Figures 41-43 compares the plasma concentration profile of azithromycin suspension to a tablet formulation administered at different dosing frequencies. Table 35 presents the PBPK model simulated pharmacokinetic parameters of azithromycin suspension in post-surgical patients. The predicted AUC post-surgery following a single dose of 500mg azithromycin suspension is 3 times higher than the AUC following a single oral dose of 500mg tablet ($p < 0.05$). The predicted AUC in post-surgical patients following 3-day and 5-day regimens of azithromycin suspension is 1.4 and 1.5 times ($p < 0.05$) higher (22.00 ± 5.16 mg.h/L vs. 15.71 ± 5.36 mg.h/L, 22.15 ± 4.47mg.h/L vs. 14.47±3.42mg.h/L) than the AUC following 3-day and 5-day regimen of azithromycin tablets. Fraction absorbed (fa) increased from 0.56 to 0.7 (1.25 times higher) following a suspension compared to tablet in gastric bypass subjects.

To evaluate the clinical efficacy of azithromycin suspension compared to the tablet formulation, AUC(24h, SS)/MIC ratios were calculated for different pathogens in post-surgical populations for 3-day and 5-day regimens. Tables 36 and 37 presents the MIC values and the calculated $AUC_{(24h,\ SS)}$/MIC for suspension and tablet formulations. The calculation of $AUC_{24,\ SS}$/MIC ratios suggests that azithromycin concentrations reached the target concentration of 5 for susceptible *H. influenzae* for suspension formulation for both 3-day and 5-day regimens in gastric bypass subjects compared to tablet formulation. However, for intermediate *H.influenze,* the threshold concentration was not reached for either dosing regimen in gastric bypass subjects for tablet or suspension formulation.

Table 35: Pharmacokinetic parameters of azithromycin suspension and tablet following single dose administration and at steady state in postsurgical population

	Cmax (mg/L)		AUC_{0-t} (mg.h/L)		Tmax (h)	
	Tablet	**Suspension**	**Tablet**	**Suspension**	**Tablet**	**Suspension**
500mg Single Dose	0.23 ± 0.05	0.41 ± 0.09	1.69 ± 0.51	5.16 ± 1.77	2.1	1.2
500mg QD for 3days	0.28 ± 0.07	0.47 ± 0.13	15.71 ± 5.36	22.0 ± 5.16	2.4	0.96
500mg day 1, 250mg day 2 - 5	0.28 ± 0.06	0.49 ± 0.10	14.47 ± 3.42	22.15 ± 4.47	2.88	1.4

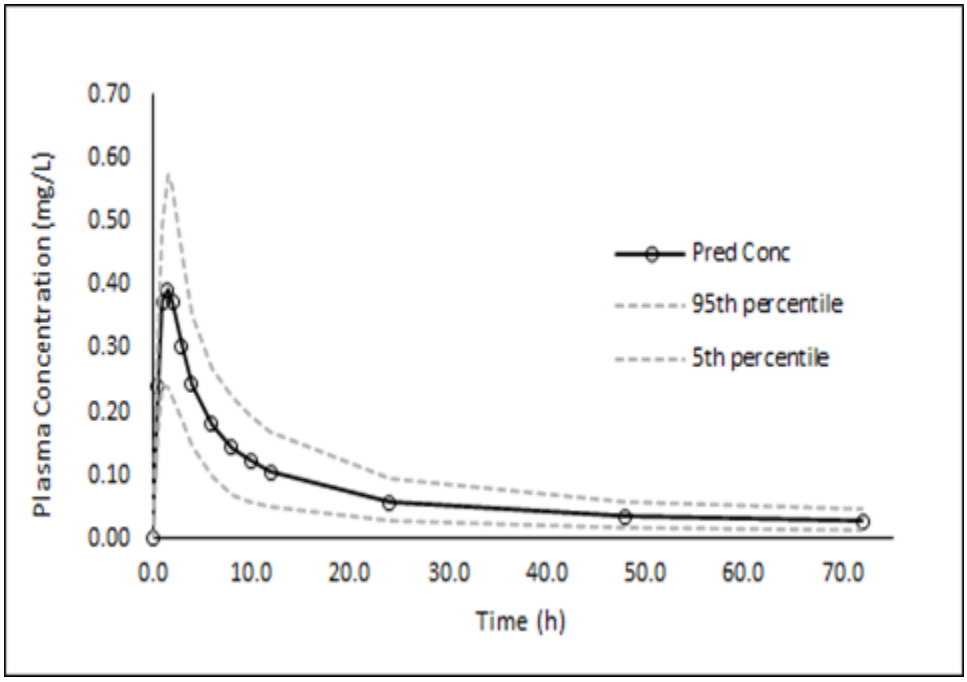

Figure 38: Predicted (solid line) concentration time profiles of 500mg oral azithromycin suspension in post RYGB surgery subjects with 5% and 95% confidence predicted interval (grey dashed lines).

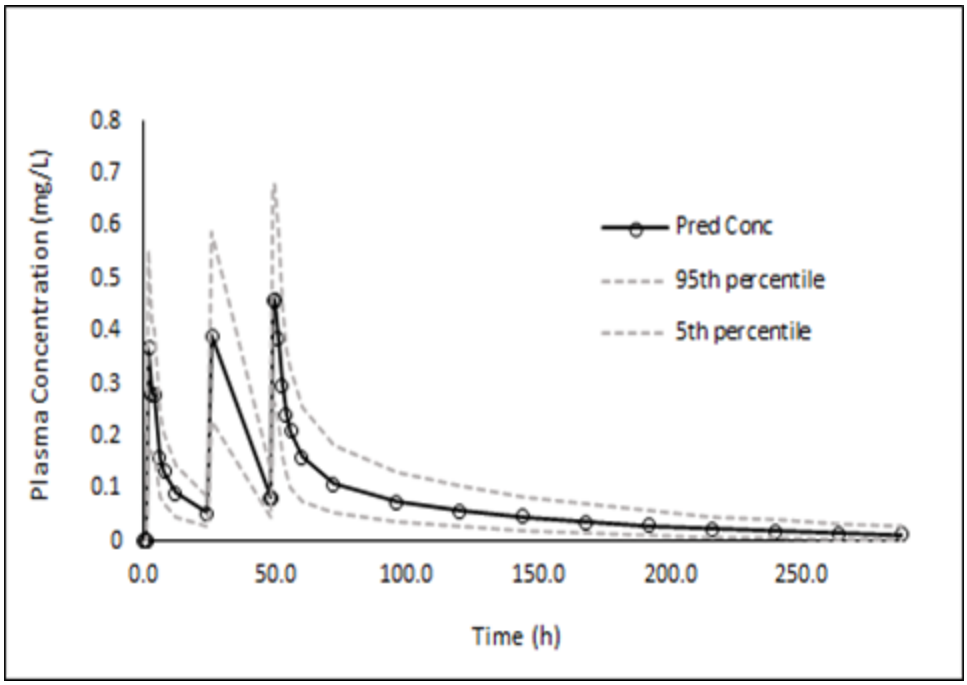

Figure 39: Predicted (solid line) concentration time profiles of 500mg oral azithromycin suspension for 3 days in post RYGB surgery subjects with 5% and 95% confidence predicted interval (grey dashed lines).

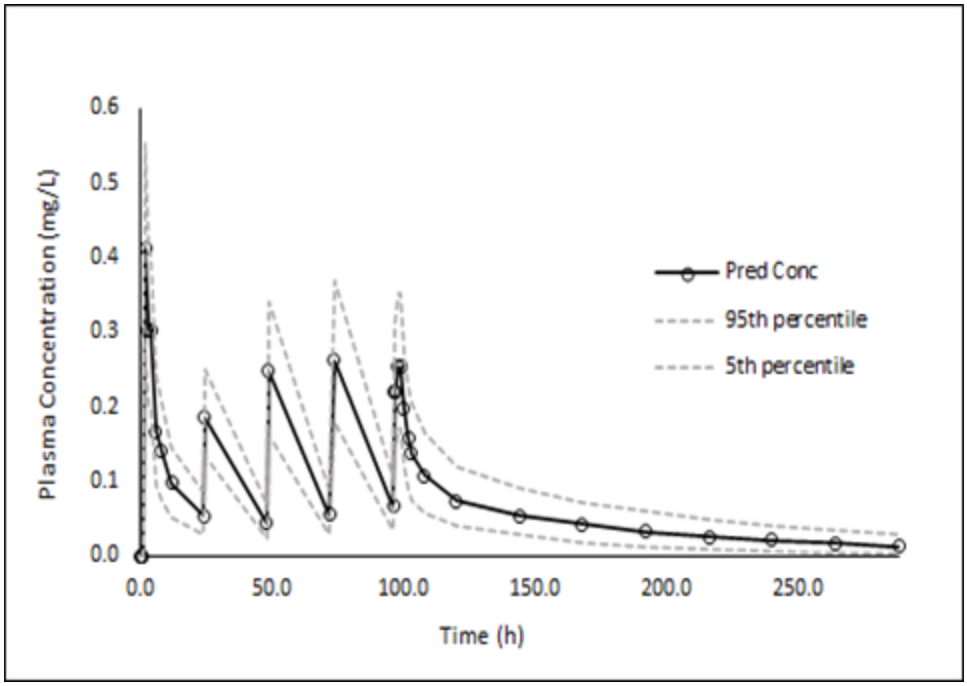

Figure 40: Predicted (solid line) concentration time profiles of 5-day regimen of oral azithromycin suspension in post RYGB surgery subjects with 5% and 95% confidence predicted interval (grey dashed lines).

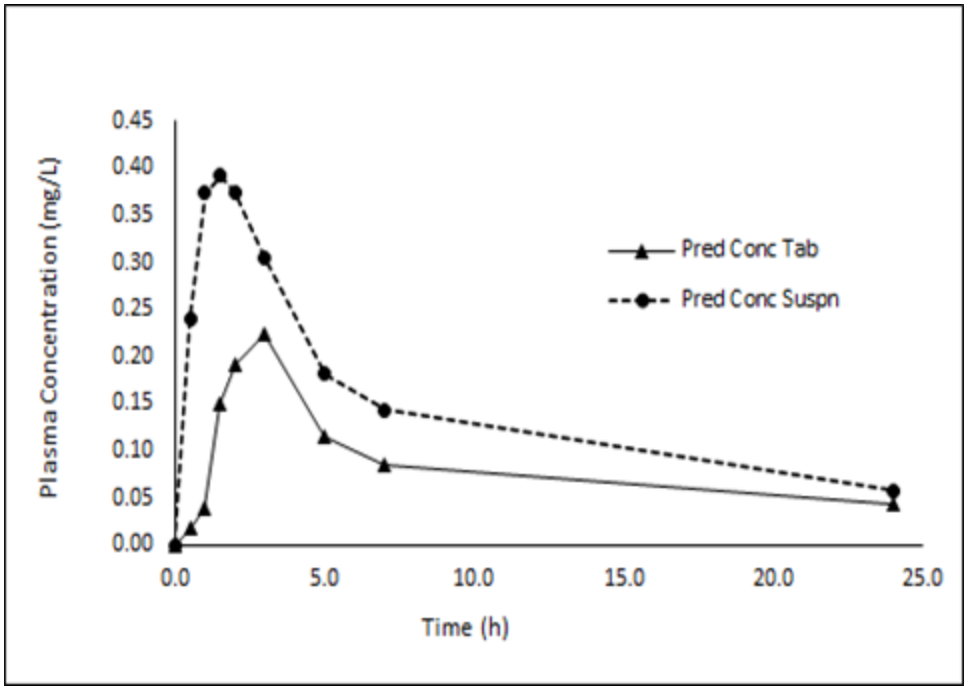

Figure 41: Predicted plasma concentration time profiles in post RYGB subjects following 500mg oral azithromycin tablet (solid triangles) and suspension (solid circles).

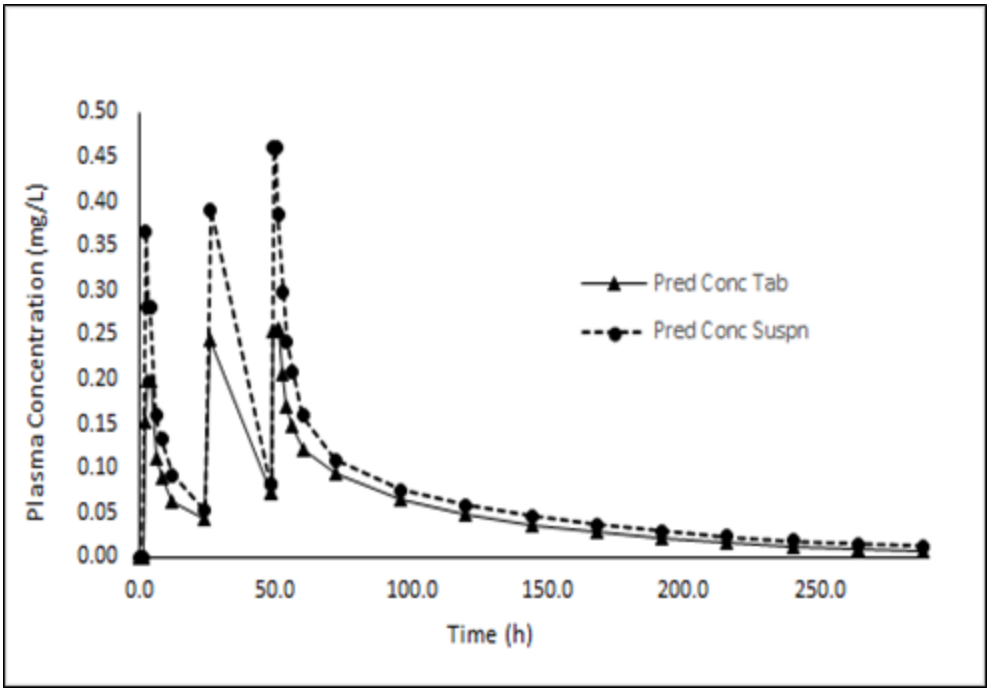

Figure 42: Predicted plasma concentration time profiles in post RYGB subjects following 500mg oral azithromycin tablet (solid triangles) and suspension (solid circles) for 3 days.

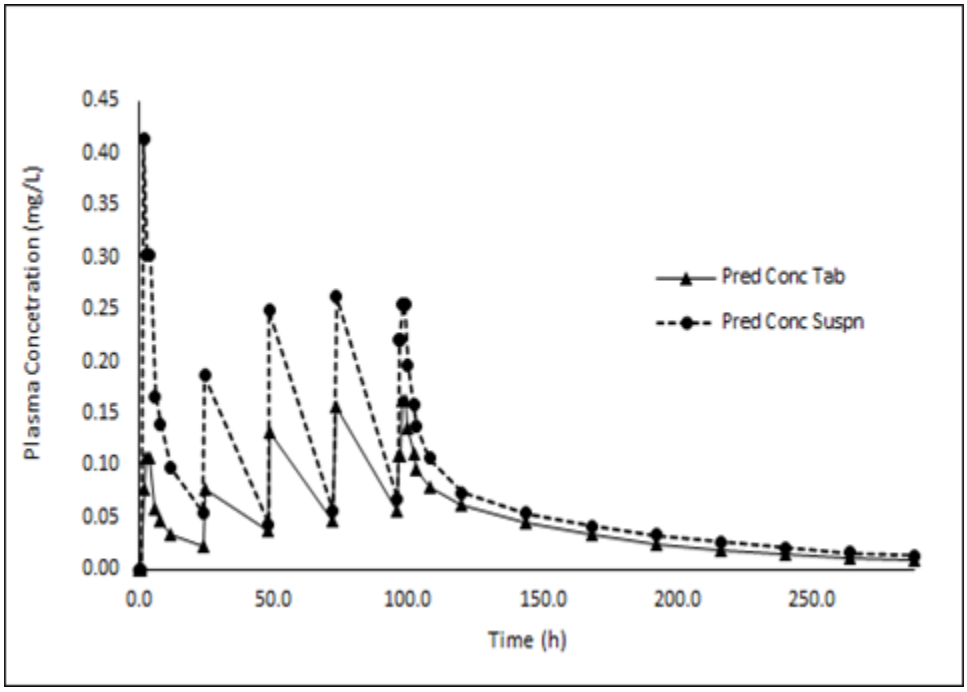

Figure 43: Predicted plasma concentration time profiles in post RYGB subjects following 5-day regimen of azithromycin tablet (solid triangles) and suspension (solid circles).

Table 36: Azithromycin suspension and tablet $AUC_{(24h, SS)}$/MIC ratios for relevant pathogens in post-surgical subjects for 3-day regimen (500mg QD for 3 days)

MIC	**AUC_{24} (mg.h/L)**		**AUC_{24} (mg.h/L)**		**AUC/MIC**		**AUC/MIC**	
	Pre-surgery		**Post-surgery**		**Pre-surgery**		**Post-surgery**	
	Tablet	**Suspn**	**Tablet**	**Suspn**	**Tablet**	**Suspn**	**Tablet**	**Suspn**
1 mg/L (*H. influenzae*)	4.25	5.2	2.38	4.1	4.25	5.2	2.38	4.1
0.5 mg/L (*H. influenzae*)	4.25	5.2	2.38	4.1	8.5	10.4	4.76	8.2
0.06 mg/L (*M.catarrhalis*)	4.25	5.2	2.38	4.1	70.83	86.67	39.67	68.33

Table 37: Azithromycin suspension and tablet $AUC_{(24h, SS)}$/MIC ratios for relevant pathogens in post-surgical subjects 5-day regimen (500mg day 1 and 250mg day 2 to day 5)

MIC	**AUC_{24} (mg.h/L)**		**AUC_{24} (mg.h/L)**		**AUC/MIC**		**AUC/MIC**	
	Pre-surgery		**Post-surgery**		**Pre-surgery**		**Post-surgery**	
	Tablet	**Suspn**	**Tablet**	**Suspn**	**Tablet**	**Suspn**	**Tablet**	**Suspn**
1 mg/L (*H. influenzae*)	3.2	3.3	2.2	3.1	3.2	3.3	2.2	3.1
0.5 mg/L (*H. influenzae*)	3.2	3.3	2.2	3.1	6.4	6.6	4.4	6.2
0.06 mg/L (*M.catarrhalis*)	3.2	3.3	2.2	3.1	53.33	55.00	36.67	51.67

The model predicted mean plasma concentration profile of cefuroxime axetil suspension following 500mg BID and 250mg BID dosing in post-gastric bypass subjects was depicted in Figures 44 and 45. Table 38 shows the predicted pharmacokinetic parameters of cefuroxime axetil suspension in post-surgical patients following two dosing frequencies. The predicted AUC post-surgery following a 500mg BID dosing of cefuroxime axetil suspension is similar to AUC following 500mg BID tablet (16.1 ± 4.4 µg.h/ml for suspension vs. 17.0 ± 5.6 µg.h/ml for tablet). A similar trend was observed for 250mg BID dosing of cefuroxime axetil suspension (9.5 ± 1.8 µg.h/ml for suspension vs. 9.5 ± 1.7 µg.h/ml for tablet).

The exposure-effect relationship for oral cefuroxime was estimated by calculating the %T>MIC value for relevant pathogens. Table 39 presents the MIC_{90} values and %T>MIC for different pathogens in (morbidly obese) and post-surgical populations for suspension and tablet formulation. %T>MIC values show that the standard dosages of 500mg q12h reached the recommended target of ≥50% for all the listed pathogens, and the %T>MIC of suspension formulation was similar to that of tablet formulation.

Table 38: Pharmacokinetic parameters of cefuroxime axetil suspension and tablet at steady state in postsurgical population

	Cmax (µg/ml)		**AUC (µg.h/ml)**		**Tmax (h)**	
	Tablet	**Suspension**	**Tablet**	**Suspension**	**Tablet**	**Suspension**
500mg BID	3.8 ± 1.5	3.7 ± 1.4	17.0 ± 5.6	16.1 ± 4.4	2.4	1.92
250mg BID	2.6 ± 0.8	2.6 ± 0.8	9.5 ± 1.7	9.5 ± 1.8	2.03	1.44

Table 39: Calculated %T$_{>}$ MIC$_{90}$ for cefuroxime axetil tablet and suspension in pre-surgery (morbidly obese) and post-surgery (gastric bypass) for relevant pathogens

Pathogen	MIC $_{90}$ (mg/L)	%T>MIC (Post-surgery)			
		500mg BID		250mg BID	
		Tablet	Suspn	Tablet	Suspn
Gram-negative bacteria					
Escherichia coli	0.5	64.58	62.50	50.00	50.00
H. influenzae	1	50.00	58.33	45.83	45.83
Gram Positive bacteria					
S. Pneumoniae (Penicillin Susceptible)	≤ 0.012	100	100	100	100

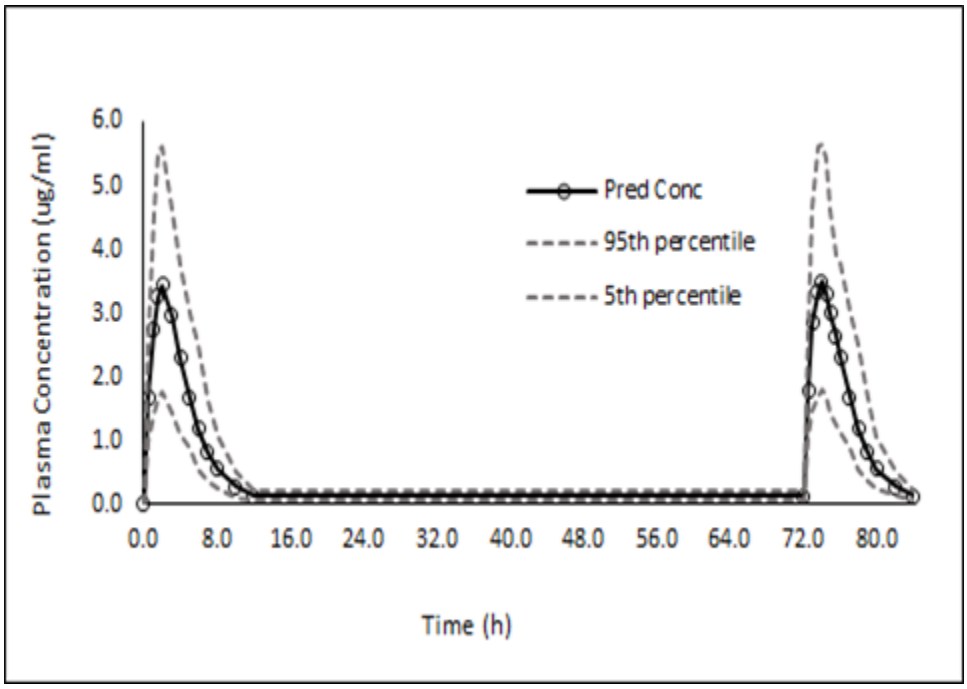

Figure 44: Predicted (solid line) concentration time profiles of 500mg BID dosing of cefuroxime axetil suspension in Post RYGB surgery subjects with 5% and 95% confidence predicted interval (grey dashed lines).

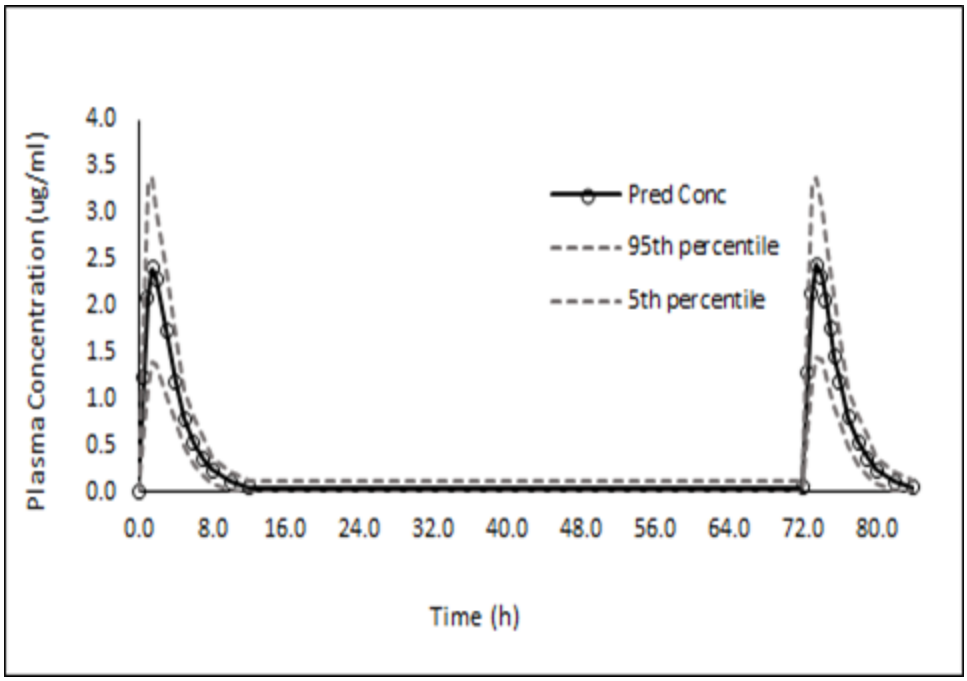

Figure 45: Predicted (solid line) concentration time profiles of 250mg BID dosing of cefuroxime axetil suspension in Post RYGB surgery subjects with 5% and 95% confidence predicted interval (grey dashed lines).

Discussion

There is an increased prevalence in obesity, resulting in an increased in the number of bariatric procedures being performed. The physiology of GIT is highly altered post gastric bypass surgery. Patients may present with absorption-related issues after surgery because of the reduced intestinal length, increased gastric pH, altered gastric motility. These physiological alterations post-surgery could alter the disintegration and dissolution of immediate-release solid dosage forms that are orally administered to patients, which could thereby affect bioavailability. In contrast, disintegration and dissolution in the stomach has a minimal role in the release of drugs from both the controlled-release oral dosage forms and even less role in the in vivo performance of liquid formulations like

suspensions, and oral solutions. As a result, switching from oral solid immediate-release drug formulations to liquid dosage forms may be beneficial for individuals who have had bariatric surgery. A recent literature analysis suggests a clear trend of switching from solid to liquid formulations across several therapeutic classes post gastric bypass surgery [199].

Minimal information is available regarding potential changes in the absorption/bioavailability of oral antibiotics post-gastric bypass surgery, which leads to ambiguity about how to prescribe oral antibiotics in this population to avoid the risk of therapeutic failure. This aspect of research aimed to characterize the relative oral bioavailability of oral formulations for antibiotics azithromycin and cefuroxime axetil in RYGB patients. The results found that azithromycin tablet formulation presented a slower rate of absorption and lower bioavailability in comparison to suspension formulation in RYGB bariatric subjects. On the other hand, no significant difference was observed for cefuroxime axetil formulations.

Azithromycin is a BCS class II drug (high permeability/low solubility). Solubility is the rate-limiting step for the bioavailability of azithromycin. At the doses used in this study, a lower Cmax and a delayed Tmax were observed for the solid oral dosage form compared to suspension formulation. The tablet formulation requires prior disintegration and dissolution of the drug to be released and thereby to be absorbed. The reduced capacity of the stomach results in a significant reduction in gastric retention time. It is expected that azithromycin tablets move at the same speed as, or slightly slower than, water directly into the distal jejunum due to the bypass of the proximal intestine, where the water is rapidly absorbed. This results in tablets losing contact with water faster, thereby affecting the process of disintegration and dissolution. Reduced bioavailability of azithromycin may

therefore be a consequence of the reduced length of the intestine and shorter gastric retention time as the azithromycin tablets may not dissolve completely and therefore affecting the absorption [200-202]. The suspension formulation, by contrast, has fewer limitations since there is no need for disintegration and dissolution of the formulation, and therefore the drug is readily available for absorption. As per the study results, PBPK model simulations demonstrated that azithromycin tablets had a lower bioavailability than the suspension formulation in RYGB patients and systemic exposure was comparable to the pre-surgical exposure of tablet formulation. PK/PD analysis of azithromycin tablets and suspension for 3-day and 5-day regimens revealed that suspension formulation reached the threshold concentration for both the dosing regimens in gastric bypass subjects for *H. Influenzae* for susceptible group whereas for intermediate susceptible group the threshold was not achieved by either tablet or suspension formulation. However, for pathogens like *M.catarhallis*. threshold concentration was reached by both tablet and suspension formulation and for both the dosing regimens. Reduced bioavailability is likely to cause a therapeutic failure in infections caused by these pathogens since the dosage regimens used in the study are the recommended doses for treating infections. Therefore, these findings suggest that suspension formulation for azithromycin could be a better alternative for respiratory infections in the gastric bypass population.

Cefuroxime axetil is also a BCS class II drug, where dissolution is the rate-limiting step for cefuroxime axetil absorption. Accordingly, a similar trend to what was seen for azithromycin was anticipated for cefuroxime axetil. However, the oral suspension of cefuroxime axetil did not meet standards of bioequivalence to tablets when tested in healthy adults. As per the study results, the bioavailability of tablet and suspension

formulations of cefuroxime axetil was similar in gastric bypass subjects. The suspension formulation of cefuroxime tends to be released in the upper intestinal region and the bypass of the upper intestine would result in release of drug in distal part of the intestine. With higher pH in Jejunum II results in lesser degradation of cefuroxime axetil to cefuroxime there by increasing the concentration of cefuroxime axetil in comparison to tablet formulation. The pharmacodynamic analysis of these different regimens of antibiotics tested in this research suggest that dose modification is necessary for azithromycin tablet formulation, however, suspension formulation seem to attain the recommended AUC24h/MIC for respiratory infections. For cefuroxime axetil dose modifications do not seem necessary for infections caused by *E.coli* in the gastric bypass population either for tablet or suspension. For infections caused by *H.influenzae* and *M.catarrhalis* 500mg BID regimen of either tablet or suspension can be preferred over 250mg BID as target %T>MIC was reached. On the other hand, the %T>MIC was above the maximum effective activity for cefuroxime axetil in pneumococcal infections.

SUMMARY & CONCLUSIONS

Summary and Conclusions

Obesity has reached epidemic proportions, and various treatment approaches, including diet, exercise, behavioral, and pharmaceutical therapy, have been employed to combat the disorder. However, if none of these treatments succeed, the morbidly obese may be qualified for bariatric surgery as a last resort, depending on various variables. The most frequent bariatric surgical procedure is the Roux-en-Y gastric bypass (RYGB). It is considered a gold standard approach due to the reproducibility of results and is the most widely performed surgical intervention globally. The Roux-en-Y gastric bypass limits the obese person's intake and absorption capacity by a combination of the small gastric reservoir with a nonabsorbent component, resulting in increased weight loss. However, anatomical alterations caused by this form of bariatric surgery may interfere with the oral absorption processes of various drugs, thereby altering their pharmacokinetic profiles. Furthermore, there are no universally accepted recommendations for the proper dosing of medications to obese people. As a result, there are some uncertainties about predicting how bariatric surgery/gastric bypass surgery may affect the pharmacokinetics of individual medications [203].

Given the rising number of bariatric surgeries and the paucity of clinical studies evaluating the effect of this surgical procedure on drug pharmacokinetics, there is a growing need to conduct this type of research to help healthcare professionals prescribe medicines safely and effectively for patients who have undergone this procedure.

In this thesis, a systems pharmacology approach was used to systemic drug exposure after oral administration with a focus on the gastrointestinal component

following gastric bypass surgery, using physiologically based pharmacokinetic modeling and simulation (PBPK M&S). The interaction between oral drug absorption and metabolism in the gut wall was explored for three oral antibiotics in order to predict changes in systemic exposure. The cases that were looked at were PBPK M&S of trends in oral drug exposure in a morbidly obese patient population undergoing gastric bypass surgery, as well as the development of the post gastric bypass model. A systematic approach was used to develop PBPK M&S for oral drug bioavailability and systemic exposure post gastric bypass PBPK models, which included identifying population-dependent intrinsic factors, characterization of systems parameters, model development, and implementation based on the Simcyp ADAM model, a mechanistic model for oral drug bioavailability and verification against clinical data was used to evaluate the developed model. The verification exercise of post-bariatric surgery PBPK models yielded results that were reflective of well-characterized system intrinsic factor parameters. The post-surgical model was highly predictive of clinical outcomes of atorvastatin acid oral drug exposure, which was used for verification of the post-surgical model. Additional verification was done prospectively through generation of clinical data of midazolam pre to post gastric bypass surgery by Chan et al., [91]. The research found that the pre- to post-surgical trend in oral exposure for atorvastatin acid was highly variable. The overall trend in simulated atorvastatin oral drug exposure pre and post RYGB was similar with the reported data. In comparison to controls, the study found a substantial increase in absorption rate with no significant change in overall exposure for midazolam after RYGB surgery.

After verifying the post gastric bypass surgery model, the interplay between oral drug absorption and metabolism occurring in the GI tract was explored for three chosen oral antibiotics azithromycin, cefuroxime axetil, and metronidazole. PBPK models for the three drugs were developed by including the physicochemical parameters and additional parameters relating to absorption, distribution, metabolism, and transport of the substrate drugs. The PBPK modeling was implemented based on the Simcyp ADAM model, a mechanistic model for oral drug bioavailability and verification against clinical data in healthy volunteers was used to evaluate the developed models.

The developed PBPK models were used to explore the impact of physiological alterations after gastric bypass surgery on the oral drug bioavailability of azithromycin, cefuroxime axetil, and metronidazole for solid and liquid administrations. The research found a decrease in pre- to post-surgical systemic exposure following oral administration of azithromycin tablets post gastric bypass surgery. Moreover, the liquid formulation displayed enhanced absorption and bioavailability compared to the tablet formulation of azithromycin. Cefuroxime axetil exposure increased post gastric bypass surgery for both solid and liquid formulation. No significant change in the oral exposure of metronidazole was observed in the post gastric bypass population.

PK/PD analysis was performed using PD indices AUC24h, ss/MIC for concentration-killing antibiotic azithromycin, and %T>MIC for time-killing antibiotics to assess the potential for either therapeutic failure cefuroxime. PK/PD evaluation revealed that threshold concentration was not achieved for azithromycin tablet formulation in gastric bypass population for respiratory infection caused by *H.influenza* compared to pre-surgical subjects. Azithromycin suspension can be a better alternative to azithromycin

tablets in gastric bypass subjects to treat respiratory infections. The recommended target of T>50% was achieved for *E.coli* and 500mg BID regimen for *H.influenze*, thereby, no dose modifications seem necessary. %T was >70% (maximum effective concentration) for *S. pneumonia* after tablet and suspension. Overall, dose modifications or therapeutic monitoring might be necessary for azithromycin for respiratory infections caused by *H. influenzae* and for cefuroxime axetil and metronidazole no dose modifications are not needed post gastric bypass surgery.

Developed post-bariatric surgery PBPK models provide a framework for theoretical exploration of physiological mechanisms associated with altered oral drug exposure pre- to post-surgery, which could be attributed to the interplay between dissolution, absorption, and gut-wall metabolism, where dissolution and formulation properties emerged as the perhaps most essential parameters in predicting the exposure following surgery. At its full potential, post-bariatric surgery models can improve pharmacotherapy, clinical decision-making, and drug regulation. User interface advances in population based PBPK software such as the Simcyp® Simulator may make it viable to apply gastric bypass surgery PBPK models in clinical pharmacology. However, utilization may be limited due to the required functionality knowledge to perform M&S of new drugs. In conclusion, developed post gastric bypass surgery models provide a framework for studying mechanisms involved in altering oral drug exposure and potentially provide a framework for pharmacotherapeutic drug optimization. Furthermore, through the successful prediction of oral drug exposure in post-bariatric surgery patient populations, the utilized template model, ADAM, incorporated into the Simcyp® Simulator, is further validated.

REFERENCES

References

1) *Obesity and Overweight. Fact sheet 311.* 2018 [cited 2018 February 16].

2) (NCD-risc)., N.R.F.C., Trends in adult body-mass index in 200 countries from 1975 to 2014: a pooled analysis of 1698 population-based measurement studies with 19·2 million participants. April 2016. 387(10026).

3) Smith, K. B., & Smith, M. S. (2016). Obesity Statistics. Primary Care - *Clinics in Office Practice*, 43(1), 121–135. Https://doi.org/10.1016/j.pop.2015.10.001.

4) Hales, C. M., Carroll, M. D., Fryar, C. D., & Ogden, C. L. (2017). Prevalence of Obesity Among Adults and Youth: United States, 2015–2016. NCHS data brief, no 288. Hyattsville, MD: *National Center for Health Statistics. NCHS Data Brief*, 288, 1–8. Https://pubmed.ncbi.nlm.nih.gov/26633046/.

5) Gloy, V. L., Briel, M., Bhatt, D. L., Kashyap, S. R., Schauer, P. R., Mingrone, G., Bucher, H. C., & Nordmann, A. J. (2013). Bariatric surgery versus non-surgical treatment for obesity: a systematic review and meta-analysis of randomised controlled trials. *BMJ (Clinical Research Ed.)*, 347(October), 1–16. Https://doi.org/10.1136/bmj.f5934.

6) Lu, Y., Hajifathalian, K., Ezzati, M., Woodward, M., Rimm, E. B., Danaei, G., Selmer, R., Strand, B. H., Dobson, A., Hozawa, A., Nozaki, A., Okayama, A., Rodgers, A., Tamakoshi, A., Zhou, B. F., Zhou, B., Yao, C. H., Jiang, C. Q., Gu, D. F., … Feskens, E. J. (2014). Metabolic mediators of the effects of body-mass index, overweight, and obesity on coronary heart disease and stroke: A pooled analysis of 97 prospective cohorts with 1·8 million participants. *The Lancet*, 383(9921), 970–983. Https://doi.org/10.1016/S0140- 6736(13)61836-X.

7) Flegal, K. M., Graubard, B. I., Williamson, D. F., & Gail, M. H. (2018). Excess Deaths Associated With Underweight, Overweight, and Obesity: An Evaluation of Potential Bias. Vital & Health Statistics. Series 3, *Analytical and Epidemiological Studies*, 0(42), 1–21. Http://www.ncbi.nlm.nih.gov/pubmed/30216148.

8) Nguyen, N. T., & Varela, J. E. (2017). Bariatric surgery for obesity and metabolic disorders: State of the art. *Nature Reviews Gastroenterology and Hepatology*, 14(3), 160– 169. Https://doi.org/10.1038/nrgastro.2016.170.

9) Fryar, C. D., Carroll, M. D., & Ogden, C. L. (2018). Prevalence of Overweight, Obesity, and Severe Obesity Among Children and Adolescents Aged 2–19 Years: United States, 1963–1965 Through 2015–2016. National Center for Health Statistics Health E-Stats, September, 1–6.

10) Kuczmarski RJ, O.C., Guo SS, Grummer-Strawn LM, Flegal KM, Mei Z, Wei R, Curtin LR, Roche AF, Johnson CL. (2002). 2000 CDC Growth Charts for the United States: methods and development. 11(246).

11) Alfonso-Cristancho, R., (2013). Bariatric Surgery for Severe Obesity: Determinants of Use and Economic Impact. Proquest Dissertation and Theses Global Washington.

12) Schauer, P. R., Bhatt, D. L., Kirwan, J. P., Wolski, K., Aminian, A., Brethauer, S. A., Navaneethan, S. D., Singh, R. P., Pothier, C. E., Nissen, S. E., & Kashyap, S. R. (2017). Bariatric Surgery versus Intensive Medical Therapy for Diabetes — 5-Year Outcomes. *New England Journal of Medicine*, 376(7), 641–651. Https://doi.org/10.1056/nejmoa1600869.62

13) Radaelli, M. G., Martucci, F., Perra, S., Accornero, S., Castoldi, G., Lattuada, G., Manzoni, G., & Perseghin, G. (2018). NAFLD/NASH in patients with type 2 diabetes and related treatment options. *Journal of Endocrinological Investigation*, 41(5), 509–521. Https://doi.org/10.1007/s40618-017-0799-3.

14) Barzin, M., Mousapour, P., Khalaj, A., Mahdavi, M., Valizadeh, M., & Hosseinpanah, F. (2020). The Relationship Between Preoperative Kidney Function and Weight Loss After Bariatric Surgery in Patients with Estimated Glomerular Filtration Rate ≥ 30 ml/min: *Tehran Obesity Treatment Study*. *Obesity Surgery*, 30(5), 1859–1865. Https://doi.org/10.1007/s11695-020-04407-5.

15) Knop, F. K., & Taylor, R. (2013). Mechanism of metabolic advantages after bariatric surgery: It's all gastrointestinal factors versus it's all food restriction. *Diabetes Care*, 36(SUPPL.2), 287–291. Https://doi.org/10.2337/dcs13-2032.

16) Ionson, A., (2015) proposed mechanisms for bariatric surgery-induced improvement and resolution of clinical manifestations of type ii diabetes, Proquest: Boston, United States.

17) Pucci, A., & Batterham, R. L. (2019). Mechanisms underlying the weight loss effects of RYGB and SG: similar, yet different. *Journal of Endocrinological Investigation*, 42(2), 117–128. Https://doi.org/10.1007/s40618-018-0892-2.

18) Van der Burgh, Y., Boerboom, A., de Boer, H., Witteman, B., Berends, F., & Hazebroek, E. (2020). Weight loss and malnutrition after conversion of the primary Roux-en-Y gastric bypass to distal gastric bypass in patients with morbid obesity. *Surgery for Obesity and Related Diseases*, 16(3), 381–388. Https://doi.org/10.1016/j.soard.2019.12.009.

19) Wilkinson, L. H., & Peloso, O. A. (1981). Gastric (Reservoir) Reduction for Morbid Obesity. *Archives of Surgery*, 116(5), 602–605. Https://doi.org/10.1001/archsurg.1981.01380170082014.

20) LI., K., (1987) A simple technique to reverse stapling gastric restriction operations. 44(6).

21) Mason, E. E., & Ito, C. (1967). Gastric bypass in obesity. *The Surgical Clinics of North America*, 47(6), 1345–1351. Https://doi.org/10.1016/S0039-6109(16)38384-0.

22) Hess, D. S., & Hess, D. W. (1998). Biliopancreatic diversion with a duodenal switch. *Obesity Surgery*, 8(3), 267–282. Https://doi.org/10.1381/096089298765554476.

23) Nicola scopinaro, ezio gianetta, dario civalleri, umberto bonalumi, v. B. (1979). Biliopancreatic bypass for obesity: 66, 1–3.

24) Singh, A. K., Singh, R., & Kota, S. K. (2015). Bariatric surgery and diabetes remission: Who would have thought it? *Indian Journal of Endocrinology and Metabolism*, 19(5), 563– 576. Https://doi.org/10.4103/2230-8210.163113.

25) Shah, K., Johnny Nergard, B., Stray Frazier, K., Geir Leifsson, B., Aghajani, E., & Gislason, H. (2016). Long-term effects of laparoscopic Roux-en-Y gastric bypass on metabolic syndrome in patients with morbid obesity. *Surgery for Obesity and Related Diseases*, 12(8), 1449–1456. Https://doi.org/10.1016/j.soard.2016.03.017.

26) Srinivas, N. R. (2016). Impact of roux-en-y gastric bypass surgery on pharmacokinetics of administered drugs: Implications and perspectives. *American Journal of Therapeutics*, 23(6), e1826–e1838. Https://doi.org/10.1097/MJT.0000000000000317.

27) Lim, R., Beekley, A., Johnson, D. C., & Davis, K. A. (2018). Early and late complications of bariatric operation. *Trauma Surgery and Acute Care Open*, 3(1), 1–7. Https://doi.org/10.1136/tsaco-2018-000219.

28) Jason Glass, A.C., Muhammad S Zeeshan, Zeeshan Ramzan, (2019). New Era: Endoscopic treatment options in obesity–a paradigm shift. 25(32).

29) Greenblatt, H. K., & Greenblatt, D. J. (2015). Altered Drug Disposition Following Bariatric Surgery: A Research Challenge. *Clinical Pharmacokinetics*, 54(6), 573–579. Https://doi.org/10.1007/s40262-015-0259-1.

30) Lloret-Linares, C. (2017). Pharmacokinetic considerations for patients with a history of bariatric surgery. *Expert Opinion on Drug Metabolism and Toxicology*, 13(5), 493–496. Https://doi.org/10.1080/17425255.2017.1290796.

31) Hachon, L., Declèves, X., Faucher, P., Carette, C., & Lloret-Linares, C. (2017). RYGB and Drug Disposition: How to Do Better? Analysis of Pharmacokinetic Studies and Recommendations for Clinical Practice. *Obesity Surgery*, *27*(4), 1076–1090. https://doi.org/10.1007/s11695-016-2535-z.

32) Anita P Courcoulas , S.H.B., Rebecca H Neiberg , Sheila K Pierson , Jessie K Eagleton , Melissa A Kalarchian , James P delany , Wei Lang , John M Jakicic. (2015). Three-Year Outcomes of Bariatric Surgery vs Lifestyle Intervention for Type 2 Diabetes Mellitus Treatment: A Randomized Clinical Trial. *JAMA Surgery*, 150(10): p. 931-940.

33) Jeffrey Mechanick, A.Y., Daniel Jones, W. Garvey, Daniel Hurley, M. Mcmahon, Leslie Heinberg, Robert Kushner, Ted Adams, Scott Shikora, John Dixon, Stacy Brethauer, (2013). Clinical Practice Guidelines for the Perioperative Nutritional, Metabolic, and Nonsurgical Support of the Bariatric Surgery Patient—2013 Update: Cosponsored by American Association of Clinical Endocrinologists, *The Obesity Society, and American Society for Metabolic & Bariatric Surgery. Endocrine Practice*, 19(2): p. 337-372.

34) Goto, T., Hirayama, A., Faridi, M. K., Jr, C. A. C., & and Kohei Hasegawa. (2017). Association of Bariatric Surgery With Risk of Infectious Diseases: A Self-Controlled Case Series Analysis. *Clinical Infectious Diseases*, 65(8), 1349–1355. Https://doi.org/DOI: 10.1093/cid/cix541.

35) April Smith, B.H., Andrew Cohen, (2011). Pharmacokinetic considerations in Roux-en-Y gastric bypass patients. *American journal of Health System Pharmacy*, 68(23): p. 2241- 2247.

36) Hamilton, R., Thai, X. C., Ameri, D., & Pai, M. P. (2013). Oral bioavailability of linezolid before and after Roux-en-Y gastric bypass surgery: Is dose modification necessary in obese subjects? *Journal of Antimicrobial Chemotherapy*, 68(3), 666–673. Https://doi.org/10.1093/jac/dks431.

37) Padwal, R. S., Ben-Eltriki, M., Wang, X., Langkaas, L. A., Sharma, A. M., Birch, D. W., Karmali, S., & Brocks, D. R. (2012). Effect of gastric bypass surgery on azithromycin oral bioavailability. *Journal of Antimicrobial Chemotherapy*, 67(9), 2203–2206. Https://doi.org/10.1093/jac/dks177.

38) Susanna R Magee, G.S., Anne Hume, (2007). Malabsorption of oral antibiotics in pregnancy after gastric bypass surgery. *Journal of the Americal Board of Family Medicine*, 20(3): p. 310-313.

39) Anvari, S., Lee, Y., Lam, M., Doumouras, A. G., & Hong, D. (2020). The Effect of Bariatric Surgery on Oral Antibiotic Absorption: a Systematic Review. *Obesity Surgery*, 30(8), 2883–2892. Https://doi.org/10.1007/s11695-020-04623-z.

40) P Periti , T.M., E Mini, A Novelli, (1989). Clinical pharmacokinetic properties of the macrolide antibiotics. Effects of age and various pathophysiological states (Part I). *ClinicalPhamacokinetics*, **16**(4): p. 193-214.

41) Zhong, S.Q.a.X., (2017). Macrolides: a promising pharmacologic therapy for chronic obstructive pulmonary disease. *Therapeutic Advances in Respiratory Disease*, **11**(3): p. 147-155.

42) Mankin, N.V.-L.a.A.S., (2018). How macrolide antibiotics work. *Trends in Biochemical Sciences*, **43**(9): p. 668-684.

43) Durdica Marosevic , M.K., Zoran Jaglic, (2017). Resistance to the tetracyclines and macrolide-lincosamide-streptogramin group of antibiotics and its genetic linkage - a review. *Annals of Agriculteral and Environmental Medicine*, **24**(2): p. 338.

44) E. F. Fiese, S.H.S., (1990). Comparison of the acid stability of azithromycin and erythromycin A. *Journal of Antimicrobial Chemotherapy*, **25**(A): p. 39-47.

45) Parnham, M. J., Haber, V. E., Giamarellos-Bourboulis, E. J., Perletti, G., Verleden, G. M.,& Vos, R. (2014). Azithromycin: Mechanisms of action and their relevance for clinical applications. *Pharmacology and Therapeutics*, *143*(2), 225–245. Https://doi.org/10.1016/j.pharmthera.2014.03.003.

46) Eric Garver , E.D.H., Shawn P Shearn, Anuradha Rao, Paul A Dawson, Charles B Davis, Chao Han, (2008). Involvement of intestinal uptake transporters in the absorption of azithromycin and clarithromycin in the rat. *Drug Metabolism and Disposition*, **36**(12): p. 2492-2498.

47) Masami Sugie, E.A., Ying Lan Zhao, Shoko Torita, Masayuki Nadai, Kenji Baba, Kiyoyuki Kitaichi, Kenji Takagi, Kenzo Takagi, and Takaaki Hasegawa, (2004) Possible Involvement of the Drug Transporters P Glycoprotein and Multidrug Resistance- Associated Protein Mrp2 in Disposition of Azithromycin. *Antimicrobial agents and chemotherapy*, **48**(3): p. 809-814.

48) Xiao-Jing He , L.-M.Z., Feng Qiu, Ya-Xin Sun, Jesse Li-Ling, (2009). Influence of ABCB1gene polymorphisms on the pharmacokinetics of azithromycin among healthy Chinese Hanethnic subjects. *Pharmacological reports* **61**(5): p. 843-850.

49) Wj, H., & Wx, H. (2014). The Role of Transporters in the Pharmacokinetics of AntibioticsAdvances in Pharmacoepidemiology & Drug Safety. *Pharmacoepidemiol Drug Saf*, *3*(4), 1–11. Https://doi.org/10.4172/2167-1052.

50) Fohner, A. E., Sparreboom, A., Altman, R. B., & Klein, T. E. (2017). Pharmgkb summary: Macrolide antibiotic pathway, pharmacokinetics/pharmacodynamics. *Pharmacogenetics and Genomics*, *27*(4), 164–167. Https://doi.org/10.1097/FPC.0000000000000270.

51) Michael, J. (1989). Formulary Forum. *Annals of Pharmacotherapy*, *23*, 839–846.

52) Stella Valentino J, Borchardt Ronald T, Hageman Michael J, Oliyai Reza, Maag Hans, T. J. W. (2008). Case Study: Cefuroxime Axetil: An Oral Prodrug of Cefuroxime. *Prodrugs*, 1195–1205. Https://doi.org/10.1007/978-0-387-49785-3_37.

53) Beate Bretschneider (1999). Intesrinal transport of beta-lactam antibiotics- analysis of the affinity at the PEPT1, the uptake into caco-2 cell monolayers and the transepithelial flux. *Pharmaceutical Research*. 16(1): p55-61.

54) Harding, S. M., Williams, P. E. O., & Ayrton, J. (1984). Pharmacology of cefuroxime as the 1-acetoxyethyl ester in volunteers. *Antimicrobial Agents and Chemotherapy*, *25*(1), 78–82. Https://doi.org/10.1128/AAC.25.1.78.

55) Cisneros-Farrar, F., & Parsons, L. C. (2007). Antimicrobials: Classifications and Uses in Critical Care. *Critical Care Nursing Clinics of North America*, *19*(1), 43–51. Https://doi.org/10.1016/j.ccell.2006.10.004.

56) PDR (2020) PDR: Concise monograph of Ceftin®. PDR.net®.

57) Dellamonica, P. (1994). Cefuroxime axetil. *International Journal of Antimicrobial Agents*, *4*(1), 23–36. Https://doi.org/10.1016/0924-8579(94)90061-2.

58) Muhammad, I. N. (2014). Pharmacokinetic and Bioequivalence Studies of Oral Cefuroxime Axetil 250 mg Tablets in Healthy Human Subjects. *Journal of Bioequivalence & Bioavailability*, *06*(05), 149–152. Https://doi.org/10.4172/jbb.10000196.

59) Olesen, S. W., Barnett, M. L., Macfadden, D. R., Lipsitch, M., & Grad, Y. H. (2018). Trends in outpatient antibiotic use and prescribing practice among US older adults, 2011-15: Observational study. *BMJ (Online)*, *362*. Https://doi.org/10.1136/bmj.k3155.

60) Salvatore M, Meyers BR. Metronidazole. Chapter 29 In: Principles and practices of Infectious diseases edit. 7th edition. *Bennetian Delin; Mandell*: 2010. p. 419-26.

61) Houghton, G., Thorne, P., Smith, J., Templeton, R., & Collier, J. (1979). Comparison of the pharmacokinetics of metronidazole in healthy female volunteers following either a single oral or intravenous dose. *British Journal of Clinical Pharmacology*, *8*(4), 337–341. Https://doi.org/10.1111/j.1365-2125.1979.tb04715.x.

62) Ralph, E. D. (1983). Clinical Pharmacokinetics of Metronidazole. *Clinical Pharmacokinetics*, *8*(1), 43–62. Https://doi.org/10.2165/00003088-198308010-00003.

63) Loft, S., & Poulsen, H. E. (1990). Metabolism of metronidazole and antipyrine in hepatocytes isolated from mouse and rat. *Xenobiotica*, *20*(2), 185–191. Https://doi.org/10.3109/004982590090471

64) T Bergan, S Aase, O Leinebo, T Harbitz, A Olsen, I Liavag, (1984). Pharmacokinetics of metronidazole and its major metabolite after a high intravenous dose. *Scand J Gastroenterol Suppl*. 91,113-23.

65) Bergan, T., Solhaug, J. H., Søreide, O., & Leinebø, O. (1985). Comparative pharmacokinetics of metronidazole and tinidazole and their tissue penetration. *Scandinavian Journal of Gastroenterology*, *20*(8), 945–950. Https://doi.org/10.3109/00365528509088853.

66) Lau, A. H., Emmons, K., & Seligsohn, R. (1991). Pharmacokinetics of intravenous metronidazole at different dosages in healthy subjects. *International Journal of Clinical Pharmacology Therapy and Toxicology*, *29*(10), 386–390.

67) Loft, S., Døssing, M., Poulsen, H. E., Sonne, J., Olesen, K. L., Simonsen, K., & Andreasen, P. B. (1986). Influence of dose and route of administration on disposition of metronidazole and its major metabolites. *European Journal of Clinical Pharmacology*, *30*(4), 467–473. Https://doi.org/10.1007/BF00607962.

68) Pearce, R. E., Cohen-Wolkowiez, M., Sampson, M. R., & Kearns, G. L. (2013). The role of human cytochrome P450 enzymes in the formation of 2-hydroxymetronidazole: CYP2A6 is the high affinity (low Km) catalyst. *Drug Metabolism and Disposition*, *41*(9), 1686–1694. Https://doi.org/10.1124/dmd.113.052548.

69) Jospeh.L.Kuti. (2016). Optimizing Antimicrobial Pharmacodynamics : A Guide For Your Stewardship Program. *Revista Médica Clínica Las Condes*, *27*(5), 615–624. https://doi.org/https://doi.org/10.1016/j.rmclc.2016.08.001

70) Jones, H. M., & Rowland-Yeo, K. (2013). Basic concepts in physiologically based pharmacokinetic modeling in drug discovery and development. *CPT: Pharmacometrics and Systems Pharmacology*, *2*(8), 1–12. Https://doi.org/10.1038/psp.2013.41.

71) Wagner, C., Zhao, P., Pan, Y., Hsu, V., Grillo, J., Huang, S. M., & Sinha, V. (2015). Application of physiologically based pharmacokinetic (PBPK) modeling to support dose selection: Report of an FDA public workshop on PBPK. *CPT: Pharmacometrics and Systems Pharmacology*, *4*(4), 226–230. Https://doi.org/10.1002/psp4.33.

72) Shardlow, C. E., Generaux, G. T., Patel, A. H., Tai, G., Tran, T., & Bloomer, J. C. (2013). Impact of physiologically based pharmacokinetic modeling and simulation in drug development. *Drug Metabolism and Disposition*, *41*(12), 1194–2003. Https://doi.org/10.1124/dmd.113.052803.

73) Rowland-Yeo, H.J.a.K., (2013). Basic Concepts in Physiologically Based PharmacokineticModeling in Drug Discovery and Development. **2**(e63).

74) Sager, J. E., Yu, J., Ragueneau-Majlessi, I., & Isoherranen, N. (2015). Physiologically based pharmacokinetic (PBPK) modeling and simulation approaches: A systematic

review of published models, applications, and model verification. *Drug Metabolism and Disposition*, *43*(11), 1823–1837. Https://doi.org/10.1124/dmd.115.065920.

75) Zhuang, X., & Lu, C. (2016). PBPK modeling and simulation in drug research and development. *Acta Pharmaceutica Sinica B*, *6*(5), 430–440. Https://doi.org/10.1016/j.apsb.2016.04.004.

76) Ina Gesquiere , Adam S Darwich , Bart Van der Schueren , Jan de Hoon , Matthias Lannoo, Christophe Matthys , Amin Rostami , Veerle Foulon, P. A. (2015). Drug disposition andmodelling before and after gastric bypass: immediate and controlled-release metoprolol formulations. *British Jounal of Clinical Pharmacology*, *80*(5), 1021–1030. Https://doi.org/10.1111/bcp.12666.

77) Adam S Darwich , Devendra Pade, Basil J Ammori, Masoud Jamei, Darren M Ashcroft, R.-H. (2012). A mechanistic pharmacokinetic model to assess modified oral drug bioavailability post bariatric surgery in morbidly obese patients: interplay between CYP3A gut wall metabolism, permeability and dissolution. *Journal of Phamacy and Phamacology*, *64*(7), 1008–1024. Https://doi.org/10.1111/j.2042-7158.2012.01538.x.

78) M J E Brill , P A J Välitalo , A S Darwich , B van Ramshorst , H P A van Dongen , A Rostami-Hodjegan , M Danhof, C. A. J. K. (2016). Semiphysiologically based pharmacokinetic model for midazolam and CYP3A mediated metabolite 1-OH-midazolam in morbidly obese and weight loss surgery patients. *CPT: Pharmacometrics & Systems Pharmacology*, *5*(1), 20–30. Https://doi.org/10.1002/psp4.12048.

79) May Almukainzi, V. L. R. L. (2014). Modelling the Absorption of Metformin with Patients Post Gastric Bypass Surgery. *Journal of Diabetes & Metabolism*, *5*(3). Https://doi.org/http://dx.doi.org/10.4172/2155-6156.1000353.

80) AS Darwich, D.P., K Rowland-Yeo, M Jamei, A Åsberg, H Christensen, DM Ashcroftand A Rostami-Hodjegan, (2013) Evaluation of an In Silico PBPK Post-Bariatric Surgery Model through Simulating Oral Drug Bioavailability of Atorvastatin and Cyclosporine. *CPT Pharmacometrics & Systems Pharmacology*, **2.**

81) Chen KF, C.L., Lin YS, (2020). PBPK modeling of CYP3A and P-gp substrates to predict drug-drug interactions in patients undergoing Roux-en-Y gastric bypass surgery. *Journal of Pharmacokinetics and Pharmacodynamics*, **47**(5): p. 493-512.

82) Sommers, D., van Wyk, M., Moncrieff, J., & Schoeman, H. (1984). Influence of food andreduced gastric acidity on the bioavailability of bacampicillin and cefuroxime axetil. *British Journal of Clinical Pharmacology*, *18*(4), 535–539. Https://doi.org/10.1111/j.1365-2125.1984.tb02501.x.

83) Maiara Camotti Montanha, T.F.d.S.M., Conrado de Souza Alcantara, Caroline Ferraz Simões, Sandra Regina Bin Silva, Cristina Megumi Kuroda, Sérgio Seiji Yamada, Lucas Eduardo Savóia de Oliveira, Daoud Nasser, Nelson Nardo Junior, Josmar Mazucheli, Andrea Diniz, Paulo Jorge Pereira Alves Paixão, Elza Kimura, (2019). Reduced bioavailability of oral amoxicillin tablets compared to 85suspensions in Roux-en-Y gastricbypass bariatric subjects. *British Journal of Clinical Phamacology*, **85**(9): p. 2118-2125.

84) Azran, C., Wolk, O., Zur, M., Fine-Shamir, N., Shaked, G., Czeiger, D., Sebbag, G., Kister,O., Langguth, P., & Dahan, A. (2016). Oral drug therapy following bariatric surgery: an overview of fundamentals, literature and clinical recommendations. *Obesity Reviews*, *17*(11), 1050–1066. Https://doi.org/10.1111/obr.12434.

85) Adela Hruby, phd, M., & Frank B. Hu, MD, phd, M. (2015). The Epidemiology of Obesity: A Big Picture. *Pharmacoeconomics.*, *33*(7), 673–689. Https://doi.org/10.1007/s40273- 014-0243-x.

86) Huttunen, R., & Syrjänen, J. (2013). Obesity and the risk and outcome of infection. *International Journal of Obesity*, *37*(3), 333–340. Https://doi.org/10.1038/ijo.2012.62.

87) M. Christopher, A. M. L. S. (2016). Mechanisms of weight loss and improved metabolismfollowing bariatric surgery. *Physiology & Behavior*, *176*(1), 100–106. Https://doi.org/10.1111/nyas.13409.

88) Roy, D. J., Langworthy, D. R., Thurber, K. M., Lorentz, P. A., Dierkhising, R. A., & Mundi, M. S. (2017). Comparison of oral antibiotic failure rates in post-Roux-en-Y gastricbypass patients versus controls. *Surgery for Obesity and Related Diseases*, *13*(9), 1524– 1529. Https://doi.org/10.1016/j.soard.2017.03.026.

89) Higaki, K., Choe, S. Y., Löbenberg, R., Welage, L. S., & Amidon, G. L. (2008). Mechanistic understanding of time-dependent oral absorption based on gastric motor activity in humans. *European Journal of Pharmaceutics and Biopharmaceutics*, *70*(1), 313–325. Https://doi.org/10.1016/j.ejpb.2008.02.022.

90) Yska, J. P., Van Der Linde, S., Tapper, V. V., Apers, J. A., Emous, M., Totté, E. R., Wilffert, B., & Van Roon, E. N. (2013). Influence of bariatric surgery on the use and pharmacokinetics of some major drug classes. *Obesity Surgery*, *23*(6), 819–825. Https://doi.org/10.1007/s11695-013-0882-6.

91) Angeles, P. C., Robertsen, I., Seeberg, L. T., Krogstad, V., Skattebu, J., Sandbu, R., Åsberg, A., & Hjelmesæth, J. (2019). The influence of bariatric surgery on oral drug bioavailability in patients with obesity: A systematic review. *Obesity Reviews*, *20*(9), 1299–1311. Https://doi.org/10.1111/obr.12869.

92) Chan LN, L.Y., Tay-Sontheimer JC, Trawick D, Oelschlager BK, Flum DR, Patton KK, Shen DD, Horn JR. (2015). Proximal Roux-en-Y gastric bypass alters drug absorption pattern but not systemic exposure of CYP3A4 and P-glycoprotein substrates. *Pharmcotherapy*, **35**(4): p. 361-369.

93) Skottheim, I. B., Stormark, K., Christensen, H., Jakobsen, G. S., Hjelmesæth, J., Jenssen, T., Reubsaet, J. L. E., Sandbu, R., & Åsberg, A. (2009). Significantly altered systemic exposure to atorvastatin acid following gastric bypass surgery in morbidly obese patients.*Clinical Pharmacology and Therapeutics*, *86*(3), 311–318. Https://doi.org/10.1038/clpt.2009.82.

94) Jamei, M., Turner, D., Yang, J., Neuhoff, S., Polak, S., Rostami-Hodjegan, A., & Tucker, G. (2009). Population-based mechanistic prediction of oral drug absorption. *AAPS Journal*, *11*(2), 225–237. https://doi.org/10.1208/s12248-009-9099-y

95) Lennernas, H. (2003). *Clinical Pharmacokinetics of Atorvastatin*. *42*(13), 1141–1160.

96) Morse, B. L., Alberts, J. J., Posada, M. M., Rehmel, J., Kolur, A., Tham, L. S., Loghin, C.,Hillgren, K. M., Hall, S. D., & Dickinson, G. L. (2019). Physiologically-Based Pharmacokinetic Modeling of Atorvastatin Incorporating Delayed Gastric Emptying and Acid-to-Lactone Conversion. *CPT: Pharmacometrics and Systems Pharmacology*, *8*(9), 664–675. Https://doi.org/10.1002/psp4.12447.

97) Wu, X., Whitfield, L. R., & Stewart, B. H. (2000). Atorvastatin transport in the Caco-2 cellmodel: Contributions of P- glycoprotein and the proton-monocarboxylic acid co-transporter. *Pharmaceutical Research*, *17*(2), 209–215. Https://doi.org/10.1023/A:1007525616017.Watanabe, T., Kusuhara, H., Maeda, K., Kanamaru, H., Saito, Y., Hu, Z., & Sugiyama, Y.(2010). Investigation of the rate-determining process in the hepatic elimination of HMG- coa reductase inhibitors in rats and humans. *Drug Metabolism and Disposition, 38*(2), 215– 222. Https://doi.org/10.1124/dmd.109.030254.

98) Watanabe, T., Kusuhara, H., Maeda, K., Kanamaru, H., Saito, Y., Hu, Z., & Sugiyama, Y. (2010). Investigation of the rate-determining process in the hepatic elimination of HMG-coa reductase inhibitors in rats and humans. *Drug Metabolism and Disposition*, *38*(2), 215–222. Https://doi.org/10.1124/dmd.109.030254.

99) Jacobsen, B.K., A Sodner, G Kirchner, K F Sewing, P A Kollman, L Z Benet, U Christians. (2000). Lactonization is the critical first step in the disposition of 3-hydroxy3-methylgultaryl-co A reductase inhibitor arovastatin. *Drug Metabolism and Disposition*. 28(11): p 1369-1878.

100) Thomayant prueksaritanont, r.s., xiaojun fang, bennett ma, yue qiu, jiunn h. Lin, paul g. Pearson, and thomas a. Baillie. (2002). Glucuronidation of statins in animals and humans: A novel mechanism of statin lactonization. *Drug Metabolism and Disposition*, **30**(5): p. 505-512.

101) Tom J. J. Schirris, T.R., Albert Bilos, Jan A. M. Smeitink, and Frans G. M. Russel. (2015).Statin Lactonization by Uridine 5′-Diphosphoglucuronosyltransferases (ugts). *Molecular pharmaceutics*, **12**(11): p. 4048-4055.

102) Karlgren M., Vildhede A, Norinder U., Wisniewski J., Kimoto E., Lai Y., Haglund U., Artursson., (2012) Classification of Inhibitors of Hepatic Organic Anion Transporting polypeptides (OATPs): Influence of Protein Expression on Drug Drug Interaction. *Journal of Medicinal Chemistry,* **55**: p. 4740-4763.

103) YY Lau, Y.H., L Frassetto and LZ Benet, Effect of OATP1B Transporter Inhibition on the Pharmacokinetics of Atorvastatin in Healthy Volunteers. *Clinical Pharmacology andTherapeutics,* 2006. **81**(2): p. 194-204.

104) Jonathan Bullman, A.N., Kevan Van Landingham, Richard Fleck, Alain Vuong, James Miller, Sarah Alexander, and John Messenheimer, (2011). Effects of lamotrigine and phenytoin on the pharmacokinetics of atorvastatin in healthy volunteers. *Epilepsia* . **52**(7):p. 1351-1358.

105) Sweta Tandra, N.C., David R Jones, Samer Mattar, Stephen D Hall, Raj Vuppalanchi, (2013). Pharmacokinetic and pharmacodynamic alterations in the Roux-en-Y gastric bypass recipients. *Annals of Surgery*, **258**(2): p. 262-269.

106) Ming Li , I.A.M.d.G., Evita van de Steeg , Marina H de Jager , Geny M M Groothuis The consequence of regional gradients of P-gp and CYP3A4 for drug-drug interactions by P-gp inhibitors and the P-gp/CYP3A4 interplay in the human intestine ex vivo. *Toxicology In Vitro,* 2017. **40**: p. 26-33.

107) M F Paine , M.K., J M Fisher, D D Shen, K L Kunze, C L Marsh, J D Perkins, K E Thummel, Characterization of interintestinal and intraintestinal variations in human CYP3A-dependent metabolism. *The Journal of Pharmacology and Experimental Therapeutics,* 1997. **283**(3): p. 1552-1562.

108) Blot, S., & De Waele, J. J. (2005). Critical issues in the clinical management of complicated intra-abdominal infections. *Drugs*, *65*(12), 1611–1620. https://doi.org/10.2165/00003495-200565120-00002.

109) Joseph S. Solomkin, John E. Mazuski, John S. Bradley, Keith A. Rodvold, E. J. C. G., Ellen J. Baron, Patrick J. O'Neill, Anthony W. Chow, E. Patchen Dellinger, S. R. E., Sherwood Gorbach, Mary Hilfiker, Addison K. May, A. B. N., & Robert G.

Sawyer, and J. G. B. (2010). Diagnosis and management of complicated intra-abdominal infection in adults and children: Guidelines by the Surgical Infection Society and the Infectious Diseases Society of America. *Surgical infections*, *11*(1), 79–109.

110) Broulette, J., Yu, H., Pyenson, B., Iwasaki, K., & Sato, R. (2013). The incidence rate and economic burden of community-acquired pneumonia in a working-age population. *American Health and Drug Benefits*, *6*(8), 494–503.

111) Jain S, Self WH, Wunderink RG, et al. Community-acquired pneumonia requiring hospitalization among U. S. adults. *N Engl J Med* 2015; 373: 415–427.

112) Sibila O, Rodrigo-Troyano A, Shindo Y, et al. Multidrug-resistant pathogens in patients with pneumonia coming from the community. *Curr Opin Pulm Med* 2016; 22: 219–226.

113) Frei, C. R., Attridge, R. T., Mortensen, E. M., Restrepo, M. I., Yu, Y., Oramasionwu, C. U., Ruiz, J. L., & Burgess, D. S. (2010). Guideline-concordant antibiotic use and survival among patients with community-acquired pneumonia admitted to the intensive care unit. *Clinical Therapeutics*, *32*(2), 293–299. https://doi.org/10.1016/j.clinthera.2010.02.006.

114) Sucher, A., Knutsen, S., Falor, C., & Mahin, T. (2020). Updated clinical practice guidelines for community-acquired pneumonia. *U.S. Pharmacist*, 45(4), 16–20.

115) Metlay, J. P., Waterer, G. W., Long, A. C., Anzueto, A., Brozek, J., Crothers, K., Cooley, L. A., Dean, N. C., Fine, M. J., Flanders, S. A., Griffin, M. R., Metersky, M. L., Musher, D. M., Restrepo, M. I., & Whitney, C. G. (2019). Diagnosis and treatment of adults with community-acquired pneumonia. *American Journal of Respiratory and Critical Care Medicine*, *200*(7), E45–E67. https://doi.org/10.1164/rccm.201908-1581ST.

116) Bakheit, A. H. H., Al-Hadiya, B. M. H., & Abd-Elgalil, A. A. (2014). Azithromycin. In *Profiles of Drug Substances, Excipients and Related Methodology* (Vol. 39). https://doi.org/10.1016/B978-0-12-800173-8.00001-5.

117) Lode, H., Borner, K., Koeppe, P., & Schaberg, T. (1996). Azithromycin - Review of key chemical, pharmacokinetic and microbiological features. *Journal of Antimicrobial Chemotherapy*, *37*(SUPPL. C), 1–8. https://doi.org/10.1093/jac/37.suppl_c.1.

118) Girard, D., Finegan, S. M., Dunne, M. W., & Lame, M. E. (2005). Enhanced efficacy of single-dose versus multi-dose azithromycin regimens in preclinical infection models. *Journal of Antimicrobial Chemotherapy*, *56*(2), 365–371. https://doi.org/10.1093/jac/dki241.

119) Luke, D. R., & Foulds, G. (1997). Disposition of oral azithromycin in humans. *Clinical Pharmacology and Therapeutics*, *61*(6), 641–648. https://doi.org/10.1016/S0009-9236(97)90098-9.

120) Zheng, S., Matzneller, P., Zeitlinger, M., & Schmidt, S. (2014). Development of a population pharmacokinetic model characterizing the tissue distribution of azithromycin in healthy subjects. *Antimicrobial Agents and Chemotherapy*, *58*(11), 6675–6684. https://doi.org/10.1128/AAC.02904-14.

121) Oszczapowicz , E Małafiej, A Horoszewicz-Małafiej, M Szelachowska, C Kuklewicz, E Sierańska. (1995). Esters of cephalosporins. Part III. Separation and properties of the R and S isomers of the 1-acetoxyethyl ester of cefuroxime. *Acta poloniae pharmaceutica,* 52(6) 47-476.

122) Sommers, D., van Wyk, M., Moncrieff, J., & Schoeman, H. (1984). Influence of food and reduced gastric acidity on the bioavailability of bacampicillin and cefuroxime axetil. *British Journal of Clinical Pharmacology*, *18*(4), 535–539. https://doi.org/10.1111/j.1365-2125.1984.tb02501.x.

123) Leder, R. D., & Carson, D. S. (1997). Cefuroxime axetil (Ceftin®): A brief review. *Infectious Diseases in Obstetrics and Gynecology*, *5*(3), 211–214. https://doi.org/ 10.1155/S1064744997000343.

124) A. Finn, a. Straughn, M. Meyer. A. J. C. (1987). Effect of Dose and Food on the Bioavailability of Cefuroxime Axetil. *Biopharmaceutics & drug disposition*, *8*(January), 519–526.

125) Rahul Lalge, Priyanka Thipsay, Vijay kumar Shankar, Abhijeet Maurya, Manjeet Pimparade, Suresh Bandari, Feng Zhang, S. Narasimha Murthya, and Michael A. Repka. (2019). Preparation and evaluation of cefuroxime axetil gastro-retentive floating drug delivery system via hot melt extrusion technology. *Int J Pharm*, 566, 520-531.

126) Holmes, A. H., Moore, L. S. P., Sundsfjord, A., Steinbakk, M., Regmi, S., Karkey, A., Guerin, P. J., & Piddock, L. J. V. (2016). Understanding the mechanisms and drivers of antimicrobial resistance. *The Lancet*, *387*(10014), 176–187. https://doi.org/10.1016/S0140-6736(15)00473-0.

127) Lamp, K. C., Freeman, C. D., Klutman, N. E., & Lacy, M. K. (1999). Pharmacokinetics and pharmacodynamics of the nitroimidazole antimicrobials. *Clinical Pharmacokinetics*, *36*(5), 353–373. https://doi.org/10.2165/00003088-199936050-00004.

128) Idkaidek, N. M., & Najib, N. M. (2000). Enhancement of oral absorption of metronidazole suspension in humans. *European Journal of Pharmaceutics and Biopharmaceutics*, *50*(2), 213–216. https://doi.org/10.1016/S0939-6411(00)00098-9.

129) Dingsdag, S. A., & Hunter, N. (2018). Metronidazole: an update on metabolism, structure-cytotoxicity and resistance mechanisms. *The Journal of Antimicrobial Chemotherapy*, *73*(2), 265–279. https://doi.org/10.1093/jac/dkx351.

130) McFarland, J. W., Berger, C. M., Froshauer, S. A., Hayashi, S. F., Hecker, S. J., Jaynes, B. H., Jefson, M. R., Kamicker, B. J., Lipinski, C. A., Lundy, K. M., Reese, C. P., & Vu, C. B. (1997). Quantitative structure-activity relationships among macrolide antibacterial agents: In vitro and in vivo potency against Pasteurella multocida. *Journal of Medicinal Chemistry*, *40*(9), 1340–1346. https://doi.org/10.1021/jm960436i

131) Foulds, G., Shepard, R. M., & Johnson, I. B. (1990). The pharmacokinetics of azithromycin in human serum and tissues. *Journal of Antimicrobial Chemotherapy*, *25*, 73–82.

132) Milić, A., Mihaljević, V. B., Ralić, J., Bokulić, A., Nožinić, D., Tavčar, B., Mildner, B., Munić, V., Malnar, I., & Padovan, J. (2014). A comparison of in vitro ADME properties and pharmacokinetics of azithromycin and selected 15-membered ring macrolides in rodents. *European Journal of Drug Metabolism and Pharmacokinetics*, *39*(4), 263–276. https://doi.org/10.1007/s13318-013-0155-8

133) Pouretedal, H. R. (2014). Preparation and characterization of azithromycin nanodrug using solvent/antisolvent method. *International Nano Letters*, *4*(1). https://doi.org/10.1007/s40089-014-0103-x

134) Luke, D. R., Foulds, G., Cohen, S. F., & Levy, B. (1996). Safety, toleration, and pharmacokinetics of intravenous azithromycin. *Antimicrobial Agents and Chemotherapy*, *40*(11), 2577–2581. https://doi.org/10.1128/aac.40.11.2577

135) Lalak, N. J., & Morris, D. L. (1993). Azithromycin Clinical Pharmacokinetics. *Clinical Pharmacokinetics*, *25*(5), 370–374. https://doi.org/10.2165/00003088-199325050-00003

136) Horita, Y., & Doi, N. (2014). Comparative study of the effects of antituberculosis drugs and antiretroviral drugs on cytochrome p450 3a4 and p-glycoprotein. *Antimicrobial Agents and Chemotherapy*, *58*(6), 3168–3176. https://doi.org/10.1128/AAC.02278-13

137) Beringer, P., Huynh, K. M. T., Kriengkauykiat, J., Bi, L., Hoem, N., Louie, S., Han, E., Nguyen, T., Hsu, D., Rao, P. A., Shapiro, B., & Gill, M. (2005). Absolute bioavailability and intracellular pharmacokinetics of azithromycin in patients with cystic fibrosis. *Antimicrobial Agents and Chemotherapy*, *49*(12), 5013–5017. https://doi.org/10.1128/AAC.49.12.5013-5017.2005

138) Amsden, G. W., Nafziger, A. N., & Foulds, G. (1999). Pharmacokinetics in serum and leukocyte exposures of oral azithromycin, 1,500 milligrams, given over a 3- or 5-

day period in healthy subjects. *Antimicrobial Agents and Chemotherapy*, *43*(1), 163–165. https://doi.org/10.1128/aac.43.1.163

139) Zakeri-Milani, P. (2010). Pharmacokinetic Study of Two Macrolide Antibiotic Oral Suspensions Using an Optimized Bioassay Procedure. *Journal of Bioequivalence & Bioavailability*, *02*(05), 111–115. https://doi.org/10.4172/jbb.1000041.

140) Long, C. M. (2014). Biopharmaceutical considerations and in vitro-in vivo correlations (IVIVCs) for orally administered amorphous formulations (Doctoral dissertation). Retrieved from https://researchportal.bath.ac.uk/en/studentTheses.

141) Barrett, M. A., Hutt, A. J., & Lansley, A . B. (1998). Involvement og P-glycoprotein in restricting the absorption of cefuroxime axetil across CACO-2 cells. *Journal of Pharmacy and Pharmacology*, 50 (Suppl. 9), 220. https://doi.org/10.1111/j.2042-7158.1998.tb02420.x

142) Arora SC, Sharma PK, Irchhaiya R, Khatkar A, Singh N, Gagoria J. (2010). Development, characterization and solubility study of solid dispersions of Cefuroxime Axetil by the solvent evaporation method. *J Adv Pharm Technol Res*, 1(3), 326-9. doi: 10.4103/0110-5558.72427.

143) Ruiz-Balaguer, N., Nacher, A., Casabo, V. G., & Merino Sanjuan, M. (2002). Intestinal transport of cefuroxime axetil in rats: Absorption and hydrolysis processes. *International Journal of Pharmaceutics*, 234(1-2). 101-111. https: //doi.org/10.1016/s0378-5173(01)00956-5.

144) Yee, K. L., Li, M., Cabalu, T., Sahasrabudhe, V., Lin, J., Zhao, P., & Jadhav, P. (2018). Evaluation of Model-Based Prediction of Pharmacokinetics in the Renal Impairment Population. *Journal of Clinical Pharmacology*, *58*(3), 364–376. https://doi.org/10.1002/jcph.1022

145) Beate Bretschneider-1999-Intesrinal transport of beta-lactam antibiotics- analysis of the affinity at the PEPT1, the uptake into caco-2 cell monolayers and the transepithelial flux. *Pharmaceutical Research*, 16(1), 55–6.

146) Rimmler, C., Lanckohr, C., Akamp, C., Horn, D., Fobker, M., Wiebe, K., Redwan, B., Ellger, B., Loeck, R., & Hempel, G. (2019). Physiologically based pharmacokinetic evaluation of cefuroxime in perioperative antibiotic prophylaxis. *British Journal of Clinical Pharmacology*, 85(12), 2864-2877. https://doi.org/10.1111/bcp.14121

147) Verhagen, C., Matties, H, & Van Strijen, E. (1994). The renal clearance of cefuroxime and ceftazidime and the effect of probenecid on their tubular excreatuib. *British Journal of clinical pharmacology*, 37(2), 193-197. https://doi.org/10.1111/j.1365-2125.1994.tb04260.x

148) Nix, D. E., Symonds, W. T., Hyatt, J. M., Wilton, J. H., Teal, M. A., Reidenberg, P., & Affrime, M. B. (1997). Comparative pharmacokinetics of oral ceftibuten, cefixime, cefaclor, and cefuroxime axetil in healthy volunteers. *Pharmacotherapy*, *17*(1), 121–125. https://doi.org/10.1002/j.1875-9114.1997.tb03684.x.

149) Donn, K. H., James, N. C., & Powell, J. R. (1994). Bioavailability of cefuroxime axetil formulations. *Journal of Pharmaceutical Sciences*, *83*(6), 842–844. https://doi.org/10.1002/jps.2600830617

150) Zhang, S., Fang, M., Zhang, Q., Li, X., & Zhang, T. (2019). Evaluating the bioequivalence of metronidazole tablets and analyzing the effect of in vitro dissolution on in vivo absorption based on PBPK modeling. *Drug Development and Industrial Pharmacy*, *45*(10), 1646–1653. https://doi.org/10.1080/03639045.2019.1648502

151) Somogyi, A., Kong, C., Sabto, J., Gurr, F. W., Spicer, W. J., & McLean, A. J. (1983). Disposition and removal of metronidazole in patients undergoing haemodialysis. *European Journal of Clinical Pharmacology*, *25*(5), 683–687. https://doi.org/10.1007/BF00542359

152) Loft, S. (1990). Metronidazole and Antipyrine as Probes for the Study of Foreign Compound Metabolism. *Pharmacology & Toxicology*, *66*, 1–31. https://doi.org/10.1111/j.1600-0773.1990.tb01611.x

153) Pearce, R. E., Cohen-Wolkowiez, M., Sampson, M. R., & Kearns, G. L. (2013). The role of human cytochrome P450 enzymes in the formation of 2-hydroxymetronidazole: CYP2A6 is the high affinity (low Km) catalyst. *Drug Metabolism and Disposition*, *41*(9), 1686–1694. https://doi.org/10.1124/dmd.113.052548

154) Larusso, N. F., Lindmark, D. G., & Müller, M. (1978). Biliary and renal excretion, hepatic metabolism, and hepatic subcellular distribution of metronidazole in the rat. *Biochemical Pharmacology*, *27*(18), 2247–2254. https://doi.org/10.1016/0006-2952(78)90084-9

155) Houghton, G., Dennis, M., & Gabriel, R. (1985). Pharmacokinetics of metronidazole in patients with varying degrees of renal failure. *British Journal of Clinical Pharmacology*, *19*(2), 203–209. https://doi.org/10.1111/j.1365-2125.1985.tb02632.x

156) Sprandel, K. A., Schriever, C. A., Pendland, S. L., Quinn, J. P., Gotfried, M. H., Hackett, S., Graham, M. B., Danziger, L. H., & Rodvold, K. A. (2004). Pharmacokinetics and pharmacodynamics of intravenous levofloxacin at 750 milligrams and various doses of metronidazole in healthy adult subjects. *Antimicrobial Agents and Chemotherapy*, *48*(12), 4597–4605. https://doi.org/10.1128/AAC.48.12.4597-4605.2004

157) Jyrki mattila, pekka t. Mannisto, raja mantyla, sirkka nykanen, a. U., & lamminsivu. (1983). Comparative Pharmacokinetics of Metronidazole and Tinidazole. *Antimicrobial Agents and Chemotherapy*, *23*(5), 721–725.

158) Houghton, G., Hundt, H., Muller, F., & Templeton, R. (1982). A comparison of the pharmacokinetics of metronidazole in man after oral administration of single doses of benzoylmetronidazole and metronidazole. *British Journal of Clinical Pharmacology*, *14*(2), 201–206. https://doi.org/10.1111/j.1365-2125.1982.tb01962.x

159) Idkaidek, N. M., & Najib, N. M. (2000). Enhancement of oral absorption of metronidazole suspension in humans. *European Journal of Pharmaceutics and Biopharmaceutics*, *50*(2), 213–216. https://doi.org/10.1016/S0939-6411(00)00098-9

160) Marsousi, N., Desmeules, J. A., Rudaz, S., & Daali, Y. (2017). Usefulness of PBPK Modeling in Incorporation of Clinical Conditions in Personalized Medicine. *Journal of Pharmaceutical Sciences*, *106*(9), 2380–2391. https://doi.org/10.1016/j.xphs.2017.04.035

161) Rodgers T, Leahy D, Rowland M. (2005). Physiologically based pharmacokinetic modeling 1: predicting the tissue distribution of moderate-to-strong bases. *J Pharm Sci.*, 94(6), 1259-76. doi: 10.1002/jps.20322.

162) Rodgers T, Rowland M. (2006). Physiologically based pharmacokinetic modelling 2: predicting the tissue distribution of acids, very weak bases, neutrals and zwitterions. *J Pharm Sci*. 95(6), 1238-57. doi: 10.1002/jps.20502.

163) Liu, P., Allaudeen, H., Chandra, R., Phillips, K., Jungnik, A., Breen, J. D., & Sharma, A. (2007). Comparative pharmacokinetics of azithromycin in serum and white blood cells of healthy subjects receiving a single-dose extended-release regimen versus a 3-day immediate-release regimen. *Antimicrobial Agents and Chemotherapy*, *51*(1), 103–109. https://doi.org/10.1128/AAC.00852-06

164) Nožinić, D., Milić, A., Mikac, L., Ralic, J., Padovan, J., & Antolovi, R. (2010). Assessment of macrolide transport using PAMPA, Caco-2 and MDCKII-hMDR1 assays. *Croatica Chemica Acta*, *83*(3), 323–331.

165) Zhou, D., Bui, K., Sostek, M., & Al-Huniti, N. (2016). Simulation and prediction of the drug-drug interaction potential of naloxegol by physiologically based pharmacokinetic modeling. *CPT: Pharmacometrics and Systems Pharmacology*, *5*(5), 250–257. https://doi.org/10.1002/psp4.12070.

166) Yoon, H. Il, Lee, C. H., Kim, D. K., Park, G. M., Lee, S. M., Yim, J. J., Kim, J. Y., Lee, J. H., Lee, C. T., Chung, H. S., Kim, Y. W., Han, S. K., & Yoo, C. G. (2013). Efficacy of levofloxacin versus cefuroxime in treating acute exacerbations of chronic obstructive pulmonary disease. *International Journal of COPD*, *8*, 329–334. https://doi.org/10.2147/COPD.S41749

167) Ralph, E. D. (1983). Clinical Pharmacokinetics of Metronidazole. *Clinical Pharmacokinetics*, *8*(1), 43–62. https://doi.org/10.2165/00003088-198308010-00003

168) Loft, S. (1990). Metronidazole and Antipyrine as Probes for the Study of Foreign Compound Metabolism. *Pharmacology & Toxicology*, *66*, 1–31. https://doi.org/10.1111/j.1600-0773.1990.tb01611.x

169) Wood, B. A., & Monro, A. M. (1975). Pharmacokinetics of tinidazole and metronidazole in women after single large oral doses. *British Journal of Venereal Diseases*, *51*(1), 51–53. https://doi.org/10.1136/sti.51.1.51

170) Cornelis Smit, S.D.H., Roger J.M. Brüggemann & Catherijne A.J. Knibbe. (2018). Obesity and drug pharmacology: a review of the influence of obesity on pharmacokinetic and pharmacodynamic parameters. *Expert Opinion on Drug Metabolism &Toxicology*, 14(3), 275-285.

171) Jill L Colquitt, K.P., Emma Loveman, Geoff K Frampton. (2014). Surgery for weight loss in adults. *The Cochrane Database of Systemic Reviews*,**8**(8).

172) Crémieux PY, Ledoux S, Clerici C, Cremieux F, Buessing M. (2010). The Impact of Bariatric Surgery on Comorbidities andMedication Use Among Obese Patients. *Obesity Surgery*, **20**: p. 861-870.

173) Eleni Sioka, G.T., Konstantinos Perivoliotis , Vissarion Bakalis, Eleni Zachari, Dimitrios Magouliotis, Vassiliki Tassiopoulou, Spyridon Potamianos, Andreas Kapsoritakis, Antigoni Poultsidi, Konstantinos Tepetes, Constantine Chatzitheofilou, and DimitrisZacharoulis, (2018). Impact of Laparoscopic Sleeve Gastrectomy on GI Motility. *Gasteroenterology Research and Practice*.

174) Dirksen C, D.M., Bojsen-Møller KN, Jørgensen NB, Kielgast U, Jacobsen SH, Naver LS,Worm D, Holst JJ, Madsbad S, Hansen DL, Madsen JL, (2013). Fast pouch emptying, delayed small intestinal transit, and exaggerated gut hormone responses after Roux-en-Y gastric bypass. *Neurogastroenterology & Motility*, **25**(4): p. 346-e255.

175) Thursky, B.J.a.K., (2012). Dosing of antibiotics in obesity. *Current Opinion in Infectious Diseases,*2012. **25**(6): p. 634-649.

176) M Ulvestad, I.S., GS Jakobsen, S Bremer, E Molden, A Åsberg, J Hjelmesæth,TB Andersson, R Sandbu and H Christensen. (2013). Impact of OATP1B1, MDR1, and CYP3A4 Expression in Liver and Intestine on Interpatient Pharmacokinetic Variability of Atorvastatin in Obese Subjects. *Clinical Pharmacology and Therapeutics,* **93**(3): p. 275-282.

177) Jens P. Kampmann, Henrik Klein, E. L. and, & Hansen, J. ens E. M. 0lholm. (1984). Ampicillin and Propylthiouracil Pharmacokinetics in Intestinal Bypass Patients Followed Up to a Year after Operation. *Clinical Pharmacokinetics, 9*, 168·176.

178) Marina Becker Sales Rocha, Gilberto De Nucci, Francisco Ney Lemos , Rodrigo Feitosa de Albuquerque Lima Babadopulos , Andrea Vieira Pontes Rohleder , Francisco VagnaldoFechine , Natalícia J Antunes , Gustavo D Mendes , Demetrius Fernandes do Nascimento. (2019). Impact of Bariatric Surgery on the Pharmacokinetics Parameters of Amoxicillin. *Obesity Surgery*, *29*, 917–927. https://doi.org/doi: 10.1007/s11695-018- 3591-3.

179) J Miskowiak, B Andersen, V. G. N. (1985). Absorption of oral penicillin before and after gastroplasty for morbid obesity. *Pharmacology*, *31*(2), 115–120. https://doi.org/doi: 10.1159/000138106.

180) S. I. Terry, J.C.G., J. P. A. McManus, and L. F. Prescott *Absorption of Penicillin and Paracetamol After Small Intestinal Bypass Surgery* European Journal of Clinical Pharmacology, 1982. **23**: p. 245-248.

181) Ana Belén Rivas, Amanda Lopez-Picado, María Del Rosario Salas-Butrón3, Ana Terleira, Andres Sanchez Pernaute , Antonio José Torres Garcia , Carmen Moreno Lopera , Luis Miguel Chicharro , Fernando Bandrés , Miguel Angel Rubio Herrera , Antonio Portolés, E. V. (2019). Effect of Roux-en-Y gastric surgery on ciprofloxacin pharmacokinetics: an obvious effect? *European Journal of Clinical Pharmacology*, *75*(5), 647–654. https://doi.org/doi: 10.1007/s00228-018-02623-8.

182) Julie De Smet, Pieter Colin, Peter De Paepe, Johannes Ruige, Hélène Batens, Yves Van Nieuwenhove, Dirk Vogelaers, Stijn Blot, Jan Van Bocxlaer, Luc M Van Bortel, K. B. (2012). Oral bioavailability of moxifloxacin after Roux-en-Y gastric bypass surgery. *The Journal of Antimicrobial Chemptherapy*, 61(1), 226–229. https://doi.org/doi: 10.1093/jac/dkr436.

183) Derendrof, S.K.B., (2016). Pharmacokinetics I: PK-PD approaches, the case of antibiotic drug development. *Clinical Pharmacology: Current topics and Case studies*: Second edition. https://doi.org/10.1007/978-319-27347-1

184) L. Alou, L. Aguilar, D.Sevillano, M.J.Gimenez, N.Gonzalez, O.Echeverria, M.Torrico, J.E. MArtin, L.Valdes, & J.Prieto. (2007). Levofloxacin vs. Azithromycin Pharmacodynamic Activity Against S. pneumoniae and H. influenzae with Decreased Susceptibility to Amoxicillin/Clavulanic Acid. *Journal of Chemotherapy*, *19*(6), 670–672. https://doi.org/doi: 10.1179/joc.2007.19.6.670

185) Biedenbach, D. J., Jones, R. N., Lewis, M. T., Croco, M. A. T., & Barrett, M. S. (1999). Comparative In Vitro Evaluation of Dirithromycin Tested Against Recent Clinical Isolates of Haemophilus influenzae, Moraxella catarrhalis, and Streptococcus pneumoniae, including Effects of Medium Supplements and Test Conditions on MIC Results. *Diagnostic Microbiology and Infectious Diseases*, *33*(4), 275–282.

186) Scott, L. J., Ormrod, D., Goa, K. L., Alexander, K., & Amsden, G. W. (2001). Cefuroxime Axetil An Updated Review of its Use in the Management of Bacterial Infections. *Drugs*, *61*(10), 1455–1500. https://doi.org/0012-6667/01/0010-1455/$27.50/0

187) Rodríguez-Gascón, A., Aguirre-Quiñonero, A., & Canut-Blasco, A. (2020). Are oral cefuroxime axetil, cefixime and cefditoren pivoxil adequate to treat uncomplicated acute pyelonephritis after switching from intravenous therapy? A pharmacokinetic/pharmacodynamic perspective. *Enfermedades Infecciosas y Microbiologia Clinica*, *38*(7), 306–311. https://doi.org/10.1016/j.eimc.2019.12.017Clinical and Laboratory Standards

Institute. Performance Standards fro Antimicrobial Susceptibility Testing: 28th Edition M100-Ed28. CLSI, Wayne,PA,USA,2018.

188) The European Committee on Antimicrobial Susceptibility Testing. Calibration of Zone Diameter breakpoints to MIC Values, Version 10.1, February 2022. EUCAST: Calibration and validation

189) Trsitram, S., Jacobs, M.R., Appelbaum, P.C. (2007). Antimicrobial Resistance in *Haemophilus influenzae*. *Clinical Microbiology Reviews*, 20(2), 368-389. https:// doi:10.1128/CMR.00040-06

190) Kastner, U., & Guggenbichler, J. P. (2001). Influence of macrolide antibiotics on promotion of resistance in the oral flora of children. *Infection*, *29*(5), 251–256. https://doi.org/10.1007/s15010-001-1072-3

191) Barrett, M. A., Hutt, A. J., & Lansley, A. B. (1998). Involvement of P-glycoprotein in restricting the absorption of cefuroxime axetil across CACO-2 cells. ***Journal of Pharmacy and Pharmacology***, **50**(SUPPL. 9), 220. https://doi.org/10.1111/j.2042-7158.1998.tb02420.x

192) Svetkey LP, Stevens VJ, Brantley PJ, Appel LJ, Hollis JF, Loria CM, Vollmer WM, Gullion CM, Funk K, Smith P, Samuel-Hodge C, Myers V, Lien LF, Laferriere D, Kennedy B, Jerome GJ, Heinith F, Harsha DW, Evans P, Erlinger TP, Dalcin AT, Coughlin J, Charleston J, Champagne CM, Bauck A, Ard JD, Aicher K; Weight Loss Maintenance Collaborative Research Group. (2008). Comparison of strategies for sustaining weight loss: the weight loss maintenance randomized controlled trial. *JAMA- Journal of the American Medical Association,* 299(10), 1139-48. doi: 10.1001/jama.299.10.1139.

193) Arterburn DE, Courcoulas AP. (2014). Bariatric surgery for obesity and metabolic conditions in adults. *BMJ.* ;349: g3961. doi: 10.1136/bmj.g3961.

194) Bal BS, Finelli FC, Shope TR, Koch TR. (2012). Nutritional deficiencies after bariatric surgery. *Nat Rev Endocrinol.*, 8(9), 544-56. doi: 10.1038/nrendo.2012.48.

195) Al-Gousous, J., & Langguth, P. (2015). Oral Solid Dosage Form Disintegration Testing - The Forgotten Test. *Journal of Pharmaceutical Sciences*, *104*(9), 2664–2675. https://doi.org/10.1002/jps.24303

196) Dahan A, Miller JM, Hilfinger JM, Yamashita S, Yu LX, Lennernäs H, Amidon GL. (2010). High-permeability criterion for BCS classification: segmental/pH dependent permeability considerations. *Mol Pharm.*, 7(5), 1827-34. doi: 10.1021/mp100175a

197) Darwich AS, Henderson K, Burgin A, Ward N, Whittam J, Ammori BJ, Ashcroft DM, Rostami-Hodjegan A. (2012) Trends in oral drug bioavailability following bariatric surgery: examining the variable extent of impact on exposure of different drug classes. *Br J Clin Pharmacol*., 74(5), 774-87. doi: 10.1111/j.1365-2125.2012.04284.x.

198) Prabhakaran, R., Janakiraman, K., & Harindran, J. (2016). Development and comparative bioavailability evaluation of cefuroxime axetil oral suspension by single dose two way cross over study in rabbits. *Journal of Pharmaceutical Sciences and Research*, *8*(1), 24–28]

199) Stano, S., Alam, F., Wu, L., Dutia, R., Ng, S. N., Sala, M., McGinty, J., & Laferrère, B. (2017). Effect of meal size and texture on gastric pouch emptying and glucagon-like peptide 1 after gastric bypass surgery. *Surgery for obesity and related diseases: official journal of the American Society for Bariatric Surgery*, *13*(12), 1975–1983. https://doi.org/10.1016/j.soard.2017.09.004

200) Wölnerhanssen, B. K., Meyer-Gerspach, A. C., Peters, T., Beglinger, C., & Peterli, R. (2016). Incretin effects, gastric emptying and insulin responses to low oral glucose loads in patients after gastric bypass and lean and obese controls. *Surgery for obesity and related diseases : official journal of the American Society for Bariatric Surgery*, *12*(7), 1320–1327. https://doi.org/10.1016/j.soard.2015.11.022

201) Nguyen, N. Q., Debreceni, T. L., Burgstad, C. M., Wishart, J. M., Bellon, M., Rayner, C. K., Wittert, G. A., & Horowitz, M. (2015). Effects of Posture and Meal Volume on Gastric Emptying, Intestinal Transit, Oral Glucose Tolerance, Blood

Pressure and Gastrointestinal Symptoms After Roux-en-Y Gastric Bypass. *Obesity surgery*, *25*(8), 1392–1400. https://doi.org/10.1007/s11695-014-1531-4

202) Brocks, Dion R; Ben-Eltriki, Mohamed; Gabr, Raniah Q; Padwal, Raj S (2012). The effects of gastric bypass surgery on drug absorption and pharmacokinetics. *Expert Opinion on Drug Metabolism & Toxicology*, 8(12), 1505–1519. doi:10.1517/17425255.2012.722757

203) Miller AD, Smith KM (2006). Medication and nutrient administration considerations after bariatric surgery. *Am J Health-Syst Pharm*. 63(19) 1852- https://doi.org/10.2146/ajhp060033\